# CONGRESS BOOK

**MSNG2024**

**11th International Conference on**

**Materials Science and Nanotechnology for**

**Future Generations**

**OEMT2024**

**6nd International Conference on**

**Organic Electronic Material Technologies**

22-25 May 2024

Troia Cultural Center- Çanakkale Onsekiz Mart University, Çanakkale/TURKEY

## COMMITTEES

**HONORARY PRESIDENT**
Prof. Dr. R. Cüneyt ERENOĞLU
Prof. Dr. Fahrettin GÖKTAŞ
Prof. Dr. Rana KİBAR

**CONFERENCE PRESIDENT**
Prof. Dr. Hava ÖZAY
Prof.Dr. Vildan BİLGİN
Prof. Dr. Osman DAYAN
Prof. Dr. Fahrettin YAKUPHANOĞLU

**ORGANIZING COMMITTEE**
Prof.Dr. Ahmet EKİCİBİL
Prof. Dr. Ayhan ORAL
Prof. Dr. Ayşe KÜÇÜKARSLAN
Prof. Dr. Cahit AKGÜL
Prof. Dr. Canan AKSU CANBAY
Prof. Dr. Diğdem ERDENER
Prof. Dr. Kadir AY
Prof.Dr. Müjdat ÇAĞLAR
Prof. Dr. Özgür ÖZAY
Prof. Dr. Şemsettin ALTINDAL
Prof. Dr. Tijen Ennil BEKTAŞ
Prof. Dr. Yusuf DİLGİN
Assoc. Prof. Dr. Ayşegül DERE
Assoc.Prof.Dr. Elif KARACAN
Assoc. Prof. Dr. Filiz UĞUR NİGİZ
Assoc. Prof. Dr. Melek TERCAN
Assoc. Prof. Dr. Serkan DAYAN
Dr. Emrah SARICA
Dr. İbrahim GÜNEŞ
Dr. Merve DANIŞMAN
Lecturer R. Nilay TEZEL
Çılga MİSLİ UÇMAZ
Sezer YİĞİT

**SCIENTIFIC COMMITTEE**

| | |
|---|---|
| Abdulhalik KARABULUT | Ağrı Ibrahim Çecen University |
| Abdulkerim KARABULUT | Erzurum Teknik University |
| Adem TATAROĞLU | Gazi University |
| Adnan KAYA | İzmir Katip Çelebi University |
| Adrian M.T. SILVA | University of Porto |
| Ahmet ALTINDAL | Yıldız Technical University |
| Ahmet CEYLAN | Erciyes University |
| Ahmet Faruk ÖZDEMİR | Süleyman Demirel University |
| Ahmet ORAL | Middle East Technical University |
| Ali Abdolahzadeh ZIABARI | Lahijan Branch, Islamic Azad University |
| Ali Cesur ONMAZ | Erciyes University |
| Ali COŞKUN | University of Fribourg |
| Ali GÜRSEL | The International University of Sarajevo |

| | |
|---|---|
| Ali Osman AYAŞ | Adıyaman University |
| Ali ÖZER | Cumhuriyet University |
| Arif KÖSEMEN | Muş Alparslan University |
| Arife GENCER İMER | Van Yüzüncü Yıl University |
| Asmaa HENDI | King Abdulaziz University |
| Atilla COŞKUN | Muğla Sıtkı Koçman University |
| Bakiye ÇAKIR | Artvin Çoruh University |
| Berna BÜLBÜL | Balıkesir University |
| Betül GÜZELDİR | Atatürk University |
| Bilgehan GÜZEL | Çukurova University |
| Buket Saatçi | Erciyes University |
| Bünyamin COŞUT | Gebze Technical University |
| Burhan COŞKUN | Kırklareli University |
| Byeong-Kwon JU | Korea University |
| Canan Aksu CANBAY | Fırat University |
| Cem ÇELEBİ | İzmir Institute of Technology |
| Christian WENGER | Leibniz Institute for Innovative Microelectronics |
| Christoph STAMPFER | RWTH Aachen University |
| Chung GWIY-SANG | Ulsan University |
| Çiğdem Karakükcü | Erciyes University |
| Cumali SABAH | Middle East Technical University |
| D. D. ZAITSEV | Moscow State University |
| D. Esra YILDIZ | Hitit University |
| D. S. PATIL | North Maharashtra University |
| Darina ARSOVA | Bulgarian Academy of Sciences |
| Denis NIKA | Moldova University |
| Deniz Sunar ÇERÇİ | Adıyaman University |
| Demet İSKENDEROĞLU | Atatürk University |
| Dever NORMAN | Henderson State University |
| Dilek ODACI | Ege University |
| Dionysios DIONYSIOU | University of Cincinnati |
| Doğan KAYA | Çukurova University |
| E. Hassan ALY | Ain Shams University |
| Ebru ŞENADIM TÜZEMEN | Cumhuriyet University |
| Ekrem AYDINER | İstanbul University |
| Elias STATHATOS | Tecnological-Educational Institute of Patras |
| Emin BACAKSIZ | Karadeniz Technical University |
| Emin ÜNAL | Iskenderun Technical University |
| Emine GÜNERİ | Erciyes University |
| Emmanuel KOUDOUMAS | Hellenic Mediterranean University |
| Emmanuel KYMAKIS | Hellenic Mediterranean University |
| Emrah SOYLU | Erciyes University |
| Emre GÜR | Eskişehir Osmangazi University |
| Emre Ozan POLAT | Kadir Has University |
| Emre YAVUZ | Erzincan Binali Yıldırım University |
| Erkan YILMAZ | Erciyes University |
| Esra ALVEROGLU | Istanbul Technical University |
| Evangelos VITORATOS | University of Patras |
| F. Ahmet ÇELİK | Bitlis Eren University |
| Faruk KARADAĞ | Çukurova University |
| Fatma Göde | Mehmet Akif Ersoy University |
| Fenghua Zhang | Harbin Institute of Technology |
| Filiz ŞENKAL | Istanbul Technical University |
| Fumihiko HIROSE | Yamagata University |
| Gabriel Constantinescui | The University of Aveiro |
| Gamze BARIM | Adıyaman University |
| Giorgio SBERVEGLIERI | Università di Brescia |

| | |
|---|---|
| Gökay UĞUR | Gazi University |
| Gökhan SAVAROĞLU | Eskişehir Osmangazi University |
| Grzegorz KARCZEWSKI | The Polish Academy of Sciences |
| Gülce ÖZTÜRK | Erciyes University |
| Gülşen AKDOĞAN | Erciyes University |
| Habibe TECİMER | Karabük University |
| Hadi HEIDARI | The University of Glasgow |
| Hakan KARAAĞAÇ | İstanbul Technical University |
| Halil İbrahim ULUSOY | Sivas Cumhuriyet University |
| Hasan ŞAHİN | İzmir Institute of Technology |
| Hatice Bekci | Kayseri University |
| Hülya METİN GÜBÜR | Mersin University |
| Hüseyin TECİMER | Karabük University |
| Hwan Kyu KIM | Korea University |
| İbrahim EROL | Afyon Kocatepe University |
| İbrahim İNANÇ | Ondokuz Mayıs University |
| İbrahim Yasin ERDOĞAN | Bingol University |
| İdris AKYÜZ | Eskişehir Osmangazi University |
| İmran AVCI | VRIJE University of Amsterdam |
| İskender ÖZKUL | Mersin University |
| Jingkun XU | Jiangxi Science & Technology Normal University |
| Jongeun RYU | North Carolina State University |
| José M. KENNY | Università di Perugia |
| Juan Carlos Martinez-ANTON | Complutense University of Madrid |
| Kamil ŞİRİN | Manisa Celal Bayar University |
| Kamuran GÖRGÜN | Eskişehir Osmangazi University |
| Katerina POMONI | University of Patras |
| Kemal Volkan ÖZDOKUR | Erzincan Binali Yıldırım University |
| Kevser Şahin Tıraş | Erciyes University |
| Khasan S. KARIMOV | GIK Institute |
| Kristina RUSIMOVA | University of Bath |
| Kübra YAKINCI | İskendurun Technical University |
| Luis BANARES | Universidad Complutense de Madrid |
| Luisa TORSI | University of Bari |
| M. Emin ARZUTUĞ | Atatürk University |
| M. Eyyüphan YAKINCI | İskenderun Technical University |
| M. Fatih EMEN | Mehmet Akif Ersoy University |
| Mahmut DOĞRU | Fırat University |
| Mahmut KUŞ | Konya Technical University |
| Marco Antonio SCHIAVON | Federal University of São João del-Rei |
| Mehmet ACET | The University of Duisburg-Essen |
| Mehmet Enver AYDIN | Dicle University |
| Mehmet PARLAK | Middle East Technical University |
| Mehmet Sait BOZGEYİK | Kahramanmaraş Sütçü İmam University |
| Merih PALANDÖKEN | İzmir Katip Çelebi University |
| Mikhail I. VASILEVSKIY | University of Minho |
| Mohamed BOUOUDINA | Prince Sultan University |
| Mohammed Saleh AL-SALIHI | King Saud University |
| Muhammad Hassan SAYYAD | Dublin City University |
| Muharrem KARAASLAN | Iskenderun Technical University |
| Mujdat ÇAĞLAR | Eskişehir Anadolu University |
| Murat ESKİL | Aksaray University |
| Murat Kaleli | Süleyman Demirel University |
| Murat SOYLU | Bingöl University |
| Mustafa TEPE | Ege University |
| MustafaTolga YURTCAN | Atatürk University |
| Nalan ÖZDEMİR | Erciyes University |

| | |
|---|---|
| Namık ÖZDEMİR | Samsun Ondokuz Mayıs University |
| Nihat TUĞLUOĞLU | Giresun University |
| Nouredine SENGOUGA | Université de Biskra |
| Nurcan DOĞAN | Gebze Technical University |
| Nurdoğan CAN | Jazan University |
| O. Mert KARATAŞ | İnönü University |
| Oğuz GÜLSEREN | Bilkent University |
| Oğuzhan AKGÖL | İskenderun Technical University |
| Oktay KARADUMAN | Munzur University |
| Ömer Faruk YÜKSEL | Selçuk University |
| Önder METIN | Koç University |
| Orhan PÜSKÜLLÜ | Erciyes University |
| Osman DAYAN | Çanakkale Onsekiz Mart University |
| Panagiotis LIANOS | University of Patras |
| Pedram Khalili Amiri | Northwestern University |
| Quanmin GUO | The University of Birmingham |
| Quentin M. RAMASSE | University of Liverpool |
| R. O. OCAYA | University of the Free State |
| Ram K. GUPTA | Pittsburg State University |
| Ramin YOUSEFI | Islamic Azad University |
| Raşit TURAN | Middle East Technical University |
| Recep ŞAHİNGÖZ | Yozgat Bozok University |
| Recep ZAN | Ömer Halisdemir University |
| Richard J. COBLEY | Swansea University |
| S. WAGEH | King Abdulaziz University |
| Sadin ÖZDEMİR | Mersin University |
| Salim ÇERÇİ | Adıyaman University |
| Sarani ZAKARIA | The National University of Malaysia |
| Savaş SÖNMEZOĞLU | Kahramanoğlu Mehmet Bey University |
| Seda BEYAZ | Balıkesir University |
| Sefa ERTÜRK | Niğde Ömer Halisdemir University |
| Şemsettin ALTINDAL | Gazi University |
| Serap GÜNEŞ | Yıldız Technical University |
| Serap ŞENTÜRK DALGIÇ | Trakya University |
| Niyazi Serdar SARIÇİFTÇİ | Johannes Kepler Linz University |
| Serhat ORKUN TAN | Karabük University |
| Seyfettin ÇAKMAK | Süleyman Demirel University |
| Sezai ALAGÖZ | Cumhuriyet University |
| Sibel DUMAN | Bingöl University |
| Şükrü KARATAŞ | Kahramanmaraş Sütçü İmam University |
| Tamer ABDALLAH | Ain Shams University |
| Tayyar GÜNGÖR | Burdur M. Akif Ersoy University |
| Thomas UNOLD | Helmholtz Zentrum Berlin |
| Tülay BAL DEMİRCİ | İstanbul University-Cerrahpaşa |
| Tülay HURMA | Eskişehir Technical University |
| Türker TÜZEMEN | Cumhuriyet University |
| W. Aslam FAROOQ | King Saud University |
| Witold Daniel DOBROWOLSKI | The Polish Academy of Sciences |
| Wojtek WLODARSKI | RMIT University |
| Wolfgang ENSINGER | Technische Universität Darmstadt |
| Yashar Azizian-Kalandaragh | Gazi University |
| Yakup KURUCU | Atatürk University |
| Yasemin ÇAĞLAR | Eskişehir Anadolu University |
| Yasemin ÇİFTÇİ ÖZTEKİN | Gazi University |
| Yasemin ŞAFAK ASAR | Gazi University |
| Zheng Liu | Nanyang Technological University |
| Zeki YARAR | Mersin University |

**Welcome Massage**

The 11th International Conference on Materials Science and Nanotechnology for Future Generations (MSNG 2024) and the 6th Organic Electronic Materials Technology Conference (OEMT 2024) are annual international scientific conferences.

This year, the two congresses will be combined and held at Çanakkale Onsekiz Mart University. MSNG2024 and OEMT2024 bring together a diverse set of research topics, including renewable energy applications, catalysis, nanomaterials, conductive materials, thin films, semiconductors, shape memory materials, and so on. Our goal was to create a platform that would connect students and colleagues to the most recent work of internationally recognized experts.

Many of our colleagues have now honored our congress by attending. The program features eight invited speakers, 34 oral presentations, and 19 posters. We thank all invited speakers, authors, and contributors to MSNG2024/OEMT2024 for visiting Çanakkale and communicating their research results.

Prof.Dr.Osman DAYAN
Conference President

**Sponsors**

Kale

Tekno-TIP

Tekno-TIP Analitik Sistemler Ltd. Şti.

Nanomat

nano-engineering

FYTRONIX

Electronic

IDASONIC

NANOCOATING SYSTEMS AND TECHNOLOGIES

DentBioChem

# PROGRAMME

| **22 May 2024 – Wednesday** | | | | **COMU Troia Culture Center** |
|---|---|---|---|---|
| **09.00** | **REGISTRATION** | | | |
| **12.00** | **LUNCH** | | | |
| **13.00** | **OPENING CEREMONY** | | | |
| **13.30** | **INVITED TALKS** | **Recent Advances in Photovoltaic Technologies** | **Raşit TURAN** | **CHAIR Fahrettin YAKUPHANOĞLU** |
| **14.00** | **INVITED TALKS** | **Introduction to KS R&D Center and Project Examples** | **Kağan KAYACI** | |
| **14.30** | **TEA, COFFEE BREAK** | | | |
| **15.00** | **Panel (Industry/University Collaborations: Examples/Suggestions)** | | **Raşit TURAN (GUNAM)**<br>**Kağan KAYACI (Kale Seramik)**<br>**Fahrettin YAKUPHANOĞLU (FYTRONİX)**<br>**Vildan BİLGİN (IDASONIC)**<br>**Murat ATEŞ (Nanochem)**<br>**Serkan DAYAN (DentBioChem)** | **CHAIR Hava ÖZAY** |
| **Cocktail** | | | | |

| 23 May 2024 – Thursday | | | | COMU Troia Culture Center |
|---|---|---|---|---|
| 09.00 | REGISTRATION | | | |
| 09.00 | INVITED TALK | Recent Advances in Zinc Oxide Based Dye-Sensitized Solar Cells | Yasemin ÇAĞLAR | CHAIR<br>Canan AKSU CANBAY |
| 09.30 | Oral-1 | Evaluation of the potential of ammonium borane as a hydrogen storage material | Canan CAN | |
| 09.45 | Oral-2 | On the Impact of Pure PVC and (Ti-doped PVC) Interlayer on the Performance Metal-Semiconductor (MS) Schottky diodes (SDs) in Wide Voltage Range ± 2.5V | Çiğdem Şükriye GÜÇLÜ | |
| 09.45 | Oral-3 | Synthesis and Characterization of Functionalized Nanoparticles for Enhanced Enzyme-Free Glucose Sensing in Biosensors | Merve KÜÇÜKOFLAZ KORKMAZ | |
| 10.15 | Oral-4 | A Computational Study On The Sensing Of Nitro-Containing Explosive Materials | Berkay SÜTAY | |
| 10.30 | TEA, COFFEE BREAK / POSTER SECTION (P1-19) | | | |
| 10.50 | INVITED TALK | New electrode material design for energy storage systems | Murat ATEŞ | CHAIR<br>AYŞEGÜL DERE |
| 11.20 | Oral-4 | W and F co-doped $SnO_2$ Films deposited by Ultrasonic Spray Pyrolysis | Emrah SARICA | |
| 11.35 | Oral-5 | Extraction and Physicochemical, Proximate and Phytochemical Analysis of Locust Beans Powder and Oil (Parkia Biglabosa) | Ibrahim Isah FAGGE | |
| 11.50 | Oral-6 | Characterization and Potential of ITO/ZnO/CuO Heterostructures for Photovoltaic Applications | İbrahim GÜNEŞ | |
| 12.05 | Oral -7 | BET surface area and TGA analyzes of some transition metal oxides used in supercapacitors | Ozan YÖRÜK | |
| 12.20 | LUNCH | | | |
| 13.30 | INVITED TALK | Scale-up Production of Polymer Fibers for Drug Delivery | Attila Levente GERGELY | CHAIR<br>AYHAN ORAL |
| 14.00 | Oral-8 | Metal-polymer composites via wet-chemistry method | Merve KÜÇÜKOFLAZ KORKMAZ | |
| 14.15 | Oral-9 | Synthesis and structural studies of aliphatic nitrile functionalized benzimidazolium salt and its respective Silver (I) and Palladium (II)-N-heterocyclic carbene complexes | Sunusi Yahaya Hussaini | |
| 14.30 | Oral-10 | Novel Poly(vinylidene Fluoride)-Baghdadite-Based Composite Membranes as Bone Scaffolds | Büşra MUTLU | |
| 14.45 | Oral-11 | N-Doped Interlayer Effects On Dielectric Properties In Diamond SBDs By Impedance Measurements | Nuray URGUN ERKUTLU | |
| 15.15 | TEA, COFFEE BREAK / POSTER SECTION (P1-19) | | | |
| 15.20 | INVITED TALK | Metal Oxides for Next-generation Photonic, and Photovoltaic Applications | Fahrettin YAKUPHANOĞLU | CHAIR<br>Vildan BİLGİN |
| 15.50 | Oral-12 | Machine-learning supported heavy metal detection by heme ring printed electrodes | Zihni Onur UYGUN | |
| 16.05 | Oral-13 | Effects of molarity on structural, optical and electrical properties of nanostructured CuO films prepared by spray pyrolysis technique using perfume atomizer | Şerif RÜZGAR | |
| 16.20 | Oral-14 | Cosmic and Gamma Radiation Test of a Developed Secondary Emission Ionization Calorimetry Module | Saleh ABUBAKAR | |
| 16.35 | Oral-15 | Investigation of the Efficiency of Photo Catalysts in Carbon Dioxide Reduction Reactions | Canan AKSU CANBAY | |
| 16.50 | Oral-16 | Spectroscopic and physical characterization of N-phenolyl amino acid derivatives of di spiro cyclotriphosphazene compound | Mahmut YILMAZ | |

| 24 May 2024 – Friday | | | | COMU Troia Culture Center |
|---|---|---|---|---|
| 09.00 | REGISTRATION | | | |
| 09.00 | INVITED TALK | Hole transport layers for perovskites solar cells: Recent progress and perspectives | Fakhra Aziz | CHAIR Serkan DAYAN |
| 09.30 | Oral-17 | An Insight into the Performance of Various Catalysts in Biodiesel Production, with Special Emphasis on Heterogeneous Based Catalysis | Abdu Muhammad Bello | |
| 09.45 | Oral-18 | A Comparison of Forward and Reverse Bias Current Transport Mechanisms (CTMs) for Au/n-Si (MS), Au/PVC/n-Si (MPS1), and Au/(Ti:PVC)/n-Si (MPS2) Type Schottky Diodes (SDs) | Çiğdem Şükriye GÜÇLÜ | |
| 09.45 | Oral-19 | Biodilecetric properties of hydroxyapatite-based materials for biomedical applications | Ayşegül DERE | |
| 10.15 | Oral-20 | Unleashing the Photovoltaic Potential: Optimizing Zn-Doped Co3O4 Films via Ultrasonic Spray Pyrolysis | İbrahim GÜNEŞ | |
| 10.30 | TEA, COFFEE BREAK / POSTER SECTION (P1-19) | | | |
| 10.50 | INVITED TALK | Electrospun nanofibers: Promising nanoscale structures in nanobiotechnology | Dilek ODACI | CHAIR Filiz UĞUR NIGIZ |
| 11.20 | Oral-21 | Conjugation of RGD on electrodeposited of carbon nanotubes to analyse glioblastoma cells | Belgüzar KARADAĞ | |
| 11.35 | Oral-22 | Sunflower Seed Shell-Derived Hard Carbon: A Sustainable Solution for Aqueous Zn-Ion Battery Electrodes | Burak TEKİN | |
| 11.50 | Oral-23 | Comparing the influence of TiO2 NPs on the activity of SDS and CTAB surfactants at air-water interface | Aminu Dabo SHIAİBU | |
| 12.05 | Oral -24 | Removal of Iron Impurities from Quartz Ores in the East Anatolian Fault Zone Region and Enhancement of Purity through Physical Methods | Canan AKSU CANBAY | |
| 12.20 | LUNCH | | | |
| 13.30 | INVITED TALK | Functional Metal/Semicoductor Devices for Organic Electronic Applications | Şemsettin ALTINDAL | CHAIR Emrah SARICA |
| 14.00 | Oral-25 | Use of active carbon produced by hydrothermal method from agricultural waste in methylene blue removal | Elif ARANCI ÖZTÜRK | |
| 14.15 | Oral-26 | Drug Doped Metal Phosphate Organic Framework Synthesis, Characterization, and Cell Viability Assay | Başak ÇELEBİ | |
| 14.30 | Oral-27 | Harnessing Turkey's First Registered Biomass: Hemp-Derived Carboneous Electrode for Advanced Zn-Ion Hybrid Supercapacitors | Burak TEKİN | |
| 14.45 | TEA, COFFEE BREAK / POSTER SECTION (P1-19) | | | |
| 15.00 | INVITED TALK | Organic photonic devices for organic electronic applications | Fahrettin YAKUPHANOĞLU | CHAIR Ayşe KÜÇÜKARSLAN |
| 15.30 | Oral-28 | Structural properties & surface morphologies of Sb doped ZnO thin films | Sibel GÜRAKAR | |
| 15.45 | Oral-29 | Effects of molarity on structural, optical and electrical properties of Hexagonal Nanocrystalline Nickel Oxide films prepared by spray pyrolysis technique using perfume atomizer | Şerif RÜZGAR | |
| 16.00 | Oral-30 | The Effect of Sulfurization Temperature on As-prepared SnS Films Deposited by Ultrasonic Spray Pyrolysis | Barbaros DEMİRSELÇUK | |
| 16.15 | Oral-31 | Cr based coatings electrodeposited by binary potential loop and their corrosion behaviour | Esra KUŞ | |
| 16.30 | Oral-32 | Analyzing the mechanical properties of an auxetic structure under compression | Gülcan AYDIN | |
| 16.45 | Oral-33 | Investigatin of Photocatalytic Properties of Rare Earth Element Oxides | Canan AKSU CANBAY | |
| 17.00 | Oral-34 | Temperature and frequency dependence of the dielectric properties of novel chalcone based methacrylate polymer | Mahmut YILMAZ | |
| 17.15 | Oral-35 | Investigation of Possible Current Transport Mechanisms (CTMs) of Quaternary Functional Semiconductor Device in a wide temperature and voltage range | S. ALTINDAL | |
| 17.30 | Oral-36 | Over- Grinding of Biocoal-Chalcopyrite Concentrate Mixture | Canan AKSU CANBAY | |
| GALA DINNER (REVGAN RESTAURANT) | | | | |

| **25 May 2024 – Saturday** |
|---|
| **SOCIAL PROGRAMS (paid)** |

| POSTER SESSION | | |
|---|---|---|
| **PosterNo** | **Title** | **Corresponding author** |
| 1 | Investigation of Voltametric Behavior of Vanillin-Based Chalcone Compound | Bahire Filiz ŞENKAL |
| 2 | Transition Metal Chalcogenide Supercapacitors | Emre GÜR |
| 3 | Breaking Barriers: Lithium Manganese Oxide (LiMnO2) Cathode Paves the Way for Next-Generation Aqueous Ammonium Ion Batteries | Burak TEKİN |
| 4 | Spinel-Derived LiMn2O4: A Promising Cathode for Environmentally Friendly Ammonium Ion Batteries | Burak TEKİN |
| 5 | Evaluation of the potential of two-dimensional (2D) Borophene material for hydrogen storage applications | Canan CAN |
| 6 | Glycoconjugates based on Mesoporous silica nanoparticles | Derya Selcan SELMANOĞLU |
| 7 | Development of Hydrogen Peroxide Biosensors Based on Poly-L-Histidine, Multi-walled Carbon Nanotubes and Ionic Liquid | Elif ULUKAN |
| 8 | Ternary rGO/MnO2/PANI hybrid nanocomposite materials in 1M KOH for Supercapacitor evaluations | Fatih NACAK |
| 9 | Synthesis and Characterization of Shape and Size-Controlled Mesoporous Silica Nanoparticle Spheres | Fatmanur UYAN |
| 10 | Synthesis of rGO@L-Arginine/Co Nanoparticles and Application Enzyme-Free Glucose Sensing | Mehtap CEYRAN |
| 11 | Synthesis, characterization, optical and electrochemical properties of poly(azomethine)s containing aliphatic chain and biphenylsulfonic acid unit | Nilay TEZEL |
| 12 | Characterization of Electrical Properties in MIS Schottky Barrier Diodes with N-Doped DLC Thin Films | Nuray URGUN ERKUTLU |
| 13 | Preparation of Alumina-Supported Pd@Ru Nano-Catalysts and Their applications | Ezginur GÜLERİŞ |
| 14 | Determination of potential use of halloysite nanotube filled alginate film for food packaging | Özde İPSALALI |
| 15 | Effect of Sulphurization Duration on Cu rich $CuSbS_2$ Films Produced by a Two-step Process | Uğur YORULMAZ |
| 16 | Cu-Based MPOF Immobilization to Strip Electrodes: Fabrication of a Glucose Biosensor | Yaren CANATAN |
| 17 | Production and Electrical/Optical Characterization of Al/NiCo2O4 /n-Si/Al Schottky Photodiode Structure | Yusuf ATMACA |
| 18 | Synthesis And Optimization Of Polyvinylimidazole By Photopolymerization Type II | Merve DANIŞMAN |
| 19 | Detailed analysis of possible current transport mechanisms (CTMs) in Au/(P3DMTFT)/n-GaAs Schottky diodes (SDs) over a wide temperature range | Ahmet Faruk ÖZDEMİR |

# INVITED SPEAKERS

**Recent Advances in Photovoltaic Technologies**

Prof. Dr. Raşit Turan
Middle East Technical University - Center for Solar Energy Research and Applications (ODTÜ-GÜNAM),
Dumlupınar Blvrd no : 1 06800 Ankara, Turkey
E-mail: turanr@metu.edu.tr

Crystalline Si photovoltaic (PV) solar cell has reached an extremely well maturity level with well-optimized material and process conditions. It is overwhelmingly dominating the commercial PV market today with a share exceeding 95%. It is generally expected that Si PV will continue to dominate the PV industry in the coming years. Like in microelectronic where Si crystal is the main and untouchable material, Si crystal will play a central role in the energy conversion technologies in the years ahead. Also a breakthrough technology based on perovskite solar cell has been developed recently and attracted a huge attention.

The conversion efficiency limit reachable with single junction Si solar cell, called Shockley–Queisser limit, is calculated to be around %30. Today, the world record realized at R&D level is already 26.7%, whereas at the industrial production lines, maximum cell efficiencies have reached 23-25 % range. Although the gap between theoretical limit and the technological achievement has narrowed down to a few percent, for an ultimate victory of solar energy over the other energy resources, efforts are still underway with new approaches to reduce cost/performance ratio even further. The performance of a solar cell, which is usually expressed in terms of the conversion efficiency, can be improved by reducing the electrical and optical losses through new material and process approaches. New c-Si PV cell architectures called TOPCon, IBC, SHJ been have been demonstrated with higher efficiency values. Also, solar cells with more than one junction made of different materials, namely, tandem solar cells have been shown to be very promising structure for future high efficiency devices. In this presentation, the current status of the PV technology and its status worldwide and future perspectives will be summarized.

The Centre for Solar Energy Research and Applications, ODTÜ-GÜNAM, was founded in 2009 and has quickly become one of the leading solar research institutes in Turkey and Europe. Starting from 2021, ODTÜ-GÜNAM has been spun off from the university and become an independent national research center Its infrastructure offers researchers an excellent working place for state-of-the-art research activities. Activities of ODTÜ-GÜNAM, its achievements and its road map in the following years will also be presented.

**Introduction to the KS R&D Center and Project Examples**

K.Kayacı[1*]

[1] *Kaleseramik Çanakkale Kalebodur Seramik Sanayi A.Ş., KS AR-GE Merkezi Çanakkale-Çan/ TURKEY*

[*]**Corresponding E-mail:** kagankayaci@kale.com.tr

Kaleseramik Research and Development Center is a research center established in April 2012 with the support of the Ministry of Industry and Technology of the Republic of Turkey under Law No. 5746. The Center is organized to meet the expectations of the Ministry of Industry and Technology and Kale Group and continues to work on a project basis with a team of 55 researchers. The projects are managed by a project management module called R&D Log. All researchers can use this module to manage their projects quickly and easily. All research projects are defined at the end of the Steering Committee and Tascom meetings. On average, 25–35 project activities are carried out each year. Tubitak, SAYEM, and EU projects are carefully monitored by our Project Management Office, and we quickly apply for appropriate calls. Sustainability projects, nano-digital effect and ink development projects, raw material research projects, cost-quality and efficiency projects, and technology development projects are the priority areas of our KS R&D Center.

**Recent Advances in Zinc Oxide-Based Dye-Sensitized Solar Cells**

Yasemin Caglar*

*Eskisehir Technical University, Department of Physics, Yunusemre Campus, Eskisehir, 26480 TURKEY*

***Corresponding E-mail:** yasemincaglar@eskisehir.edu.tr

The global increase in energy consumption is closely tied to population growth and rising wealth. As of 2022, world energy demand stands at 25.5 terawatts, which is anticipated to continue its upward trajectory. Post-pandemic recovery is expected to boost energy consumption, with a projected growth of 1.8% in 2024, compared to 1.2% in 2023. This expansion will be driven by robust demand in Asia, particularly a 3.1% increase, despite uncertainties surrounding China's economic outlook. Renewable energy is poised for significant growth in 2024, with combined solar and wind energy consumption projected to increase by approximately 11% annually. Capacity additions are set to reach a record high of around 400 GW in 2023, continuing to rise in 2024. The escalating energy demand, depletion of oil resources, and concerns about global warming underscore the need for clean and renewable energy technologies. Among various sustainable energy options like tidal power, solar thermal, hydropower, and biomass, photovoltaic technology utilizing solar energy is considered the most efficient. Solar energy, particularly through photovoltaic cells converting photons to electrons, is recognized as a clean and low-carbon energy source. Over the last three decades, dye-sensitized solar cells (DSSCs) have gained significant attention due to their simple preparation, cost-effectiveness, ease of production, and low toxicity. Initial research involved the extraction of chlorophyll from spinach at the University of California, Berkeley, leading to the synthesis of the first chlorophyll-sensitized ZnO electrode in 1972. Although ZnO-single crystals were initially explored, the efficiency of DSSCs was limited. Improvements were achieved by optimizing the porosity of the electrode made from fine oxide powder, enhancing dye absorption, and subsequently improving light harvesting efficiency. A typical DSSC comprises a photoanode, a sensitizer (dye), an electrolyte, and a counter electrode. The photoanode semiconductors, such as $TiO_2$, ZnO, or $SnO_2$, facilitate dye adsorption, accept electrons from the excited dye, and conduct them to generate an electric current. Among these semiconductors, $TiO_2$ has been widely used, but recent studies highlight ZnO as a potential replacement due to its comparable physical properties and higher electron mobility. ZnO's superior electron mobility contributes to increased charge separation and enhanced device performance, crucial for optoelectronic and photovoltaic devices. Recent advancements in ZnO-based nanoparticles, composites, and modified materials are explored for applications in energy storage, conversion devices, and biological applications. In this invited talk, we discuss the numerous studies conducted by researchers in the last decade to modify ZnO photoanodes and their progress. We also look at different types of nanostructures, such as fabrication methods, doping, nanocomposites, and deposition parameters, that improve the efficiency of ZnO-DSSCs.

**New electrode material design for energy storage systems**

M.Ates[1*]

[1] *Tekirdag Namik Kemal University, Department of Chemistry, Tekirdag, 59030 TURKEY*
[*]**Corresponding email:** mates@nku.edu.tr

New electrode design is very important to obtain high electrochemical performance of energy storage systems such as supercapacitors and batteries. Electrochemical energy storage systems have some superior properties, such as fast charging and discharging capability, high energy density, long-term stability, etc. In addition, they have been used in various applications, such as wind power stations, electric or hybrid electric products, etc. There are many electroactive materials used in energy storage technology. The most used electroactive materials are inorganic and organic materials. These materials are inserted into flexible matrixes. These are including mainly carbonaceous materials, such as carbon foam,carbon-basedn based-cloth, etc. and metal based (Cu, Ni foams, etc) have been used as a host for cathode and anode materials.

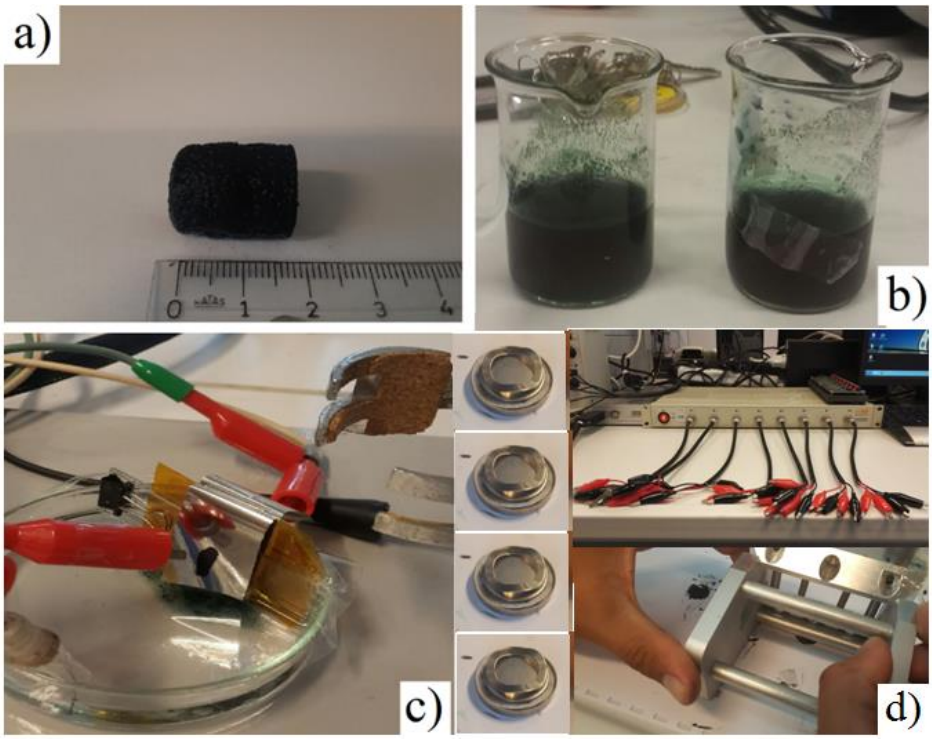


Fig.1. a) Graphene hydrogel (GH), b) GH/Polyaniline (PANI) composite c) GH/PANI electrode designed in symmetrical supercapacitor in two electrode system, d) CR2032 coin cell preparation and cell measurements.

**Scale-up Production of Polymer Fibers for Drug Delivery**

Attila Levente GERGELY[1*]

[1] *The Sapientia Hungarian University of Transylvania, Department of Mechanical Engineering, Targu Mures, 540485* ROMANIA

[*]**Corresponding E-mail:** agergely@ms.sapientia.ro

Recently, nanofibers have garnered significant attention across various applications owing to their nanometer-scale size and impressive surface-to-volume ratio. Notably, fiber-based drug delivery systems have emerged, aiming either for localized, sustained drug release or for improving the bioavailability and solubility of drugs with low solubility. Electrospinning has emerged as the preferred method for nanofiber fabrication due to its cost-effectiveness and relatively straightforward setup. This technique utilizes an electric field to spin nanofibers from a polymer solution, with the solvent evaporating during the process, leaving behind dry fibers on a collector. Despite its advantages, electrospinning also has drawbacks, notably its low production rate, which hampers its scalability for industrial applications. This study introduces three methods to address this limitation: disc- and corona electrospinning, and centrifugal spinning. Additionally, the data presented lays the groundwork for exploring centrifugal spinning as a promising approach for producing drug-loaded fiber-based amorphous solid dispersions.

**Keywords:** polimer nanofibers, electrospinning, centrifugal spinning, drug delivery system.

**Electrospun nanofibers: Promising nanoscale structures in nanobiotechnology**

Dilek Odaci[1*]

[1] *Ege University, Faculty of Science, Department of Biochemistry, Izmir, 35100 TURKEY*
[*]**Corresponding E-mail:** dilekodaci.od@gmail.com

Electrospinning is a very economical and efficient technique for obtaining excellent features of electrospun nanofibers (ESNFs) from many types of natural and synthetic polymer. ESNFs can be used in various applications such as biomedical, drug delivery system, environmental, water treatment (affinity membranes), electromagnetic interference (EMI) shielding, industrial applications such as food packaging, energy storage/conversion, and sensors with their high surface area and porosity properties [1]. Additionally, ESNFs are flexible nanomaterials suitable for catalysts in electrodes. Notably, ESNFs are among the promising nanomaterials for sensor applications due to their huge surface areas. ESNFs can be produced with different structures such as spring/helical ESNFs, porous ESNFs, core–shell ESNFs, hollow electro-spun fibers, and triaxial ESNFs. ESNFs can serve as an immobilization matrix to create a biofunctional surface. Combining electrospinning with novel materials may benefit the production of smart fibers that respond to pH, light, electric field, and magnetic field using responsive polymers. Furthermore, the highly porous structure of nanofibers supplies advanced catalytic efficiency due to low mass transfer resistance. ESNFs in biosensor systems have many advantages; including adjustable size (micro to nano), a large surface area, biocompatibility, suitability as a good immobilization matrix, cost-effectiveness, and the ability to be decorated with other nanomaterials [2]. Here, a description of nanomaterials such as nanofibers, dendrimers, carbon nanotubes, graphene, gold nanoparticles, and their applications in biotechnology will be provided.

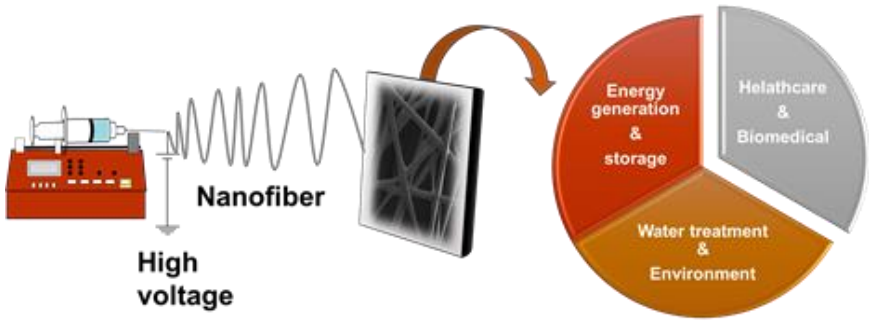


Fig.1. Schematic illustration of electrospinning and examples for applications of ESNFs [1].

References

[1] N.M. Kilic, S.S. Gelen, S.E. Zeybekler, D. Odaci, ACS Omega 2024, 9, 1, 3–15.

[2] N.M. Kilic, S. Singh, G. Keles, S. Cinti, S. Kurbanoglu, D. Odaci, Biosensors 2023, 13(6), 622.

**Functional Metal/Semicoductor Devices for Organic Electronic Applications**

Şemsettin ALTINDAL

*Department of Physics, Faculty of Science, Gazi University, Ankara-Türkiye*
***Corresponding E-mail:** altundal@gazi.edu.tr

In this study, (Zn:Cd:Ni:$TiO_2$) and (CdO:ZnO:NiO:Ti) with different ratios quaternary alloy was used as interlayer instead of traditional insulator between metal (Al) and semiconductor (p-Si). These functional interlayers were deposited onto p-Si wafer by using spin coater method to develop new type diodes/structures. Some important electric parameters of them such barrier height, ideality factor (n), reverse-saturation current, rectification-ratio ($I_{forward}/I_{reverse}$) at a certain voltage, series/shunt-resistances ($R_s/R_{sh}$) were calculated from the current-voltage (I-V) measurements. Energy dependent profiles of surface-sates ($N_{ss}$) were also obtained using I-V data by considered voltage dependence of n and BH for each diode. The other some important electrical parameters such as doping acceptor atoms (Na) into semiconductor, BH, Rs, and Nss were calculated the (capacitance/conductance)-voltage (C/G-V) measurements at 1 MHz. The comparison of all the experimental results suggests that the prepared Al/p-Si structure with (Zn:Cd:Ni:$TiO_2$) and (4:2:2:2) ratios has the best performance in terms of low leakage/saturated current, n, $N_{ss}$ and hig RR, BH and so it can be successfully used instead of conventional metal-insulator-semiconductor (MIS) type structures in electronic and optic applications.

**Keywords:** Functional metal/semiconductor devices; Basic electrical properties; Energy dependent profile of surface states; Current transport mechanisms

# ORAL PRESENTATIONS

**Evaluation of the potential of ammonium borane as a hydrogen storage material**

C.Can[1*], M.Kamislioglu[2,3*], B.Buyuk[4*]

*[1]Bandırma Onyedi Eylül University, Department of Alternative Energy Sources PhD Program, Bandırma, 10200 TURKEY*
*[2]National Boron Research Institue (BOREN), Ankara, 06530 TURKEY*
*[3]Bandırma Onyedi Eylül University Department of Medical Imaging, Vocational School of Health Services, Bandırma, 10200 TURKEY*
*[4]Bandirma Onyedi Eylül University, Faculty of Engineering and Natural Sciences, Bandırma, 10200 TURKEY*

**[*]Corresponding E-mail:** canan.can92@hotmail.com

**ABSTRACT**

Most of the countries need different energy sources for their increasing populations due to the fact that fossil fuels are both limited in terms of reserves and cause high carbon emissions that cause global warming. As a result of scientific studies carried out worldwide in recent years, it has been determined that boron minerals and boron technologies developed accordingly constitute an alternative to fossil fuels. While boron minerals alone are widely used, the technologies created with boron derivatives today enable hydrogen conversion and nuclear fusion production, which are shown as the energy source of the future. However, it is widely recognised that the controlled storage and release of hydrogen is the biggest obstacle to the large-scale implementation of hydrogen energy. Boron hydride compounds have recently come to the fore as an energy source for hydrogen production and storage. Ammonium borane ($NH_3BH_3$, AB) has been recognised as an ideal hydrogen storage material for portable hydrogen production due to its high hydrogen content (19.6 wt%), non-toxicity, stability under ambient conditions and excellent hydration and dehydration properties. Ammonium borane methanolysis technology seems to be the safest, effective and suitable technology route for portable hydrogen production applications due to its mild reaction conditions and low temperature suitability. The synthesis of ammonium borane using efficient and cheaper boron compounds and the use of cheap catalysts in the dehydrogenation process enables the production of hydrogen with a lower cost production process, increasing its usability as hydrogen storage material and contributing to the hydrogen economy. Ammonium borane was investigated from a fundamental point of view when it was first discovered and its possible use in laser-induced nuclear fusion was predicted. In the 21st century, it was considered mainly suitable for chemical hydrogen storage and studies are still continuing. In this study, in order to advance the practical use of ammonium borane, which is a hydrogen energy storage material, a prediction for future expectations was created by drawing attention to the structure, properties, synthesis and dehydrogenation processes of ammonium borane.

*Keywords: Ammonium borane, hydrogen storage, boron minerals*

**On the Impact of Pure PVC and (Ti-doped PVC) Interlayer on the Performance Metal-Semiconductor (MS) Schottky diodes (SDs) in Wide Voltage Range ± 2.5V**

Çiğdem Şükriye Güçlü[1*]

[1] *Department of Physics, Faculty of Science, Gazi University, 06500 Ankara, Turkey*

[*]**Corresponding E-mail:** cigdemguclu@gazi.edu.tr

The aim of this study is to determine the impacts of pure PVC and (Ti-doped PVC) interlayer on the performance Au/n-Si (MS) SDs. For this purpose, MS, MPS1 (Au/PVC/n-Si) and MPS2 (Au/(Ti:PVC)/n-Si) were grown on the same n-Si wafer under the same conditions. XRD, SEM and energy dispersive (EDX) techniques were applied to the prepared tin interlayers. By means of the Debye-Scherrer formula, the average size of the crystallites was estimated to be 31 nm. The basic electrical parameters of the MS, MPS1, and MPS2 type SDs were obtained based on Thermionic-emission (TE) model, modified-Norde, and Cheung functions by using the forward bias $I_F$-$V_F$ measurements and they were compared with each other. The energy-dependent distribution of the surface states ($N_{ss}$) of these were also obtained and compared with each other. Experimental results show that the use of PVC and (Ti:PVC) interlayer leads to increased performance of MS SD in terms of lower values of ideal factor (n), leakage current, Nss, and higher values of barrier height (BH), rectifying ratio (RR).

**Keywords:** Schottky diodes with/without PVC and (Ti:PVC) interlayer; Series resistance and surface states; Basic electrical parameters; TE, Norde, and Cheung models

**Acknowledgement**: This study was supported by Scientific and Technological Research Council of Türkiye (TÜBİTAK) with the research project number 121C396.

**Synthesis and Characterization of Functionalized Nanoparticles for Enhanced Enzyme-Free Glucose Sensing in Biosensors**

Merve Kucukoflaz Korkmaz[1], Rümeysa Kisi[1], Mehtap Ceyran[1], Serkan Dayan [*1,2]

[1] *Drug Application and Research Center, Molecular Synthesis & Industrial Application Research Laboratory (MSIA-Lab), Erciyes University, 38039 Kayseri, Turkey.*
[2] Faculty of Pharmacy, Department of Pharmaceutical Basic Sciences, Kayseri, Turkey.

[*]**Corresponding E-mai:** serkandayan@erciyes.edu.tr

Biosensors, in which biological sensors and physical transducers are integrated, are used to detect signals at different analyte concentrations. Research focuses on electrochemical biosensors as well as enzymatic and enzyme-free biosensors, whose applications include the detection of hormones, glucose, and DNA/RNA [1]. The integration of nanomaterials such as graphene oxide (GO) and reduced graphene oxide (rGO) into biosensors is currently being investigated to increase the surface area and adsorption of analytes [2]. L-arginine, which is considered a therapeutic dietary supplement, plays a crucial role as a protein precursor in the body. Among other things, it contributes to ammonia degradation, wound healing and increasing blood flow by stimulating nitric oxide production [3].

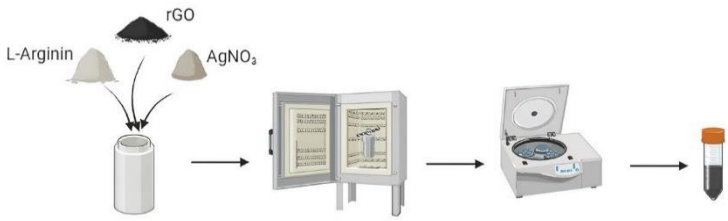


Figure 1. Synthesis of rGO@L-arginine/Ag nanomaterial.

This study involves the synthesis of rGO@L-arginine/Ag nanomaterials by a hydrothermal method (Figure 1). The characterization of the synthesised nanomaterial was carried out using field emission scanning electron microscopy, elemental mapping, energy dispersive X-ray analysis and Fourier transform infrared spectroscopy. This comprehensive analysis aims to elucidate the structural and chemical properties of the synthesised nanomaterials and provide insights into their potential applications, particularly in biosensing.

1. Amor-Gutiérrez, O., et al., *Bioelectroanalysis in a drop: Construction of a glucose biosensor.* Journal of Chemical Education, 2017. **94**(6): p. 806-812.
2. Rahsepar, M., F. Foroughi, and H. Kim, *A new enzyme-free biosensor based on nitrogen-doped graphene with high sensing performance for electrochemical detection of glucose at biological pH value.* Sensors and Actuators B: Chemical, 2019. **282**: p. 322-330.
3. Verma, N., A.K. Singh, and M. Singh, L-arginine biosensors: A comprehensive review. Biochemistry and biophysics reports, 2017. 12: p. 228-239..

# A Computational Study On The Sensing Of Nitro-Containing Explosive Materials

M. Erdem Sözbir [1], Berkay Sütay [1] *

[1] *Istanbul Technical University, Department of Chemistry, Istanbul, 34485 TURKEY*

ABSTRACT

Detection of nitro-based explosives has become a rising priority in recent years in homeland and border security. There is a need for fast and reliable new generation sensors with high power, low cost and portable usage in order to detect possible threats like monitoring the mentioned environments and detecting hidden explosive devices. In this study, the methods computational chemistry were used to reduce human involvement in enhancing the detection of mines in hazardous areas where landmines cannot be safely removed. What is aimed to achieve through these calculations is to explore the molecular-scale detection mechanism of explosives and to assess their compatibility with newly developed polymeric materials, particularly focusing on nitroaromatics and nitramines like RDX, HMX, etc. This investigation is crucial due to the challenges posed by the low vapor pressures of these explosives. In the present study, Super-yellow polymer was used as the target system. All computations were conducted using density functional theory (DFT) at the B3LYP/6-31G(d,p) level. These calculations were executed utilizing resources provided by the ITU National Center for High Performance Computing (ITU UHeM). The detection mechanism was examined in terms of the intermolecular interaction energies, including basis set superposition error (BSSE) and zero-point energy (ZPE) corrections, and theoretical fluorescence spectra of target/explosive molecular complexes. Theoretical results were found in agreement with the experimental data for 2,4-DNT explosive. Theoretical predictions have also been reported regarding the detection of certain explosives where experimental data are lacking. The outcomes of this *a priori* study can provide a substantial amount of time saving and financial gain against the experimental fieldwork.

*Keywords: : explosive, preconcentration, fluorescence quenching, density functional method*

Corresponding author: Berkay Sütay (sutay@itu.edu.tr)

## 1. Introduction

The identification of chemicals associated with explosives has become an increasingly important focus in homeland and border security in recent years. Detecting nitroaromatic, nitramine, or nitro explosive compounds can pose significant challenges, particularly when the target analyte is present in trace amounts in the open air. Explosives typically contain both oxidizing and reducing groups within their chemical structures. These substances commonly have nitro, peroxo, azide, etc groups, which make them reactive, biologically active and hazardous to living species (Bener et.al. (2022), Jiao et.al. (2022), Santiwat et.al. (2023)). The current investigation delves into two distinct processes involved in explosive detection studies, each presenting its own unique challenges. These processes, namely "sample collection" and "detection" mechanisms, are discussed separately, considering their individual characteristics and difficulties. In this direction, the noncovalent complexes of ten different explosive molecules with Aflas and Super yellow systems were modeled with density fucntional theory (DFT) which reveal the relevant quenching via the intermolecular forces such as hydrogen bond, π-π and or CH/π interaction, etc.

The sampling process involves collecting air from the vicinity of a potential mine into a polymer. The collected sample is then labeled and sent to specialized centers off-site, where trained sniffer dogs are employed to detect the presence of explosives. This determination is made before sending operatives back to the field. However, it is a slow and costly procedure. Therefore, there is a powerful need in alternative methods both to collect samples across explosive-suspected field without wandering the field, and to detect sensitively any sampled explosive residues, as fast as posible (Gillanders et al., 2017, 2019; Glackin et al., 2020, Gillanders et al. (2021)). Luminescent organic semiconductor films

have been attracting a high level of attention in recent years as explosive vapour sensing films. Super yellow polymeric system was used in the present study, Figure 1. Aflas polymer is used in this study to accumulate explosive vapours to the surface, based on the hydrogen bond acidity between polymer and target vapour, Figure 2.

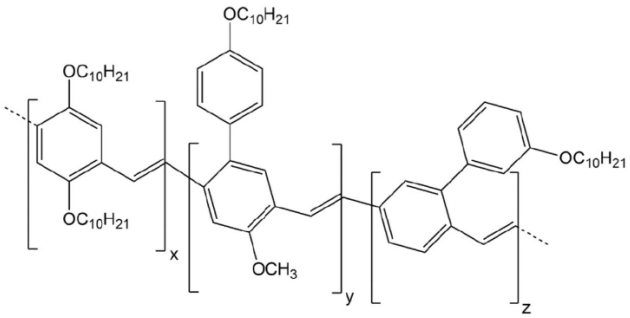


***Figure 1**. Super Yellow.*

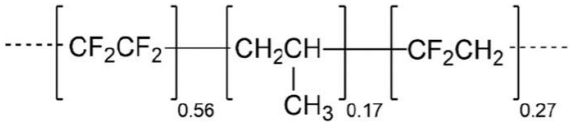


***Figure 2**. Aflas polymer*.

**2. Computational details**

Gas-phase geometry optimizations were conducted for noncovalent complexes of explosive molecules with Aflas and Super Yellow systems using the DFT method employing the M06-2X functional with a 6-31G(d,p) basis set. All computations were executed within Gaussian '16 program. Interaction energies were computed for all optimized structures to quantitatively interpret inter- and intramolecular hydrogen bonds, with consideration given to the basis set superposition error in all calculations. Additionally, interaction energies were corrected for zero-point energy. TD-DFT calculations were carried out for the most thermodynamically stable explosive-Super Yellow complexes to examine changes in emission and absorption spectra concerning fluorescence quenching.

**3. Results and discussion**

The molecular interaction of 2,4-DNT and TNT explosives with Aflas system was shown in Figure 3 and 4.

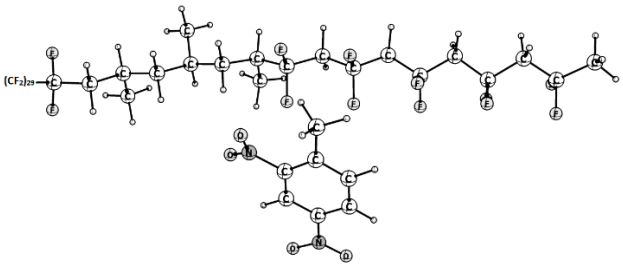

***Figure 3.** Aflas+2,4-DNT complex.*

The interaction energy of Aflas+2,4-DNT complex was found in the order of -7 kcal/mol.

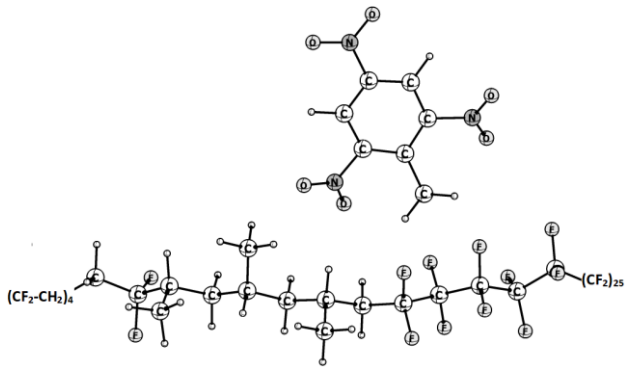


***Figure 4.*** *Aflas+TNT complex.*

The interaction energy of Aflas+TNT complex corresponding to the lowest energy structure was found to be -9 kcal/mol. The hydrogens of both Aflas and TNT molecules lie in a proper distance in the range to form typical classical hydrogen bonds. The methyl groups on Aflas are in attraction with nitro groups of the explosive and the fluorine atoms attract to the methyl hydrogens of TNT.

The most stable 2,4-DNT and TNT complexes of super-yellow molecule were shown in Figure 5 and 6.

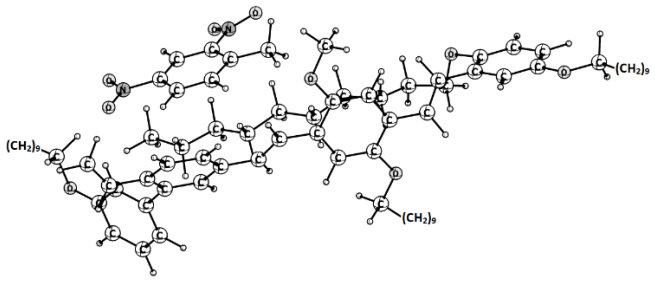


***Figure 5.*** *The lowest energy configuration of SY+2,4-DNT complex.*

The SY+2,4-DNT complex has an interaction energy in the order of -15 kcal/mol. The C-H bond lengths of SY molecule in the interaction site with the explosive molecule increased which indicates the presence of hydrogen bonds. In addition, the π electrons of the aromatic ring in 2,4-DNT interact with the hydrogens of the oligomeric chains of super-yellow molecule and affects on the C-H bond length of the related hydrogen donor. That indicates the presence of CH/π aromatic hydrogen bond interaction.

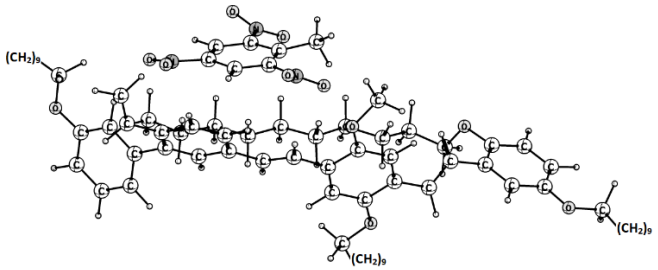


***Figure 6***. *The lowest energy configuration of SY+TNT complex.*

The SY+TNT complex has an interaction energy in the order of -15 kcal/mol.

In order to explain the quenching mechanism of the emission of super yellow in the presence of an explosive was also shown, Figure 7.

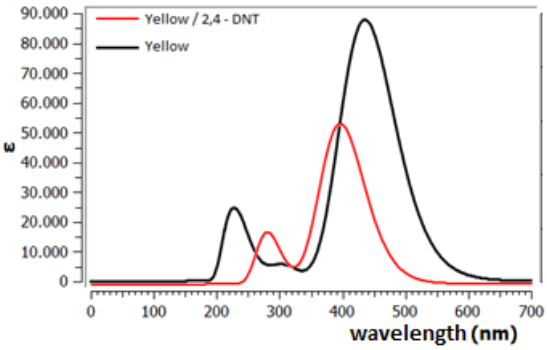


***Figure 7.*** *The fluorescence spectrum of superyellow w/o 2,4-DNT.*

The fluorescence quenching of SY in the presence of 2,4-DNT was found to be 40 percent.

**4. Conclusion**

The present study focused on examining noncovalent molecular complexes formed by various nitroaromatic, nitramine, and nitro-type explosive molecules with Aflas and Super Yellow systems. The strength of the interaction of super yellow complexes was predicted in decreasing order as follows (including BSSE and ZPE corrections): TNP ~ RDX > 2,6-DNT > TNT > 2,4-DNT. When we consider the quenching ratios in the emission spectra of the complexes, the following trend has been predicted upon increasing order of quenching: 2,6-DNT < RDX < TNP < TNT < 2,4-DNT. The results of this study constitutes a strong argument that Super yellow can be used as a target for a variety of explosives as well. In particular, the fact that each explosive has a different quenching percentage and emission shift in the fluorescence spectrum which is very important in terms of its potential to offer a plausible approach to the segregation problems experienced in explosive detection.

This study investigated the factors directly influencing the interaction between the polymer and analyte, as well as the distinctive quenching process. It examined structural parameters of the target including pore size, molecular internal volume, and collisional diameter, along with the molecular interactions of target-analyte systems. The necessary information has been obtained to assist in the determination of standard features, for future studies and applications on this field.

**5. Acknowledgement**

Computing resources used in this work were provided by the National Center for High Performance Computing (UHeM) under grant number 1010722021.

**References:**

[1] Bener, M.; Burak Şen, F.; Apak, R., 2022. Protamine gold nanoclusters – based fluorescence turn-on sensor for rapid determination of trinitrotoluene (TNT). Spectrochim. Acta, Part A, 279, No. 121462.

[2] Jiao, X.; Marin, L.; Cheng, X., 2022. Fluorescent cellulose/testing paper for the sensitive and selective recognition of explosives 2,4,6-trinitrophenol and 2,4-dinitrophenylhydrazin. J. Photochem. Photobiol. A, 424, No. 113632.

[3] Santiwat, T.; Sornkaew, N.; Srikittiwanna, K.; Sukwattanasinitt, M.; Niamnont, N., 2023. Electrospin nanofiber sheets mixed with a novel triphenylamine-pyrenyl salicylic acid fluorophore for the selective detection of picric acid. J. Photochem. Photobiol., A, 434, No. 114258.

[4] Gillanders, R.N., Samuel, I. D. W., Turnbull, G. A., 2017. A low-cost, portable optical explosive-vapour sensor," Sens Actuators B Chem, vol. 245, pp. 334–340.

[5] Gillanders, R. N., Glackin, J. M. E., Filipi, J., Kezic, N., Samuel, I. D. W., Turnbull, G. A., 2019. Preconcentration techniques for trace explosive sensing, Science of the Total Environment, vol. 658, pp. 650–658.

[6] Glackin, J. M. E., Gillanders, R. N., Eriksson, F., Fjallgren, M., Engblom, J., Mohammed, S., Samuel, I. D. W., Turnbull, G. A., 2020. Explosives detection by swabbing for improvised explosive devices, Analyst, vol. 145, no. 24, pp. 7956–7963.

[7] Gillanders, R. N., Glackin, J. M. E., Babic, Z., Mustra, M., Simic, M., Kezic, N., Turnbull, G. A., Filipi, J., 2021. Biomonitoring for wide area surveying in landmine detection using honeybees and optical sensing, Chemosphere, vol. 273.

**W and F co-doped SnO2 Films deposited by Ultrasonic Spray Pyrolysis**

İ Gunes[1], E. Sarica[2*], M. Terlemezoglu[3], H. B. Ozcan[4], İ. Akyuz[5],

[1]Canakkale Onsekiz Mart University, Department of Electricity and Energy, Canakkale, 17200, Turkey
[2]Baskent University, Department of Electrical and Electronics Engineering, Ankara, 06790, Turkey
[3]Gazi University, Department of Physics, Ankara, 06500, Turkey
[4]Bursa Technical University, Department of Physics, Bursa, 16310, Turkey
[5]Eskisehir Osmangazi University, Department of Physics, Eskisehir, 26040, Turkey

[*]**Corresponding E-mail:** emrahsarica@baskent.edu.tr

Tin oxide films ($SnO_2$) are frequently used in various applications. Their wide band gap (>3.6 eV) and high optical transparency, coupled with chemical stability and inertness, make them resistant to corrosion and degradation in harsh environments. Additionally, their stability at high temperatures is another important advantage. These key features make SnO2 films technologically important. In this study, $SnO_2$ films co-doped with F and W were deposited on Corning Eagle XG glass substrates using the user-friendly ultrasonic spray pyrolysis technique, and the changes in their physical properties were examined. High optical transparency (>80%) and low resistivity ($\rho = 8.5 \times 10^{-4}$ Ωcm) were achieved by 30% F and 7% W doping.

Keywords: $SnO_2$ thin films, co-doping, ultrasonic spray pyrolysis, transparent conductive oxides

This study was supported by Scientific and Technological Research Council of Turkey (TUBITAK) under the Grant Number 121F025. The authors thank to TUBITAK for their supports.

**Characterization and Potential of ITO/ZnO/CuO Heterostructures for Photovoltaic Applications**

I.Gunes[1*]

[1] *Canakkale Onsekiz Mart University, Department of Electricity and Energy, Canakkale, 17200, TURKEY*

[*]**Corresponding E-mail:** ibrahimgunes@comu.edu.tr

Copper oxide (CuO), recognized as a non-toxic, p-type metal oxide semiconductor, is distinguished by its suitability for photovoltaic applications, owing to its adjustable band gap ranging from 1.3 to 2.1 eV and a high absorption coefficient of approximately $10^5$ $cm^{-1}$. In this study, to examine the properties of CuO films and reveal the potential of the ITO/ZnO/CuO heterostructures, the CuO layer was deposited onto ITO-coated glass substrates at varying spray durations of 15, 20, and 25 minutes. Structural analyses confirm the successful formation of this heterostructure. Optical transmittance and absorption spectra indicated that the absorption edges for ZnO and CuO are approximately 380 nm and 800 nm, respectively. Furthermore, Hall effect measurements verified the n-type conductivity of ZnO and p-type conductivity of CuO in the deposited layers.

***Keywords:*** *CuO films;* Heterostructures, *Ultrasonic spray pyrolysis; Optical and electrical properties.*

**BET surface area and TGA analyzes of some transition metal oxides used in supercapacitors**

O. YORUK[1,*], M. ATES[2,*], Y. BAYRAK[1]

[1] *Trakya University, Department of Chemist, Edirne, 22030 TURKEY*
[2]*Tekirdag Namik Kemal University, Department of Chemistry, Tekirdag, TURKEY.*

[*]**Corresponding E-mails:** ozanyoruk@trakya.edu.tr; mates@nku.edu.tr

Supercapacitors are widely used in energy storage systems today due to their many superior features such as fast charge- discharge, stable cycle life, safe and higher columbic efficiencies. There are three types of supercapacitors: double layer supercapacitors, pseudo supercapacitors, and hybrid supercapacitors consisting of the combination of double layer supercapacitors and pseudo supercapacitors. The electroactive materials used in pseudo supercapacitors are transition metal oxides (NiO, $TiO_2$, $RuO_2$, CuO vb.) and conductive polimers(PANI, Pyrrole, PEDOT etc.). In this study, BET surface area parameters and Thermo Gravimetric analysis (TGA) effects of some transition metal oxides were examined on electrochemical performances of supercapacitors. Moreover, electrode material is critical important on specific capacitance, energy and power densities, etc. Therefore, TGA-DTA analysis of these materials were examined to understand thermal behavior effects on durability and cycle life of supercapacitor devices.

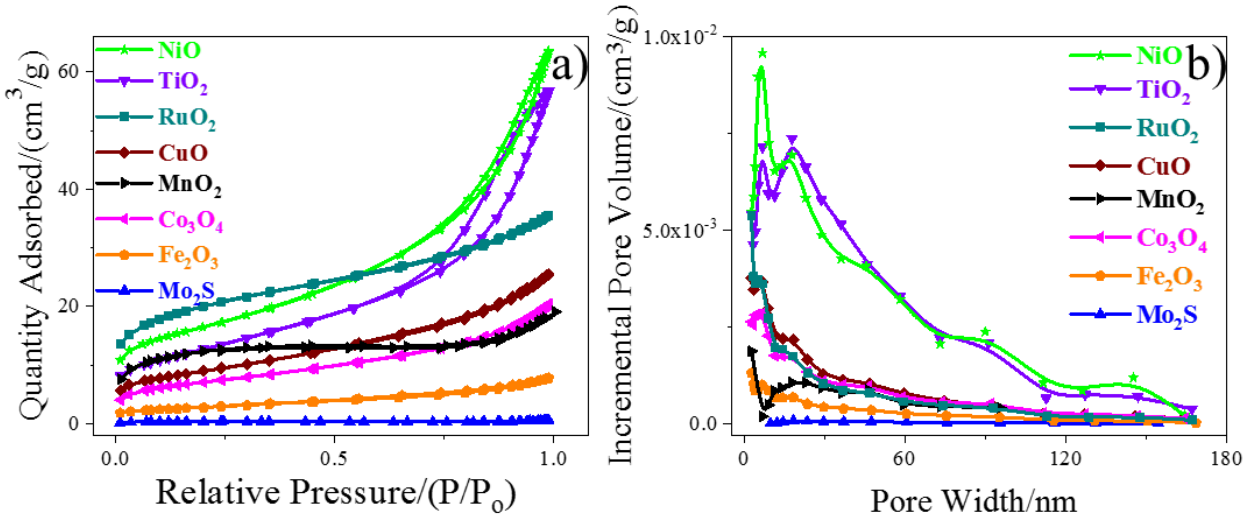


Fig.1. BET analysis of some metal oxides, a)Nitrogen adsoption-desorption izoterms and b) Pore size distrubition curves of metal oxides.

**Metal-polymer composites via wet-chemistry method**

M. Kucukoflaz Korkmaz[1, *], K. Sahin Tiras[2], H. Bulduk Karakaya[1], Serkan Dayan [1,3]

[1] Erciyes University, Drug Application and Research Center, Molecular Synthesis & Industrial Application Research Laboratory, Kayseri, 38039, *Türkiye*

[2] *Erciyes University, Department of Physics, Kayseri, 38280, Türkiye*

[3] Erciyes University, Faculty of Pharmacy, Basic Pharmaceutical Sciences, Kayseri, 38280, *Türkiye*

[*]**Corresponding E-mail:** kucukoflazmerve@gmail.com

With the advancement of nanotechnology, a variety of nanostructure materials have been created by arranging nanosized particles into ordered shapes. These materials have generated a great deal of interest because of their numerous distinctive optical, electrical, magnetic, and catalytic capabilities. In this work, composite materials were studied because they have special physical and biological features and can be created by coating and depositing metal nanoparticles on polymers. Metal nanoparticles are frequently surface modified during the production process to improve their stability in solution. These alterations allow stable metal nanoparticles to exhibit a variety of surface properties, including electric charge, hydrophilic/hydrophobic, etc. Metal-polymer composites can be produced by these specific and controlled modifications of metal particles. Wet-chemistry method was used to create nanoparticles-coated composites. Optical and morphological characterizations of the composites were evaluated.

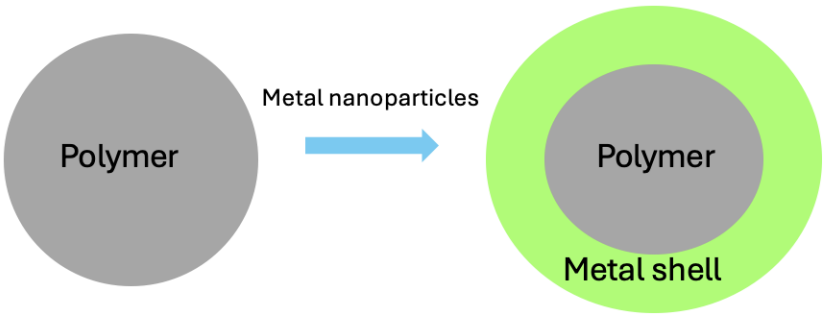


Fig.1. Metal nanoparticles coated polymer.

**Novel Poly(vinylidene Fluoride)-Baghdadite-Based Composite Membranes as Bone Scaffolds**

B.Mutlu[1,2*], F.Demirci[3], Ş. Duman[1]

[1]*Bursa Technical University, Department of Metallurgical and Materials Engineering, Bursa, TURKEY*
[2]*Bursa Technical University, Central Research Laboratory, Bursa, TURKEY*
[3]*Bursa Technical University, Department of Polymer Materials Engineering, Bursa, TURKEY*

[*]**Corresponding E-mail:** busra.bulut@btu.edu.tr

Poly(vinylidene fluoride) (PVDF) is attracting significant interest due to its exceptional properties such as high biocompatibility, thermal stability, ease of processing, and superior electroactivity, which open up a wide range of potential applications. Bagdadite (Ca3ZrSi2O9) (BAG), incorporated into the matrix to enhance the properties of the polymer, is preferred in bone regeneration for its excellent bioactivity, favorable absorption and high biological performance through the release of Ca, Si and Zr ions. This study presents the characterization of PVDF-BAG membrane scaffolds, developed using the non-solvent induced phase separation technique, as support materials. The results demonstrate that the produced scaffolds have interconnected cross-sectional pores and adequate pore size. The incorporation of BAG into the PVDF matrix improves the hydrophilicity while reducing the degree of swelling of the scaffolds. Mechanical tests show that the scaffolds closely resemble native bone, exhibiting good tensile strength and elongation at break properties. Additionally, the scaffolds possess a semi-crystalline structure with a significant fraction of the PVDF β-phase. Moreover, the scaffolds significantly enhance biactivity, cell viability and proliferation without exhibiting cytotoxic effects. These results suggest that the novel composite membrane scaffolds could potentially serve replacements in bone repair.

**Keywords:** polyvinylidene fluoride, bagdadite, membrane scaffold, bone regeneration.

**N-Doped Interlayer Effects On Dielectric Properties In Diamond SBDs By Impedance Measurements**

N.Urgun[1*], A.Feizollahi Vahid[2], B.Avar[3], S.O.Tan[4], Ş.Altındal[5]

[1] *Department of Mechatronics Engineering, Faculty of Engineering, Karabük University, Karabük, 78050, Turkey*
[2]*Department of Nanotechnology Engineering, Zonguldak Bülent Ecevit University, Zonguldak, 67100, Turkey*
[3]*Department of Metallurgy and Material Engineering Faculty of Science, Zonguldak Bülent Ecevit University, Zonguldak, 67100, Turkey*
[4]*Department of Electrical Engineering, Faculty of Technology, Karabük University, Karabük, 78050, Turkey*
[5]*Department of Physics, Faculty of Sciences, Gazi University, Ankara, 06500, Turkey*
[*]**Corresponding E-mail:** nuray1erkutlu@gmail.com

Interlayer usage has been a parameter adjuster in MIS devices for a long time. Since the passivation of unbalanced bonds between MS interfaces promotes the electric charge-storing properties due to the rising dielectric characteristics related with the polarization, this advantage of mid-layer effect can be employed to shape the device behaviors in desired working conditions. Moreover, the usage of impurities in semiconducting or dielectric materials also develops conduction properties in MS-based designs. So, the material and design preferences of MS devices can alter cost-effective switches. As a durable material, DLC films, which have been used in industry primarily for protective coatings, can help with the devices' barrier functions in MIS structures when used as an insulator layer. Besides, the electrical conductivity parameter can be changed when DLC films are doped. This study uses DLC film as an interlayer of an MIS SBD by N doping. Electrochemical deposition technic (ECD) is used to fabricate the studied structure. The capacitance-voltage (*C-V*) and the conductance-voltage (*G/ω-V*) measurements at 3 kHz and 1 MHz for -2.8 V to 3.8 V are utilized for dielectric parameter extraction by impedance spectroscopy. The parameter changes such as high dielectric constant $\varepsilon'$ above 400 at 3kHz, apparent peaks of complex electric modulus ($M^*$) and tangent loss ($tan\delta$) values in the depletion stage, distinct separation of conductive and non-conductive phases of working scales show that the fabricated structure has properties of a unique MIS capacitor. Additionally, the noticeable trend gaps in parameter values between high and low frequencies in the plots indicate that the employed diamond interlayer is effective within the designed MIS structure. The decreasing heat loss and rising ac conductivity by rising frequency show that the frequency successfully eliminates the surface states and series resistance effects while rising source voltage promotes both the carrier activity and losses related with rising conduction. The fabricated structure distinguishes itself by its high energy storage capacity and efficient switching mechanism compared to similar MIS structures produced by conventional interlayers.

**Keywords**: diamond SBD, interlayer effect, N-doping, MIS device

**Cosmic and Gamma Radiation Test of a Developed Secondary Emission Ionization Calorimetry Module**

Nejdet Paran[a,b,], Emrah Tiras[a,c,*], Burak Tekgun[b], Saleh Abubakar[a,*]

[a] *Department of Physics, Erciyes University, Kayseri, Türkiye, 38039*
[b] *Department of Electrical and Electronics Engineering, Abdullah Gül University, Kayseri, Türkiye, 38030*
[c] *Department of Physics and Astronomy, University of Iowa, Iowa City, Iowa, USA, 52241*

[*]**Corresponding E-mail:** salehbinabubakar@gmail.com and etiras@fnal.gov

Due to the increasing instantaneous luminosity and unprecedented radiation conditions at particle physics and high-energy physics accelerators, the demand for precision, robustness, and reliability in radiation-resistant particle detectors and ionization calorimeters remains significant. Secondary Emission (SE) Ionization Calorimetry is a new design technology that measures the energy of hadronic and electromagnetic particles, especially in high-radiation environments. In this study, we investigated the cosmic and gamma radiation test of a developed SE ionization calorimetry module. The modules were developed by modifying the conventional Hamamatsu single anode R7761 Photomultiplier Tubes (PMTs). Three distinct voltage configurations were created for each module. The results show that all three modes have good sensitivity to electromagnetic showers and are suitable for high-radiation environments. Here, we discuss the technical design, test characteristics, and cosmic and particle interaction results of the newly developed SE modules.

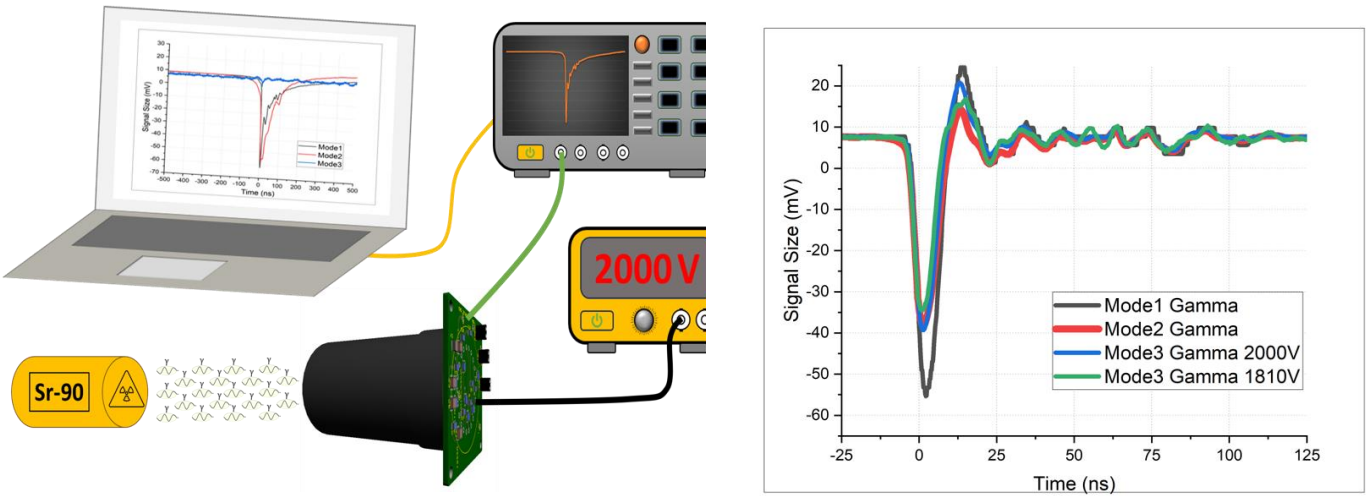


Fig.1. An image of the developed SE module for cosmic and gamma radiation tests, and characterization and analysis.

**Investigation of the Efficiency of Photo Catalysts in Carbon Dioxide Reduction Reactions**

Canan AKSU CANBAY*[1] Ece KALAY*[2] İskender ÖZKUL*[2] Ömer GÜLER*[3]

[1] Fırat University, Faculty of Science, Department of Physics, Elazig, TURKEY
[2] Mersin University, Faculty of Engineering, Department of Mechanical Engineering, Mersin, TURKEY
[3] Munzur University, Faculty of Engineering, Department of Mechanical Engineering, Tunceli, TURKEY

## ABSTRACT

The escalating levels of carbon dioxide emissions due to rapid urbanization and reliance on non-renewable resources necessitate urgent action to mitigate their impact on global warming. Photo catalytic carbon dioxide reduction reactions present a promising solution by harnessing sunlight and employing suitable catalysts to convert greenhouse gases into valuable chemical products. While conventional photo catalysts like titanium dioxide ($TiO_2$) tungsten trioxide ($WO_3$), bismuth-based compounds, $C_3N_4$-based catalysts, copper-based semiconductors etc. have been extensively studied, their limitations, such as wide bandgaps and limited visible light absorption, hinder their full potential. However, recent advancements in high-entropy alloys (HEA) offer a novel approach to catalysis, leveraging their unique properties to enhance efficiency and stability. HEA demonstrate remarkable catalytic activity in various reactions, including carbon dioxide conversion, due to their adjustable composition design and solid solution structure. As collaborative efforts between researchers and industry stakeholders continue to drive innovation in photo catalytic processes, the transition towards a sustainable future becomes increasingly feasible. Through the integration of photo catalysis and renewable energy sources, we can effectively combat climate change and achieve energy sustainability.

*Keywords: photo catalyst, $CO_2$ reduction, high entropy alloys*

Corresponding author: eecekalay@gmail.com

# Spectroscopic and physical characterization of N-phenolyl amino acid derivatives of di spiro cyclotriphosphazene compound

Mahmut Yılmaz[1*], Eray Çalışkan[2], Fatih Biryan[1], Kenan Koran[1]

[1]*Firat University, Department of Chemistry, Elazig, 23200 Türkiye*
[2]*Bingol University, Department of Chemistry, Bingöl, 12000 Türkiye*

[*]**Corresponding E-mail:** yilmaz886@hotmail.com

In this study, we is aimed to synthesize new spiro cyclotriphosphazene structures containing cinnamic acid derivatives carrying amino acid structures in the side groups, in which biphenol substituted cyclotriphosphazene is located in the center, which is not included in the literature, and to explain their structural characterization by spectroscopic methods. In the first step, N-phenolyl amino acid derivatives were obtained from the reaction of 4-hydroxycinnamic acid compound[1] derived from 4-hydroxybenaldehyde with alanine and phenylalanine amino acid esters. In the last step, new cyclotriphosphazene compounds were obtained for the first time in this study from the reactions of dispiro cyclotriphosphazene (DFF) compound[2] and N-phenolyl amino acid derivatives. The physical and thermal properties of the compounds were characterized by UV-vis and DSC/TGA methods, and their spectroscopic characterizations by FT-IR, NMR and mass spectroscopy, respectively.

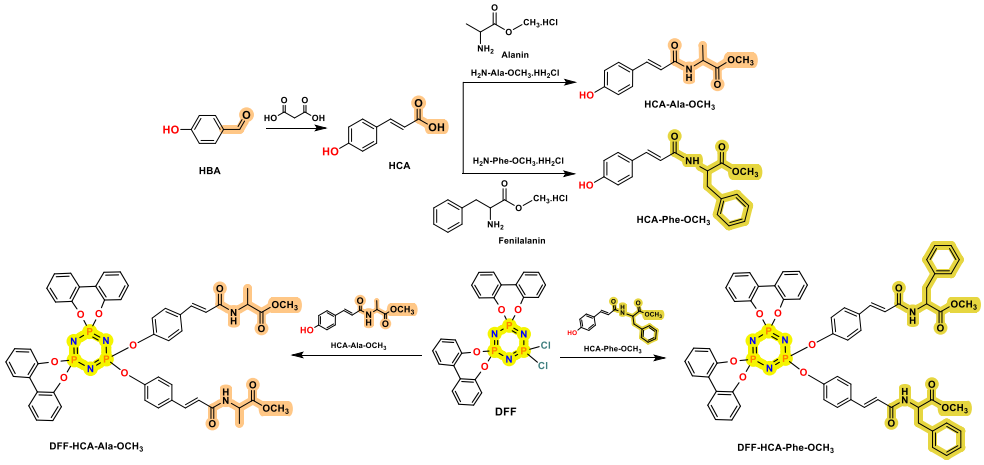


Fig.1. N-phenolyl amino acid derivatives of di spiro cyclotriphosphazene compound.

**Acknowledgement:** This work was supported by Scientific Research Projects Coordination Unit of Firat University. Project number FF.23.15.

**References**

1. Narasimhan, B., Belsare, D., Pharande, D., Mourya, V., Dhake, A. (2004). European Journal of Medicinal Chemistry, 39(10), 827-834.
2. Carriedo, G. A., Fernández-Catuxo, L., García Alonso, F. J., Gómez-Elipe, P., González, P. A. (1996). Macromolecules, 29(16), 5320-5325.

**A Comparison of Forward and Reverse Bias Current Transport Mechanisms (CTMs) for Au/n-Si (MS), Au/PVC/n-Si (MPS1), and Au/(Ti:PVC)/n-Si (MPS2) Type Schottky Diodes (SDs)**

Çiğdem Şükriye Güçlü[1]*

[1] *Department of Physics, Faculty of Science, Gazi University, 06500 Ankara, Turkey*

[*]**Corresponding E-mail:** cigdemguclu@gazi.edu.tr

In this study, the CTMs of the prepared Au/n-Si (MS), Au/PVC/n-Si (MPS 1) and Au/(Ti:PVC)/n-Si (MPS2) type SDs were investigated in a wide range of voltages. For this purpose, the plots of the forward bias $Ln(I_F)$-$Ln(V_F)$ and the reverse bias $Ln(I_R)$-$V_R^{0.5}$ were drawn and analyzed. The forward bias $Ln(I_F)$-$Ln(V_F)$ plots show there linear parts which correspond to the low, intermediate and high bias voltages and obeyed the power-law $I \sim V^m$. The slope (m) values were found as 1.11 and 1.91 for MS, 1.09, 2.50, and 3.30 for MPS1, and 1.33, 5.25, and 4.03 for MPS2. From these slopes, the CTMs were estimated as ohmic, space-charge limited current (SCLC) and trap-charge limited current (TCLC) mechanisms for regions I, II and III, respectively. The CTMs of these three SDs were also examined in the reverse bias region, considering the potential for either Schottky-emission (SE) or Poole-Frenkel emission (PFE) processes. The $Ln(I_R)$-$V_R^{0.5}$ plots show a good linear part and their slopes are indicated that for MS SD SE and for MPS SDs PF are the predominant mechanisms.

**Keywords:** Forward and reverse bias I-V characteristics; MS and MPS type Schottky diodes; Ohmic, space charge/trap charge limited current (SCLC/TCLC) conduction mechanism; Schottky-emission (SE) and Poole-Frenkel emission (PFE)

**Acknowledgement**: This study was supported by Scientific and Technological Research Council of Türkiye (TÜBİTAK) with the research project number 121C396.

**Biodielectric properties of hydroxyapatite-based materials for biomedical applications**

A.Dere[1*], Burhan Coşkun[2], Niyazi Özdemir[3],F.Yakuphanoglu[4]

[1] *Vocational School of Technical Science, Department of Electric and Energy, Firat University, Elazig, Türkiye*
[2]*Kırklareli University, Department of Physics, Kırklareli, Türkiye*
[3] *Türkiye Firat University, Department of Metallurgical and Materials Engineering, Elazig 23119, Türkiye*
[4] *Firat University, Department of Physics, Elazig, 23200*

[*]**Corresponding E-mail:** a.dere@firat.edu.tr

Biomaterials are materials used to perform the functions of tissues and organs in the body or to support them. For this reason, it is very important to produce materials that are compatible with the body in all conditions in scientific applications. In the study, the biodielectric properties of HAp-based Sr-doped materials were examined. Strontium and hydroxyapatite were produced using the hydrothermal method. Biodielectric properties were investigated by analyzing the dielectric properties of Sr-doped HAp-based materials at 1%, 3%, 5% and 10% molar rates as a result of a 10-hour reaction. After determining that doping had occurred with ATR-IR and SEM-EDX analyses, dielectric analyzes of the samples were performed. The transmittances of the samples increases as the doping increases. The real dielectric coefficient of the samples varied depending on the amount of additive. It has been observed that the dielectric constant is constant up to a certain frequency and shows a sudden increase after approximately 18MHz. The change in dielectric constant at high frequencies shows that the materials can be used in biodielectric applications.

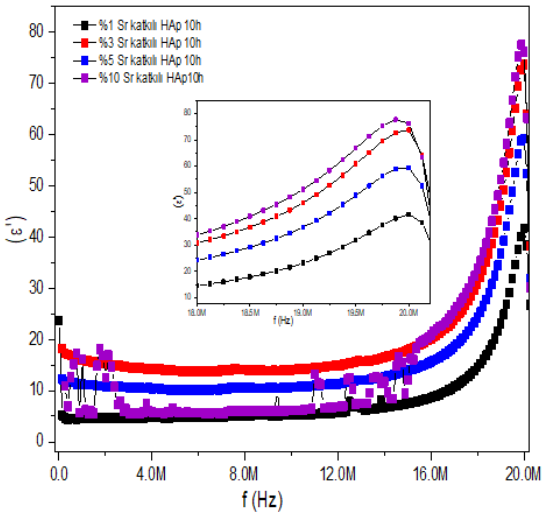


Fig.1. Dielectric constant of 10h pure HA and 1%, 3%, 5% and 10% Sr-doped HA powder samples

**Unleashing the Photovoltaic Potential: Optimizing Zn-Doped Co3O4 Films via Ultrasonic Spray Pyrolysis**

I.Gunes[1*], E.Sarica[2], I.Akyuz[3], A.Kucukarslan[4], V.Bilgin[4]

[1] *Canakkale Onsekiz Mart University, Department of Electricity and Energy, Canakkale, 17200, TURKEY*
[2] *Baskent University, Department of Electrical and Electronics Engineering, Ankara, 06790, TURKEY*
[3] *Department of Physics, Eskisehir Osmangazi University, Eskisehir, 26480, TURKEY*
[4] *Canakkale Onsekiz Mart University, Department of Physics, Canakkale, 17020, TURKEY*

[*]**Corresponding E-mail:** ibrahimgunes@comu.edu.tr

In this study, undoped and zinc-doped cobalt oxide ($Co_3O_4$) films were deposited on microscope glass substrates using the ultrasonic spray pyrolysis technique at a substrate temperature of 375 °C. The effect of different Zn doping concentrations (3%, 6%, and 9%) within the film structure on the morphological, structural, and optical properties of $Co_3O_4$ films was investigated to optimize their optoelectronic and photovoltaic applications. Morphological, structural, and optical analyses of all films were carried out using atomic force microscopy (AFM), scanning electron microscopy (SEM), X-ray diffraction (XRD), and UV-visible spectroscopy, respectively. The morphological and structural analyses revealed noticeable changes on the surfaces with increasing doping concentration, while no significant change in the crystallite size was observed. For optical analyses, the optical transmittance and absorption spectra of the films were obtained in the wavelength range of 300-1000 nm, and some optical parameters such as optical band gaps and Urbach parameters were determined using these spectra. As a result, it was observed that the deposited films could be successfully obtained for photovoltaic applications using the ultrasonic spray pyrolysis method.

***Keywords:*** *Zn-doped $Co_3O_4$ thin films; Ultrasonic spray pyrolysis; Physical properties.*

**Acknowledgements:** This work was supported by the Canakkale Onsekiz Mart University Scientific Research Projects Committee under the Project Number FBA-2021-3661.

**Conjugation of RGD on electrodeposited of carbon nanotubes to analyse glioblastoma cells**

B. Karadag[1*], S. Er Zeybekler[1], S.S. Gelen[1], L. Sabour-Takanlou[2], M. Sabour-Takanlou[2], C. Biray Avci[2], D. Odaci[1]

*[1] Ege University, Department of Biochemistry, Faculty of Science, Izmir, 35100 TURKEY*
*[2] Ege University, Department of Medical Biology, Faculty of Medicine, Izmir, 35100 TURKEY*

[*]**Corresponding E-mail:** dilekodaci.od@gmail.com
cbavci@gmail.com
belguzar.karadag@hotmail.com

The discovery of carbon nanotubes helped give rise to the concepts of nanotechnology and nanomaterials. There are many studies on Multi-Walled Carbon Nanotube (MWCNT) [1]. In this study, MWCNT was modified with 4-aminothiophenol (4ATP). Electrochemical deposition of the synthesized MWCNT-4ATP was carried out on gold electrodes. Then, after conjugating RGD-peptide onto Poly(MWCNT-4ATP), the adhesion of glioblastoma cells were monitored by electrochemical techniques. The synthesized Poly(MWCNT-4ATP) and the obtained Poly(MWCNT-4ATP)/RGD surfaces were characterized using Scanning Electron Microscopy-Energy Dispersive X-Ray Spectrometer (SEM-EDS), Attenuated Total Reflection Fourier Transform Infrared Spectroscopy (ATR-FTIR), X-Ray Photoelectron Spectrometer (XPS). The linear detection range of U-87MG glioblastoma cells was found to be $10^2$-$10^6$ cells/mL. The developed Poly(MWCNT-4ATP)/RGD cell adhesion platform enabled following of U-87MG glioblastoma cells using both electrochemical techniques and fluorescence imaging results.

**Keywords:** Nanobiotechnology, biosensor, cell adhesion, glioblastoma

**Reference:**

[**1**]. Yang, N., Chen, X., Ren, T., Zhang, P., & Yang, D. (2015). Carbon nanotube based biosensors. Sensors and Actuators B: Chemical, 207, 690-715.

**Sunflower Seed Shell-Derived Hard Carbon: A Sustainable Solution for Aqueous Zn-Ion Battery Electrodes**

Buse Ecevit[1], Yıldıray Topcu[1], Burak Tekin[1]*

[1] *Ondokuz Mayıs University, Chemical Engineering Department, Samsun, 55139, TURKEY*

***Corresponding E-mail:** burak.tekin@omu.edu.tr

The growing global energy demand and reliance on fossil fuels underscore the urgent need for sustainable and efficient energy storage solutions. In this context, zinc-ion hybrid supercapacitors have emerged as a promising technology, bridging the gap between traditional supercapacitors and batteries. Offering both high energy and power densities, zinc-ion hybrid supercapacitors represent an innovative approach to meet the increasing demand for high-performance energy storage systems. In the quest for novel energy storage materials, the selection of appropriate materials plays a pivotal role in achieving sustainability and cost-effectiveness. Recognizing the potential of locally abundant resources, we have explored the utilization of hard-carbon material derived from sunflower seed shells. Leveraging the high cellulose content and widespread availability of sunflower seed shells, we synthesized hard carbon material through a pyrolysis process. The synthesized hard carbon material was subjected to comprehensive characterization using advanced techniques such as X-ray Diffraction (XRD), Fourier-Transform Infrared (FTIR), and Thermogravimetric Analysis (TGA). XRD analysis confirmed the amorphous carbon structure of the material, while FTIR analysis revealed the presence of functional groups within the hard carbon structure. TGA provided insights into the thermochemical transformation processes within the material and quantified the volatile matter ash content to be 2.5%. To evaluate the electrochemical performance of the hard carbon material, various electroanalytical methods including Cyclic Voltammetry (CV), constant-current charge-discharge, and Electrochemical Impedance Spectroscopy (EIS) were employed. Specifically, the influence of electrolyte concentration ($ZnSO_4$) on Zn-ion hybrid supercapacitor performance was investigated using aqueous $ZnSO_4$ electrolytes with concentrations ranging from 0.5 to 2M. Remarkably, the hard carbon material exhibited optimal electrochemical performance in 1.5M $ZnSO_4$ electrolyte. During charge-discharge tests, the hybrid cell demonstrated a gravimetric capacitance of approximately 80 $F/cm^2$ at a current density of 80 A/g, while retaining 99.9% of its initial capacity after 500 cycles. These results highlight the potential of locally abundant sunflower seed shells as a viable source for producing electroactive electrodes for next-generation zinc-ion hybrid batteries.

**Keywords**: Biomass, Zn-ion hybrid supercapacitor, Electrochemical tests, Energy Storage.

# Removal of Iron Impurities from Quartz Ores in the East Anatolian Fault Zone Region and Enhancement of Purity through Physical Methods

Canan AKSU CANBAY [a]* Mustafa BOYRAZLI[b] Gulsah CAKMAK[c] Ugur CALIGULU[d] Ayse Didem KILIC[e] Ozlem ERDEM[f]

[a]* Firat University, Faculty of Science and Literature, Department of Physics, Elazig, Turkey

[b]Firat University, Faculty of Engineering, Department of Metallurgy and Materials Engineering, Elazig, Turkey

[c]Firat University, Faculty of Engineering, Department of Mechanical Engineering, Elazig, Turkey

[d]Firat University, Faculty of Technology, Department of Metallurgy and Materials Engineering, Elazig, Turkey

[e]Firat University, Faculty of Engineering, Department of Geological Engineering, Elazig, Turkey

[f]Munzur University, Faculty of Engineering, Department of Civil Engineering, Tunceli, Turkey

ABSTRACT

This study was conducted to investigate the role of piezoelectric minerals in sustainable energy conversion. For this purpose, minerals with a relatively high $SiO_2$ content, obtained from various sources in the Elazığ region, were used. It was determined that almost all these ores contained iron oxide impurities, and efforts were made to enrich the quartz by applying ore dressing and beneficiation processes. In the process of removing iron impurities from quartz ores and increasing their purity through physical methods under laboratory conditions, steps such as collecting rock samples, preparing thin sections, and determining mineralogical compositions were taken. The high field intensity wet magnetic separation technique was used to purify quartz samples from different depths determined in active tectonic and recent earthquake zones. Neutron analysis methods were used to determine the structure and crystallographic orientations of quartz. According to the data obtained, the $SiO_2$ content of the initial quartz sample, which was 67.12%, was increased to up to 96% by the ore dressing and beneficiation process.

*Keywords: Piezoelectric minerals, Quartz Purification, Neutron analysis, Flotation, Sustainable Energy*

Corresponding author: caksu@firat.edu.tr

## 1. Introduction

With the increasing demand for energy due to growing energy needs, there is a rising interest in renewable and sustainable energy sources. In this context, the potential of our geological resources for energy production is gaining importance. Particularly, the energy conversion properties of piezoelectric minerals draw attention to the utilization of geological materials as alternative energy sources [1].

The piezoelectric effect is based on the principle of generating electricity on the surface of a crystal when mechanical pressure is applied, and conversely, generating mechanical stress when electricity is applied to the surface. The piezoelectric properties of common minerals like quartz are particularly noteworthy in industrial applications. However, research on the potential of the piezoelectric effect in our geological resources and energy production from these minerals is limited. Therefore, further research is needed to understand the role of piezoelectric minerals in energy production and to evaluate our geological resources in terms of energy [2].

It is known that natural minerals can convert mechanical energy into electrical energy and vice versa (actuator property), but how the mechanical stress created by active tectonics affects this energy in minerals is not yet fully understood. There are 207 minerals with ferroelectric, pyroelectric, or piezoelectric properties, with quartz being the most common among them. Quartz can be found in a wide range of rocks, from granites to sandstones. It has been observed that the piezoelectric property is higher in multi-mineral rocks compared to single-mineral rocks. The East

Anatolian Fault Zone is a rich area in various mineral and ore resources, and if it can be determined that piezoelectric crystals in this region can produce low-frequency (LF) and medium-frequency (MF) electromagnetic emissions, piezoelectric polarization may exist in the minerals under investigation [3].

The East Anatolian Fault (EAF) is one of Turkey's most important active faults and has been extensively studied by many researchers since the early 1960s. Until now, numerous studies have been conducted, especially for geological purposes. In a study conducted by Duman and Emre [4], the geometry and segmentation of the EAF were extensively discussed and divided into three main parts: the southern (main) branch, the northern branch (Sürgü-Misis fault), and the Karasu Basin. The southern (main) branch forms the northeast with the North Anatolian and Varto Faults and the Karlıova Triple Junction, and the southwest with the Dead Sea Fault (DSF) and the Cyprus Arc at the Amik Triple Junction. The total length of the EAF is about 580 km, and segments such as Karlıova, Ilıca, Palu, Pütürge, Erkenek, Pazarcık, and Amanos have been identified on it. This study covers the rocks and minerals within the Palu segment. The Palu segment extends approximately 77 km along the K60°E direction between the Gök River compressional fold and the Hazar Lake releasing fold. The Palu segment is not a single piece but is divided into three sub-sections of a fault section. From the past to the present (especially in 2020 and 2023), severe earthquakes have been observed on the Palu segment, and its activity continues.

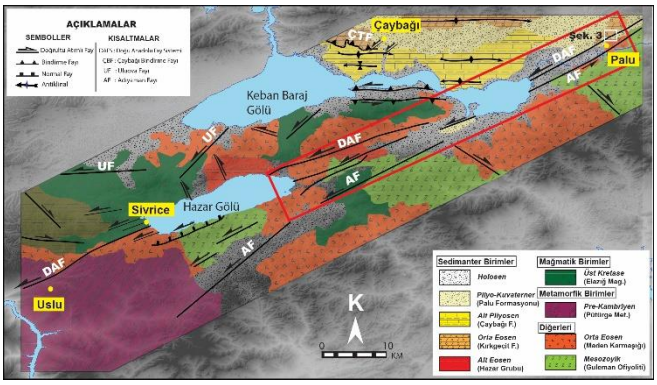


**Figure 1.** Geological map of the study area and significant tectonic structures [4]

The Eastern Anatolia Region boasts a wide variety of rocks, making it a geologically rich area. The study area encompasses age ranges from the Cretaceous to the present. Within this range, various geological units such as the Late Cretaceous (Senonian) Elazığ Magmatic rocks, the Early Eocene Hazar Group, and the Middle Eocene-Oligocene Kırkgeçit Formation are present. The study area comprises both igneous and sedimentary rock types. Among these are the Elazığ Magmatic rocks, which consist of granite, granodiorite, tonalite, diorite, norite, and gabbro, as well as the Kırkgeçit Formation, composed of sandstone, shale, and siltstone [5].

Quartz, a common mineral found in these rocks, has a trigonal crystal geometry. The density of quartz is 2.65 g/cm³, its Mohs hardness is 7, and its α-β phase transition temperature is 573°C. At this temperature, quartz transforms from hexagonal α-quartz to non-piezoelectric hexagonal β-quartz. Quartz crystals have a zero temperature coefficient over a wide temperature range at room temperature and exhibit excellent frequency-temperature characteristics. Due to these properties, quartz crystals are preferred as industrial raw materials for providing accurate reference signals in devices such as communication devices, televisions, digital cameras, and computers [6-8].

The use of quartz alongside natural minerals like tourmaline, olivine, and cubic zirconia provides an alternative to costly energy sources. The superior physical properties of quartz have also made its use possible in jewelry and ornaments. The most common everyday use of quartz is in quartz crystal clocks, which provide much higher accuracy compared to mechanical clocks. The significant role of quartz in various industries necessitates the study of energy production from natural minerals and their industrial applications.

There are numerous studies on the energy efficiency of minerals [9-11]. These studies demonstrate how the cation content of the mineral affects its purity and how electrical properties vary depending on the mineral's chemistry. Researchers [12] have shown that quartz can be termed "high purity" when the trace element content is less than 50 mg/g, and that trace elements such as Al, Ge, and Ti can substitute for silicon within the quartz structure, either within a fluid or enclosed within a mineral. Another study stated that pure quartz should have specific elemental ratios and quantities, including Al/Li around 12, with individual amounts for Li, Na, K, Mg, Ca, Fe, Cu, Cr, Mn, Al, and Ti [13]. In studies by Götze and Weil [14, 15], pegmatitic quartzites were identified with varying concentrations of Al, Ti, and Ge, and quartz with these properties was termed pure quartz. These elements can substitute for Si4+ in the quartz structure. Preliminary data from neutron activation analysis of quartz selected from examined diorite rock ($SiO_2$ %45-52) indicated low levels of various impurities [16]. Some of these disadvantages, especially high Al and Fe contamination, can be overcome using chemical and physical processes. In a study on processing quartz mineral into semi-industrial fusion powder, Santos et al. [17] found that quartz with less than 100 ppm of impurities, particularly pyrite, is used in industrial applications requiring high thermal stability. Quartz containing less than 10 ppm of pyrite is considered ultra-high purity and is used in the production of semiconductor chips and solar cells. Alkali oxides such as $K_2O$, $Na_2O$, CaO, and MgO found in quartz contribute to the durability of glass in glass production. Recently, the use of SiO2 in the photovoltaic and flat-panel display industries has increased. In an experimental study on quartz minerals, a 33% increase in energy was observed at 125 kHz frequency, with smaller crystalline quartz showing increases ranging from 10% to 40% [18-20].

The area highlighted with a red frame in Figure 1 indicates the most suitable location for the purification of quartz crystals based on data obtained from drilling studies on the East Anatolian Fault. This region is predominantly characterized by rocks from the Elazığ Magmatic suite, such as granite, tonalite, and rhyolite, which typically have quartz contents ranging from 20% to 60%. Additionally, these rocks often contain feldspar ranging from 10% to 90%, and amphibole and biotite ranging from 10% to 50%. These data indicate the widespread occurrence of quartz in this region and provide an important reference point for determining mineral contents.

The aim of this study is to explore the potential of minerals with piezoelectric properties in energy production and to evaluate how our geological resources can be utilized in sustainable energy production. Understanding how our geological resources can be utilized in sustainable energy production may support a more reliable and environmentally friendly approach to energy in the future.

**2. Experimental method**

In this study, the methods utilized for detailed application in a local area are as follows:

- Rock samples were collected from the study area.

- Thin sections were prepared from selected rock samples in the laboratory, and their mineralogical compositions were determined.

Subsequently, quartz was separated into different grain sizes.

- Quartz samples from different depths identified within active tectonic and recent seismic zones were categorized.

Finally, the removal of iron oxide in quartz was carried out using a wet high intensity magnetic separator.

After the chemical analysis and sieve analysis values of the quartz ore were determined, it was subjected to enrichment at 1000 Gause, 3000 Gause and 6000 Gause magnetic field strength using a high field strength Wet Magnetic Separator on a laboratory scale.

To determine the Dielectric/Ferroelectric or Piezoelectric properties of a material, it is necessary to first cut the selected mineral in the appropriate symmetry direction. Intensive neutron analysis methods such as Instrumental Neutron Activation Analysis (INAA) and X-ray diffraction are used to determine the structure and crystallographic orientations of quartz. However, unlike X-ray diffraction measurements, neutron diffraction (ND) analyses can determine large-volume textures such as mineral orientation in rocks. This method also provides data on the crystallographic orientation of coarse-grained materials and their magnetic properties.

The representation of the electrical polarization generated by the piezoelectric effect when a mechanical force is applied to a quartz crystal (Figure 2) can be visualized using diffraction results obtained for a specific polycrystalline sample. In this representation, the location of the electrical center, defined by Si+ and O- atoms, changes as a result of the application of a compressive force along the X-axis, and piezoelectric polarization planes develop in the quartz, with an electrical charge polarization in the X-direction.

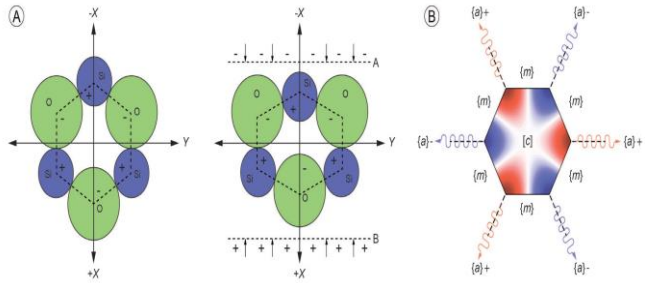


**Figure-2**. A) The effect of a mechanical stress applied parallel to the X-axis on a quartz crystal lattice. When the lattice is distorted, the electric field becomes unbalanced, resulting in polarization. B) Distribution of piezoelectric polarization in a quartz crystal (red positive; blue negative). It is noteworthy that only {a} axes are piezoelectrically active [20].

**3. Results and discussion**

In the optical microscope images of the ore, which was separated into different grain sizes by crushing, grinding and screening processes, the grain size of liberation from iron oxides was determined as 100 microns (Figure 3).


**Figure 3.** (A) Pulp prepared for magnetic separation process, (B) High-gradient wet magnetic separator, (C) Magnetic product obtained after passing through the magnetic separator.

Cumulative sieve curves plotted logarithmically according to the results obtained from the sieving processes performed after grinding for different periods of time are given in Figure 4.

According to the graph in Figure 4, after 15 minutes of grinding, 9.33% of the total material passed through the 106-micron sieve, while after 30 minutes of grinding, this rate became 24.52%. Again, for 60 minutes of grinding, 59.56% and 90 minutes of grinding, 88.33% of the total material passed through the 106-micron sieve.

The composition and mineralogical properties of an ore are crucial for determining the most suitable method for enriching industrial minerals. One of the most significant impurities found in quartz ores is iron. The iron content in

industrial minerals can be reduced through physical separation methods such as abrasion, magnetic separation, or flotation. Alternatively, hydrometallurgical methods can be used to remove iron compounds by dissolving them with appropriate reagents [24].

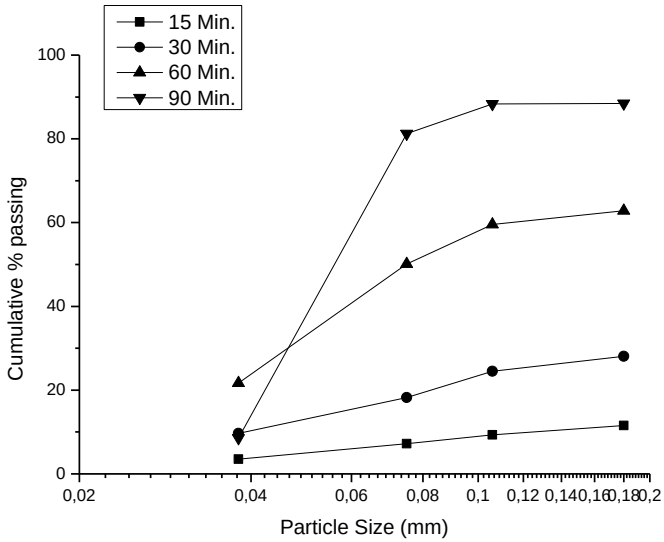


**Figure 4.** Cumulative under-sieve curves obtained as a result of the grinding process performed at different times.

The sample with a grain size of 106 microns underwent magnetic separation at different field intensities. Table 2 displays the $SiO_2$ and $Fe_3O_4$ contents of the tailings and concentrate as a result of magnetic enrichment through the application of varying magnetic field intensities. In Figure 5 (a) and (b), the changes in iron oxide and silicate content in the concentrate and tailings depending on the magnetic field intensity are shown.

**Table 2.** $SiO_2$ and $Fe_3O_4$ contents in products as a result of enrichment at different magnetic field intensities.

| Magnetic field (Gauss) | Concentrate | | Tailing | |
|---|---|---|---|---|
| | ($SiO_2$ ,%) | ($Fe_3O_4$ , %) | ($SiO_2$ ,%) | ($Fe_3O_4$ , %) |
| 0 | 67,12 | 21,42 | 67,12 | 21,42 |
| 1000 | 87,54 | 10,42 | 24,06 | 66,31 |
| 3000 | 96,10 | 1,28 | 7,31 | 86,23 |
| 6000 | 85,13 | 8,14 | 18,41 | 72,11 |

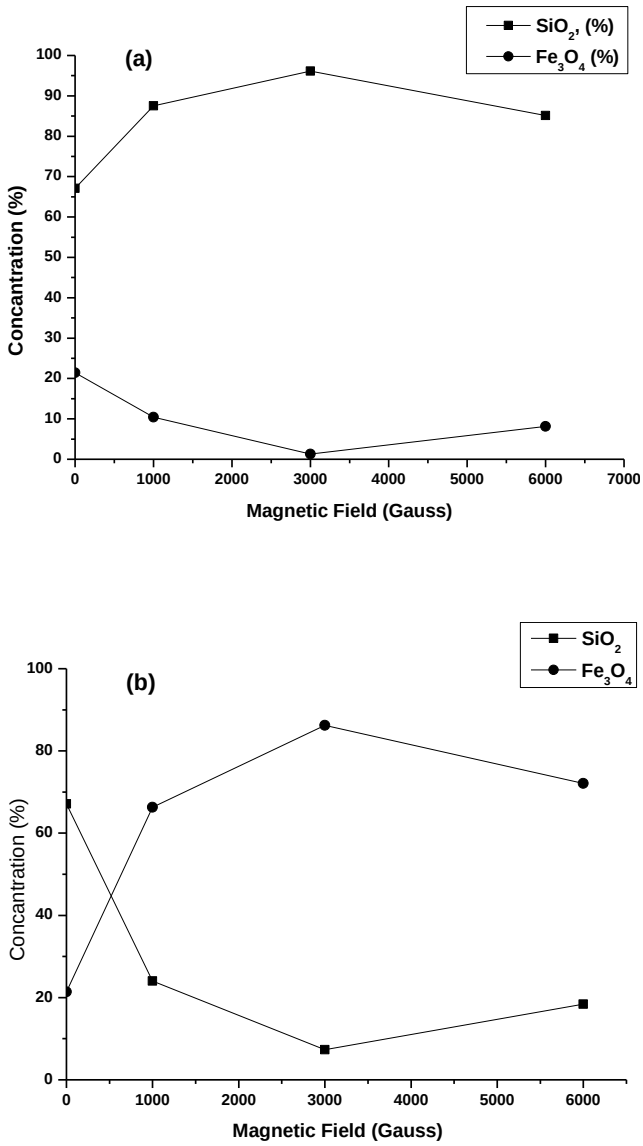


**Figure 5.** The change of iron oxide and silicate content (a)in the concentrate and (b) in the waste, depending on the magnetic field intensity.

As shown in Figure 5 (a) and (b), the initial sample contained 67.12% $SiO_2$ and 21.42% $Fe_2O_3$. When a magnetic field intensity of 1000 Gauss was applied, the concentrate had 87.54% $SiO_2$ and 10.42% $Fe_3O_4$. At a magnetic field strength of 3000 Gauss, the concentrate contained 96.10% $SiO_2$ and 1.28% $Fe_3O_4$. However, when the magnetic field strength was increased to 6000 Gauss, the $SiO_2$ content in the concentrate decreased to 85.13%.

Very fine particles can be enriched at low magnetic field strengths if they possess sufficient magnetic properties. However, when a higher intensity magnetic field is applied to the same particles, the non-magnetic particles remaining between the magnetic particles are also attracted to the magnet. Thus, the proportion of non-magnetic particles in the concentrate increases as a result of the enrichment process.

Our aim in this study was to increase the concentration of $SiO_2$ and reduce the concentration of $Fe_3O_4$. In the sample to which a magnetic field of 6000 Gauss was applied, $SiO_2$ particles were trapped between the $Fe_3O_4$ particles and caught by the magnet, resulting in a decrease in the $SiO_2$ content in the concentrate.

For the determination of phase analyses of the concentrate, measurements were taken using a DTA-DTG device (Figure 6). The crystallographic phase transformations, decomposition, dehydration, desorption, melting, boiling,

evaporation, oxidation, and other physical/chemical behaviors in response to external heat and resulting temperature changes that the selected samples could exhibit were observed to provide insight into their physical properties. To achieve this, each sample was heated from room temperature to 850°C at a constant rate of 20°C per minute using a Shimadzu DTG-60 AH model DTA-DTG device, and simultaneous measurements of the differential thermal analysis (DTA) and accompanying mass changes, as shown by thermogravimetric analysis (TGA), were conducted in an air atmosphere.

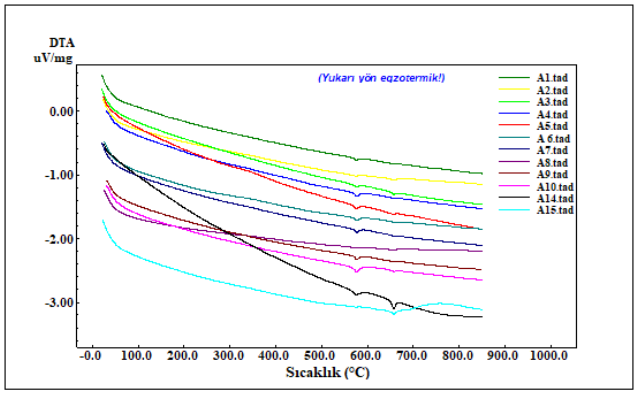


**Figure 6.** Multiple DTA measurement curves of the samples

In the conducted physical measurements, upon In the conducted physical measurements, upon examining the DTA-TGA graphs of the samples, it was observed that certain metal oxides, such as $K_2O$, decomposed around 574-576°C. Additionally, the loss of chemically adsorbed water (crystalline water) occurred within the same temperature range. Alongside the measured endothermic peaks, a polymorphic transformation of quartz ($SiO_2$) from the α-quartz phase to the β-quartz phase was thermally observed. These transformations occurred consistently with the studies reported in the literature [25-27].

## 4. Conclusion

This study has examined the purification and enrichment process of quartz ores obtained from granite rocks. The data gathered through various physical processes and analyses conducted in the laboratory have provided important insights for determining the most suitable methods for enriching industrial minerals.

As a result of enriching the quartz ore with a magnetic separator, the $SiO_2$ content was increased from 67.12% to 96.10%, and the magnetic minerals were largely removed.

Another significant finding of the study is the data obtained from DTA-TGA analysis. These analyses have provided an opportunity to examine the thermal behaviors of the samples in detail. Thermal properties such as the decomposition of certain metal oxides and the polymorphic phase transformations of quartz are critically important in the characterization and processing of the material.

Lastly, the results obtained from this study can be regarded as an important step in increasing the industrial usage potential of quartz ores and contributing to sustainable energy production. The high-purity quartz obtained can be used in various industrial applications and can contribute to the development of renewable energy technologies. This study has provided a fundamental reference point that will guide future research and industrial applications.

**5. Acknowledgement**

This study is supported by TUBITAK under the code "223M574" and titled "Doğu Anadolu Fay Zonu İçerisindeki Deprem Kaynaklı Enerjinin Mineraller Üzerine Etkisinin Araştırılması"

**References:**

[1] Elçi, H., and Bayır, S. (2021). Piezoelectric Materials: Energy Conversion, Properties, and Applications. In: Energy Conversion - Current Technologies and Future Trends. Intech Open. https://doi.org/10.5772/intechopen.97657

[2] Römer, Y., El-Soury, M. (2015). Piezoelectric Materials and Devices: Applications in Engineering and Medical Sciences. Wiley-VCH

[3] Griffiths, S. D., Jackson, J. A., Priestley, K. F. (2004). Earthquake-induced deformation cycles in continental rifts. Journal of Geophysical Research: Solid Earth, 109(B6). https://doi.org/10.1029/2003JB002735

[4] Duman, T.Y., Emre, Ö. (2004). Geological and seismological characteristics of the Palu fault zone, Eastern Turkey: implications for long-term seismic activity. Geophysical Journal International, 157(3), 1065-1080. https://doi.org/10.1111/j.1365-246X.2004.02259.x

[5] Goncuoglu, M. C., & Okay, A. I. (1996). Tertiary evolution of the eastern Pontides (Turkey): implications for the Neotethyan closure. Geological Society, London, Special Publications, 100(1), 327-350. https://doi.org/10.1144/GSL.SP.1996.100.01.19

[6] Li, W., Li, Q., Li, H., Zhang, Z., & Hao, J. (2021). Recent progress in piezoelectric materials for energy harvesting: Principle, mechanisms, and applications. Nano Energy, 81, 105670. DOI: 10.1016/j.nanoen.2020.105670

[7] Wang, Y., Yao, Y., Jiang, X., Zhang, Y., & Chen, L. (2020). Piezoelectric materials: Energy harvesting, sensors, and actuators. Advanced Functional Materials, 30(12), 1906696. DOI: 10.1002/adfm.201906696

[8] Nguyen, V. V., Park, D. Y., & Jeong, C. K. (2021). Piezoelectric materials for sensing and energy harvesting: Recent progress and future challenges. Materials Today Energy, 21, 100730. DOI: 10.1016/j.mtener.2021.100730

[9] Smith, J. D., & Johnson, R. W. (2020). Mineral Energy Efficiency: Effect of Cation Content on Mineral Purity. Journal of Energy Efficiency in Minerals, 8(2), 123-135.

[10] Kim, Y. H., & Lee, S. M. (2019). Potential Role of Piezoelectric Minerals in Energy Conversion. Journal of Renewable Energy Resources, 6(1), 45-58.

[11]Chen, L., & Wang, H. (2021). Electromechanical Properties and Industrial Applications of Quartz. Journal of Materials Science & Technology, 37(3), 289-302.

[12] Smith, J. D., & Johnson, A. B. (2018). Analysis of Trace Elements of Quartz and Its Effect on Energy Efficiency. Journal of Mineralogical Research, 25(3), 321-335.

[13] Heraeus, 2014. HLQ 200. http://lamp-materials.heraeusquarzglas.com/en/materialgrades/hlq200/HLQ200.aspx (accessed 16.02.14.)

[14] Götze, J. (2009). Chemistry, texture and physical properties of quartz–geological interpretation and technical application. Mineralogical Magazine, 73(4), 645-671.

[15] Weil, J. A. (1993). A review of EPR spectroscopy in alpha-quartz: the decades of 1982e1992. In: Helms, C.R., Deal, B.E. (Eds.), Physics and Chemistry of $SiO_2$ and the Si-$SiO_2$ Interface 2. Plenum press, New York, pp. 131e144..

[16] Santos, M.F.M., Fujiwara, E., Schenkel, E.A., Enzweiler, J., Suzuki, C.K. (submitted for publication). Processing quartz lumps rejected by silicon industry into silica glass raw material. International Journal of Mineral Processing.

[17] Unimin. (2014). A History in Havelock. Canadian Nepheline Modernization. Retrieved from http://canadiannepheline.ca/#our-history, accessed: 12.02.2018.

[18] Arvamangala, H., Natarajan, K. A. (2011). Microbially Induced Flotation of Alumina, Silica/calcite from Hematite. International Journal of Mineral Processing, 99, 70-77.

[19] Bond, W. L. (1943). A Mineral Survey for Piezo-Electric Materials. 22: 2, 145-152.

[20] Homand-Etienne, H., Houpert, R. (1989). Thermally induced microcracking in granites: characterization and analysis. International Journal of Rock Mechanics, Mining Sciences & Geomechanics Abstracts, 26(2), 125-134.

[21] Nye, J. (1957). Physical Properties of Crystals: Their Representation by Tensors and Matrices, Oxford.

[22] Mason, W. P. (1950). Piezoelectric crystals and their application to ultrasonics, New York, D. Van Nostrand Company, Inc.

[23] Tuncuk, A., Akçıl, A. (2013). Asit Liçi Uygulamasıyla Yüksek Kalitede Kuvars Üretiminde Çözücü ($H_2SO_4$ ve $C_6H_8O_7$) ve İndirgeyici ($H_2O_2$) Etkisi. Madencilik, 52(2-3), 9-20.

[24] Akçıl, A., Tuncuk, A., Deveci, H. (2007). Kuvarsın Saflaştırılmasında Kullanılan Kimyasal Yöntemlerin İncelenmesi. Madencilik, 46(4), 3-10.

[25] Xuesong, J., Jian, C., Mengnan, W., Feifei, L., Boyuan, B., Jingwei, L. (2020). Effect of Impurity Content Difference Between Quartz Particles on Flotation Behavior and Its Mechanism. Powder Technology, 375, 504-512.

[26] Tuck, G., Stacy, F. D., Starcky, J. (1977). A search for the piezo-electric effect in quartz-bearing rocks. Tectonophysics, 39, 7-11.

[27] Hou, S., Cui, L.L., Xu, X.A. (2019). A piezoelectric-based three-direction normal stress sensor for concrete structures. Journal of Intelligent Material Systems and Structures, 30, 1850-1867.

**Use of active carbon produced by hydrothermal method from agricultural waste in methylene blue removal**

M. Boyrazlı [1], E. Aranci Ozturk [2*], E. Celik[1], M.A. Yasli[1]

[1] *Firat University, Faculty of Engineering, Department of Metallurgical and Materials Engineering, Elazig, 23119 TURKEY*

[2]*Balikesir University, Balikesir Vocational School, Department of Machine and Metal Technologies, Balikesir, 10145 TURKEY*

[*]**Corresponding E-mail:** elif.ozturk@balikesir.edu.tr

In this study, the use of activated carbon produced from an agricultural waste by hydrothermal method in the removal of methylene blue from solution was examined. In the study, Pistachio Roasting Facility Waste (FTA) was chosen as agricultural waste. For activated carbon production, carbonized products were processed in a hydrothermal device (HTC) in the presence of an activator for various periods of time. In the processes carried out at constant temperature, high pressure values were reached, enabling activated carbon to reach a high adsorption capacity. As a result of the studies, it was determined that the sample with a KOH impregnation ratio of 1:1 in HTC for 480 min at 160 °C could remove MM with 99.85% extraction efficiency in a solution with 350 ppm MM concentration.

**Keywords:** Hydrothermal Carbonization, Activated Carbon, Pistachio, Organic Waste, Methylene Blue, Adsorption

# Drug Doped Metal Phosphate Organic Framework Synthesis, Characterization, and Cell Viability Assay

Başak ÇELEBİ[1], Rümeysa BEYAN TAŞDEMİR[1], Fatmanur UYAN[1], Funda ÖZDEMİR GÜNEY[1,2], Hatice BEKCİ[1,3], Serkan DAYAN[1,4]*

[1] *Drug Application and Research Center, Molecular Synthesis, and Industrial Applications Laboratory (MSIA-Lab), Erciyes University, 38280 Kayseri, Turkey*
[2] *ERNAM – Erciyes University, Nanotechnology Application and Research Center, Kayseri 38039, Turkey*
[3] *Kayseri University, Develi Hüseyin Şahin Vocational School, Kayseri, Turkey*
[4] *Erciyes University, Faculty of Pharmacy, Department of Pharmaceutical Basic Sciences, 38039, Kayseri, Turkey*
***Corresponding E-mail:** celebibasak200128@gmail.com or serkandayan@erciyes.edu.tr

Metal-organic frameworks (MOFs) are hybrid nanoparticles that have porous structures due to metal-organic interactions. Due to their physical and chemical properties, they play a very important role in drug delivery and disease diagnosis. They have properties such as a well-defined structure, an adaptable framework, high porosity, different types of pores, low toxicity, large surface area, and easy chemical functionalization. MOFs are particularly useful in cancer research [1,2]. The focus is on the delivery of doxorubicin (DOX), the first anticancer drug encapsulated in liposomes, to tumor sites using nanocarrier-based components such as MOFs. Compared to other nanocarrier materials, MOFs deliver higher local concentrations of DOX and transport more drugs [3,4].

In this study, metal phosphate organic frameworks (MPOFs) were synthesized with Cu/Sr metals and organic DOX ligands. Fourier transform infrared spectroscopy (FTIR) for molecular bonding, X-ray diffraction (XRD) for elemental composition, and field emission scanning electron microscopy (FESEM) for surface morphology and energy dispersion analysis were then performed. The analyses were followed by an in vitro cell viability assay using cytotoxicity measurement techniques.

**Keywords:** metal-phosphate organic framework (MPOF), doxorubicin, anti-cancer.

**References:**

1. Al Sharabati, M.; Sabouni, R.; Husseini, G. A. Nanomaterials. 2022, 12(2), 277.
2. Valizadeh Harzand, F., Mousavi Nejad, S. N., Babapoor, A., Mousavi, S. M., Hashemi, S. A., Gholami, A., ... & Lai, C. W. (2023). Recent advances in metal-organic framework (MOF) asymmetric membranes/composites for biomedical applications. *Symmetry*, *15*(2), 403.
3. Rivankar, S. *Journal of cancer research and therapeutics*. **2014**, *10(4)*, 853–858.
4. Ibrahim, M.; Abuwatfa, W. H.; Awad, N. S.; Sabouni, R.; Husseini, G. A. *Pharmaceutics*. **2022**, *14(2)*, 254

**Harnessing Turkey's First Registered Biomass: Hemp-Derived Carboneous Electrode for Advanced Zn-Ion Hybrid Supercapacitors**

Burak Tekin*, Yıldıray Topcu

[1] *Ondokuz Mayıs University, Chemical Engineering Department, Samsun, 55139, TURKEY*
***Corresponding E-mail:** burak.tekin@omu.edu.tr

The cornerstone of any energy storage system resides in its electrodes, serving as either anodes or cathodes. Thus, the efficacy of energy storage and conversion systems heavily relies on their sustainability and electrochemical functionality. This research delves into the utilization of carbonaceous material derived from hemp biomass for water-based Zn-ion hybrid supercapacitors. Notably, the hemp biomass employed in this study represents not only the first national biomass but also heralds the introduction of hemp-derived carbon as a cathode material for aqueous Zn-ion hybrid capacitors. To achieve this, hard carbon electrodes were crafted from hemp biomass through a combination of hydrothermal synthesis and chemical activation with potassium hydroxide (KOH). The resulting hard-carbon material boasts a crucial porous structure vital for efficient energy storage. Comprehensive structural characterization of the hard-carbon material was conducted using various advanced techniques, including X-ray Diffraction (XRD), Scanning Electron Microscopy (SEM), Energy-Dispersive X-ray Spectroscopy (EDS), Thermogravimetric Analysis (TGA), Fourier-Transform Infrared (FTIR) spectroscopy, Brunauer-Emmett-Teller (BET) analysis, and X-ray Photoelectron Spectroscopy (XPS). In the final stage, a hybrid supercapacitor was assembled by incorporating hard carbon and metallic Zn in a swagelock cell. This hybrid cell exhibits an exceptional specific capacitance of 220 F/g over 2000 cycles, demonstrating outstanding cycling stability, and an energy density of 65 Wh/kg. In conclusion, this study underscores the potential of integrating hemp biomass-derived carbon materials into water-based electrolytes, thus advancing the frontier of emerging aqueous zinc-ion hybrid supercapacitors in the international arena of novel electrode materials for energy systems.

**Keywords**: Hemp Biomass, Hard-Carbon electrodes, Hybrid Zn-ion supercapacitor, Water-based electrolyte

**Structural properties & surface morphologies of Sb doped ZnO thin films**

Sibel Gürakar[1*]

[1] *Ankara University, Department of Physics Engineering, Ankara, 06100 TURKEY*

[*]**Corresponding E-mail:** sgurakar@eng.ankara.edu.tr

Sb doped ZnO thin films with different doping ratios of 0, 1, 2, and 3 at % are grown by sol-gel dip coating method on glass substrates. The deposition voltage and temperature for 10 cycles of dipping are chosen as 24 V and 500 °C, respectively. The structural properties of Sb doped ZnO thin-films are analyzed by X-ray diffraction (XRD) method. The lattice parameters of the films are determined from XRD patterns. The crystallite size, strain and stress are obtained for all films using Williamson Hall Uniform Deformation Model (UDM), Uniform Stress Deformation Model (USDM), and Uniform Deformation Energy Density Model (UDEDM). Surface morphologies are investigated using atomic force microscope (AFM) measurements.

Keywords: ZnO, thin film, structural properties, surface morphologies

**The Effect of Sulfurization Temperature on As-prepared SnS Films Deposited by Ultrasonic Spray Pyrolysis**

I.Gunes[1], B. Demirselcuk[2*], E. Sarica[3], I. Akyuz[4], A. Kucukarslan[5], V. Bilgin[5]

*[1] Canakkale Onsekiz Mart University, Department of Electricity and Energy, Canakkale, 17200, TURKEY*
*[2] Canakkale Onsekiz Mart University, Department of Electricity and Energy, Canakkale, 17020, TURKEY*
*[3] Baskent University, Department of Electrical and Electronics Engineering, Ankara, 06790, TURKEY*
*[4] Department of Physics, Eskisehir Osmangazi University, Eskisehir, 26480, TURKEY*
*[5] Canakkale Onsekiz Mart University, Department of Physics, Canakkale, 17020, TURKEY*

[*]**Corresponding E-mail:** bdemirselcuk@comu.edu.tr

In this study, SnS films were deposited onto glass substrates using the ultrasonic spray pyrolysis technique at a substrate temperature of 350°C. Following deposition, the films were subjected to a sulfurization process by annealing in a tubular furnace with 50 mg of sulfur powder at three different temperatures (300°C, 350°C, and 400°C). The effect of sulfurization on the structural, morphological, and optical properties of the SnS films was investigated using X-ray diffraction (XRD), scanning electron microscopy (SEM), atomic force microscopy (AFM), and UV-vis spectrophotometry techniques. Structural analysis has revealed that all films were formed in an orthorhombic structure, and the crystallization levels of the films were significantly affected by the sulfurization process. Morphological analysis showed that the particles had a longitudinally elongated, rice-shaped surface structure. The optical band gaps were calculated to range from 1.60 eV to 1.86 eV.

***Keywords:*** *SnS thin films, Sulfurization temperature, Ultrasonic spray pyrolysis*

**Acknowledgements:** This work was supported by the Canakkale Onsekiz Mart University Scientific Research Projects Committee under the Project Number FBA-2022-3992.

**Cr based coatings electrodeposited by binary potential loop and their corrosion behaviour**

E.Kus[1*], M.Hacıismaıloglu[1] and M.Alper[1]
[1] *Uludag University, Department of Physics, Bursa, 16059 TURKEY*
[*]**Corresponding E-mail:** esrakus@uludag.edu.tr

Chromium (Cr) based coatings are widely used in industrial applications due to their high hardness, high corrosion and wear resistance, and low friction. The main problem is the cracks formed during the electrodeposition of the Cr coatings, which strongly affects the coating performance and life by reducing the mechanical strength and corrosion resistance. Up to now the electrodeposition modes and the parameters have been experimented to overcome this problem. In this study, Cr coatings were electrodeposited from an aqueous solution containing trivalent Cr ions ($Cr^{3+}$) as given in the schematic diagram in Fig. 1(a). A binary potential loop was designed for which -0.7 and -1.8 V were applied sequentially as shown in Fig. 1(b). The corresponding current density-time graph is presented in Fig. 1(c). Ni-Cr and Ni-Cr-Fe coatings were also electrodeposited by the binary potential loop. The corrosion behaviour of the coatings was investigated by open circuit potential, Tafel extrapolation and electrochemical impedance spectroscopy in 3.5% salt water (NaCl) solution. The corrosion potential, current and resistance were calculated from the Tafel curves (Fig. 1(d)). Based on these values, the corrosion resistance and corrosion rate were determined. Coatings electrodeposited by binary potential loop were found to have lower corrosion rates and higher resistance compared with those electrodeposited at constant potential and current. The structural and morphological properties were examined by using X-ray diffraction and scanning electron microscope, respectively. Some structural parameters such as the average grain size and lattice constants were calculated from XRD patterns. In the SEM images, it was seen that the size of the cracks on the surface of the Cr coatings decreased to nano-scale and the surface became smoother. As a result, the designed binary potential loop may be a promising method to improve the properties of the Cr-based coatings without using many chemicals.

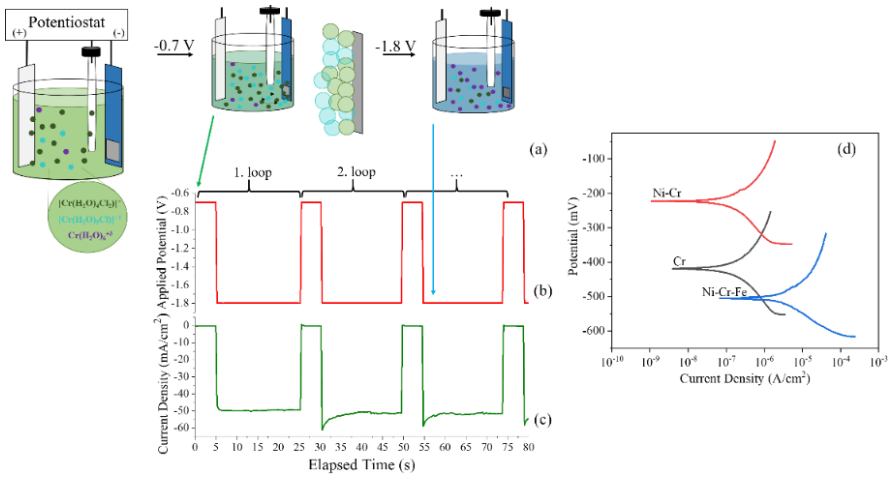


Fig.1. (a) Schematic diagram of the binary potential deposition, (b) the potential-time, (c) corresponding current-time transients recorded during Cr coating and (d) Tafel curves.

**Keywords:** Electrodeposition, Cr coating, corrosion, XRD, EIS

**Acknowledgements:** This work was supported by Uludag University under Grant No. FDK-2022-1262, FAY-2022-811 and UAP(F)-2010/56, and by TAI under Grant No. Ar-Ge-21-044.

**Analyzing the mechanical properties of an auxetic structure under compression**

Gülcan Aydin[1,2*], Sait Eren San[1]

[1] *Kocaeli University, Department of Physics, Kocaeli, 41001 TURKEY*
[2] *CMS Glass Machinery, Kocaeli, 41400 TURKEY*

[*]**Corresponding E-mail:** gulcan.aydin@kocaeli.edu.tr

Auxetic metamaterials, with their unique mechanical traits and negative Poisson's ratios, offer a promising path in material innovation. This study employs finite element analysis to explore into the mechanical dynamics of auxetic metamaterials, particularly focusing on re-entrant lattice structures. By investigating geometric array configurations, unit cell sizes, and thicknesses, it examines their impact on displacement, strain, von Misses stress, and Young's modulus. Meticulous numerical simulations reveal significant correlations between these parameters and structural integrity. These findings highlight the critical role of geometric arrangement, unit cell dimensions, and thickness in optimizing the design and performance of auxetic metamaterials across various engineering fields. By enhancing our understanding and offering valuable insights, this research advances the development and application of auxetic metamaterials.

# Investıgatıon Of Photocataltic Properties Of Rare Earth Element Oxides

Ece KALAY*1 İskender ÖZKUL*1 Ömer GÜLER*2 Canan AKSU CANBAY*3

*1 Mersin University, Faculty of Engineering, Department of Mechanical Engineering, Mersin, TURKEY
*2 Munzur University, Faculty of Engineering, Department of Mechanical Engineering, Tunceli, TURKEY
*3 Fırat University, Faculty of Science, Department of Physics, Elazig, TURKEY

ABSTRACT

This research extensively explores the photocatalytic efficacy and potential environmental utility of nanoparticles composed of rare earth oxides (REOs). REOs play a pivotal role in photo catalysis due to their efficiency across a wide spectrum of light and exceptional stability in photocatalytic processes. Photo catalysis encompasses crucial environmental functions like the decomposition of organic compounds and the electrolysis of water into hydrogen and oxygen. The study systematically investigates how various synthesis techniques and conditions influence the photocatalytic characteristics of REOs, holding promise for the effective elimination of organic contaminants. The findings shed light on diverse factors governing the photocatalytic efficiency of REOs. Notably, the selection of synthesis techniques and the incorporation of additives emerge as pivotal factors impacting the photocatalytic efficacy of REOs. Consequently, further investigation is warranted, particularly to delve into the influence of different additives and supporting materials on photocatalytic performance. The insights gleaned from this study could inform the development of more potent and efficient photo catalysts for environmental applications. Nevertheless, a comprehensive grasp and optimization of the photocatalytic attributes of REOs necessitate additional research. Therefore, it is recommended to delve deeper into exploring the effects of varied synthesis techniques and conditions on the photocatalytic efficacy of REOs.

*Keywords: rare earth metal oxides, photo catalytic activity,*

Corresponding author: eecekalay@gmail.com

## 1. Introduction

In today's world, environmental pollution and water contamination have become a globally increasing concern. Human activities such as industrialization, agriculture, and urban development are polluting water sources and harming natural systems. Especially, heavy metals, phenols, antibiotics, benzene, dyes, and other organic pollutants are causing water sources to become contaminated and unhealthy. This situation threatens the use of water and human health, and it causes serious damage to ecosystems. The need for innovative and effective solutions to deal with these threats is increasing day by day (Im et al., 2021).

In this context, photocatalytic reactions have emerged as a promising technology for reducing environmental pollution and purifying water sources, becoming one of the topics researchers are increasingly focusing on. By harnessing solar energy, photocatalytic materials can break down pollutants in environments such as water and air, transforming them into harmless compounds (Van Gerven, Mul, Moulijn, & Stankiewicz, 2007). Chemical stability and surface preparation are key features of semiconductor catalysts such as titanium dioxide ($TiO_2$), zinc oxide (ZnO), iron oxides ($Fe_2O_3$), and copper oxide (CuO), which are commonly employed in photocatalytic processes (Badvi & Javanbakht, 2021; Y. Liu et al., 2021; Truong et al., 2021). In recent years, the use of rare earth oxide (REO) as photo catalysts has gained attention. REOs demonstrate high activity in photocatalytic reactions, making them suitable for various applications such as water purification, air cleaning, and energy production. Particularly, the effectiveness of rare earth oxide in photocatalytic reactions such as the degradation of organic pollutants and hydrogen production has become a

frequently studied topic (Balaram, 2019). The aim of this study is to comprehensively examine the photocatalytic performance of rare earth oxide and its potential in environmental applications.

**2. Rare earth oxides and their photocatalytic efficiencies**

Photo catalysis is the process of accelerating or triggering chemical reactions using light, typically ultraviolet (UV) or visible light. These reactions are catalyzed by a special substance called a photocatalyst. Photo catalysis is employed in various applications including environmental remediation, water and air purification, solar energy conversion, and chemical synthesis (Sudha & Sivakumar, 2015). Photocatalytic reactions typically involve the following stages:

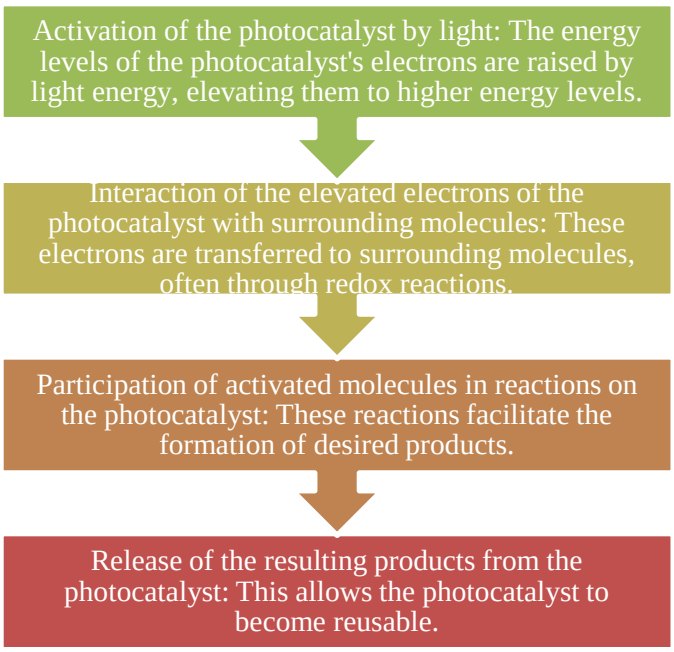


**Figure 1.** Photocatalytic reaction stages (De Lasa, Serrano, & Salaices, 2005)

Photocatalyst play three fundamental roles in photocatalytic reactions. Firstly, they absorb certain wavelengths of light, stimulating the excitation of electrons within them. This enables the photocatalyst to become active and initiate chemical reactions. Additionally, they create active catalytic sites on their surfaces or arrange molecules participating in reactions in suitable configurations, thereby facilitating the occurrence of reactions in a specific order and the formation of desired products (Van Gerven et al., 2007). Rare earth oxide is obtained through various methods such as oxidation, fractional crystallization, ion exchange, and hydrometallurgical methods. In the oxidation method, rare earth ores are subjected to oxidation by heating at high temperatures (usually in heated air or oxygen environment) (Patil, Patil, Dighavkar, Adole, & Tupe, 2022). As a result of this process, rare earth elements are converted into oxides. In the fractional crystallization method, rare earth ores are first washed and then processed using acids or bases. This process dissolves the rare earth elements, followed by obtaining their oxides. In the ion exchange method, minerals containing rare earth elements are exchanged with specific ions. Subsequently, compounds obtained from ion exchange are converted into oxides through thermal treatment or other chemical processes. In the hydrometallurgical method, ores are dissolved using acids or bases. The solution is then processed, and various chemical treatments are applied to separate and purify rare earth elements. Oxides are obtained as a result of these processes. (Leger, Yacoubi, & Loriers, 1981). The various rare earth elements are presented in Table 1 (Hussein, 1996).

**Table 1.** Rare earth element oxides (Hussein, 1996

| Elements | Oxides |
|---|---|
| Lantan | $La_2O_3$ |
| Cerium | $CeO_2$ |
| Praseodim | $Pr_6O_{11}$ |
| Neodim | $Nd_2O_3$ |
| Samarium | $Sm_2O_3$ |
| Europium | $Eu_2O_3$ |
| Gadolinium | $Gd_2O_3$ |
| Terbium | $Tb_4O_7$ |
| Holmium | $Ho_2O_3$ |
| Erbium | $Er_2O_3$ |
| Thulium | $Tm_2O_3$ |
| Ytterbium | $Yb_2O_3$ |
| Lutetium | $Lu_2O_3$ |
| Uranium | $UO_2$ |
| Plutonium | $PuO_2$ |
| Neptunium | $NpO_2$ |
| Americium | $AmO_2$ |

)

Lanthanum oxide ($La_2O_3$) among these REOs is a p-type semiconductor with tremendous dielectric constant, low cage energy, and a wide bandgap (Huo, Zhang, Jin, Zhu, & Li, 2008). Samarium, neodymium, and holmium oxide compounds hold significance as rare earth substances owing to their appropriateness in optical, ceramic, photovoltaic, nano electronic, semiconductor, detection, and catalytic purposes. They find utility across a broad spectrum of uses, spanning from everyday household products to cutting-edge aerospace technologies (T. Liu, Zhang, Shao, & Li, 2003). $CeO_2$, another oxide of a rare earth element, enjoys extensive utilization across diverse fields thanks to its exceptional attributes, including minimal toxicity and expense, robust oxygen retention capabilities, and remarkable chemical resilience (Escudero, Maffiotte, & Serrano, 2021). These properties of $CeO_2$ can promote the formation of abundant oxygen vacancies and enhance photocatalytic activity. However, $CeO_2$ has some disadvantages such as low specific surface area, wide bandgap (2.8 - 3.1 eV), and characteristics like high electron-hole recombination with low absorption in the visible range up to 400 nm. Therefore, various modifications are being attempted to address these drawbacks (Wen, Niu, Ruan, Zhang, & Zeng, 2017). The photocatalytic activity of rare earth element oxides is typically associated with their effectiveness across a wide spectrum of light and high photochemical stability. These oxides are particularly notable for their ability to catalyze various chemical reactions, especially using sunlight. For instance, a photocatalyst composed of rare earth element oxides can facilitate hydrogen production through the photocatalytic splitting of water. Additionally, certain crystallographic structures on the surface of rare earth element oxides can facilitate surface reactions and enhance their photocatalytic performances. These structures often contain high surface area and reactive surface groups, which in turn increase photocatalytic efficiency. Photo catalysis occurs in the presence of a photocatalyst (Hatch, 2012). Light-activated and capable of participating in chemical reactions, a material is under the influence of sunlight, electrons on the surface of the photocatalyst are elevated, enabling the catalyst to engage in chemical reactions (De Lasa et al., 2005). These reactions typically involve environmentally significant processes such as the breakdown of organic compounds or the splitting of water into hydrogen and oxygen. Photo catalysis involves the generation and interaction of active species (e.g., hydroxyl radicals, superoxide radicals) bound to the surface. These active species engage with molecules of interest on the surface of the photocatalyst, instigating chemical changes. It is established that pristine REOs exhibit desirable catalytic traits. For instance, they facilitate Hoffmann elimination reactions during the dehydration of 2-alcohols such as 2-butanol (Tanabe, Misono, Hattori, & Ono, 1990). Ytterbium (III) oxide, $Yb_2O_3$, is the most selective catalyst for the formation of alkenes: 4-methyl-2-pentanol and 2-butanol are dehydrated to form 4-methyl-1-pentene and 1-butene, respectively (Lundeen &

VanHoozer, 1967). It's established that fundamental $La_2O_3$ and $Sm_2O_3$ initiate methane activation for oxidative coupling reactions (Kennedy & Cant, 1991).

Rare earth element oxides have significant potential in the field of photo catalysis. Their crystallographic structures can facilitate surface reactions and enhance photocatalytic performances. Properties such as high surface area and reactive surface groups contribute to increased photocatalytic efficiency. They can be effectively utilized in processes such as hydrogen production through the photocatalytic splitting of water, degradation of air pollutants, and purification of water from contaminants. Rare earth element oxides play an important role in areas such as clean energy production, environmental protection, and chemical synthesis, and they have been the subject of researchers' studies in recent years. In the research led by Narasimharao and collaborators, three distinct rare earth metal oxides (samarium, neodymium, and holmium) were fabricated utilizing both organic and inorganic pathways. The impact of the synthesis approach on their physicochemical characteristics was explored employing various methods including X-ray diffraction (XRD), Fourier-transform infrared spectroscopy (FT-IR), thermogravimetric analysis, microscopy, and diffuse reflectance ultraviolet-visible spectroscopy. The examination uncovered that specimens produced through the organic pathway showcased notable effectiveness. Specifically, samarium oxide ($Sm_2O_3$) crafted via the organic technique displayed enhanced photocatalytic efficacy attributed to its diminished bandgap energy, augmented surface area, pore volume, and the existence of active surface -OH groups. Additionally, it was found that the synthesized rare earth metal oxide catalysts exhibited excellent recyclability for photocatalytic degradation of crystal violet (Narasimharao & Ali, 2020). In another study conducted by Chen and colleagues, a novel solid-state chemical synthesis method for the successful production of $CeO_2$ samples at room temperature was introduced by combining substances such as polyethylene glycol 400 (PEG 400), cetyltrimethylammonium bromide (CTAB), and sodium dodecyl sulfate (SDS). The specimens underwent characterization through methods including X-ray diffraction (XRD), transmission electron microscopy (TEM), scanning electron microscopy (SEM), BET analysis, and UV spectroscopy. It was established that the samples demonstrated elevated efficacy in the photocatalytic breakdown of methylene blue (MB). Additionally, it was concluded that samples supported by surfactants showed higher photocatalytic activity compared to samples without surfactants. Particularly, the sample containing SDS demonstrated the highest photocatalytic activity, achieving a methylene blue degradation rate of 89.6%. Under optimum conditions, the $CeO_2$ sample achieved a maximum MB degradation rate of up to 96.5%, surpassing commercial $TiO_2$ P25 under the same conditions. These results suggest that $CeO_2$ could be used as a potential photocatalyst for the removal of organic pollutants (Chen, Cao, & Jia, 2011). In recent years, $CeO_2$-based photo catalysts have become a frequently studied rare earth element oxide due to their superior properties such as unique fluorite-type structure, rigid framework, and the ability to easily reduce and oxidize between cerium tetravalent ($Ce^{4+}$) and trivalent ($Ce^{3+}$) valence states. In a study by Fauzi and colleagues, it was noted that due to the wide energy bandgap of $CeO_2$, the efficiency of solar energy utilization is low, thereby limiting its application in wastewater treatment. They emphasized the potential use of various modifications of $CeO_2$ to enhance its photo degradation performance. These modifications include metal and non-metal doping, addition of support materials, and coupling with another semiconductor. (Fauzi et al., 2022). In a study analyzing the dye degradation performance in wastewater treatment, remarkable photocatalytic activity was observed for $CeO_2$, $Gd_2O_3$, and GO (graphene oxides) nanocomposites (NCs). During the synthesis of NCs, the adapted and developed specific morphologies, surface areas, and properties such as having a bandgap that allows for the absorption of a wide spectrum of light, which is critical for photo catalysis, were found to enhance the photocatalytic efficiency (Al-Wafi, Hammad, & Mansour, 2024). In another study conducted by Singh and colleagues, the efficiency of mixed metal oxide nanocomposites, particularly those based on rare earth elements, in photocatalytic, electrochemical, and biological applications was investigated. The NiOCGSO [$NiO\text{-}Ce_{0.8}Gd_{0.2}O_{2-d}–Ce_{0.8}Sm_{0.2}O_{2-d}$] nanomaterial was synthesized via a wet chemical method. A crystal structure with a face-centered cubic (FCC) arrangement was identified, with XRD examination indicating the absence of any secondary phases. Metal-oxygen linkages were detected via FTIR analysis. The sample's morphology and elemental makeup underwent scrutiny via EDAX and SEM. UV-Vis spectroscopy was

employed to analyze the optical bandgap. Noteworthy responses were noted during electrochemical assessments (at a voltage of 1.3 V, spanning a frequency spectrum from 42 Hz to 5 kHz). Furthermore, the photocatalytic and antibacterial properties of the prepared NiO-CGSO nanocomposites were investigated. The studies demonstrated that this novel composite catalyst removed 92% of toxic pollutants from wastewater and exhibited superior antibacterial performance against bacterial pathogens such as Aeromonas hydrophila, E. coli, and S. epidermis. (Singh, Kumar, Srivastava, & Chowdhury, 2017).

**3. Results**

Rare earth oxide (REO) nanoparticles possess significant potential in photocatalytic reactions. This potential is associated with their effectiveness across a broad spectrum of light and their high photochemical stability. Their crystallographic structures can facilitate surface reactions and enhance photocatalytic performance, particularly through high surface area and reactive surface groups, which are crucial factors in increasing photocatalytic efficiency. Photocatalytic reactions typically involve environmentally significant processes such as the degradation of organic compounds and the splitting of water into hydrogen and oxygen. In these processes, rare earth oxide nanoparticles stand out for their ability to catalyze various chemical reactions using sunlight. Particularly, they can be effectively utilized in processes such as hydrogen production through the photocatalytic breakdown of water, as well as the degradation of air and water pollutants.

These studies demonstrate the significant potential of rare earth oxide nanoparticles in environmental applications and their effectiveness in removing organic pollutants. However, further research is needed to enhance their photocatalytic performance. Specifically, more investigation into various modifications is required to optimize their properties. It is crucial to explore in detail the effects of different synthesis methods and conditions on the photocatalytic properties of rare earth oxide nanoparticles. Additionally, the impact of different additives and support materials on photocatalytic activity needs to be investigated. The results of these studies could contribute to the development of more effective and efficient photocatalysts for environmental applications.

**References:**

Al-Wafi, R., Hammad, M. S., & Mansour, S. (2024). Superior dye degradation for wastewater treatment based on nanocomposites of cerium oxide, gadolinium oxide and graphene oxide. Ceramics International, 50(10), 16736-16746.

Badvi, K., & Javanbakht, V. (2021). Enhanced photocatalytic degradation of dye contaminants with $TiO_2$ immobilized on ZSM-5 zeolite modified with nickel nanoparticles. Journal of Cleaner Production, 280, 124518.

Balaram, V. (2019). Rare earth elements: A review of applications, occurrence, exploration, analysis, recycling, and environmental impact. Geoscience Frontiers, 10(4), 1285-1303.

Chen, F., Cao, Y., & Jia, D. (2011). Preparation and photocatalytic property of $CeO_2$ lamellar. Applied surface science, 257(21), 9226-9231.

De Lasa, H. I., Serrano, B., & Salaices, M. (2005). Photocatalytic reaction engineering (Vol. 590): Springer.

Escudero, M., Maffiotte, C., & Serrano, J. (2021). Long-term operation of a solid oxide fuel cell with MoNi–$CeO_2$ as anode directly fed by biogas containing simultaneously sulphur and siloxane. Journal of Power Sources, 481, 229048.

Fauzi, A., Jalil, A., Hassan, N., Aziz, F., Azami, M., Hussain, I., . . . Vo, D.-V. (2022). A critical review on relationship of $CeO_2$-based photocatalyst towards mechanistic degradation of organic pollutant. Chemosphere, 286, 131651.

Hatch, G. P. (2012). Dynamics in the global market for rare earths. Elements, 8(5), 341-346.

Huo, Y., Zhang, X., Jin, Y., Zhu, J., & Li, H. (2008). Highly active $La_2O_3/Ti_{1-x}B_xO_2$ visible light photocatalysts prepared under supercritical conditions. Applied Catalysis B: Environmental, 83(1-2), 78-84.

Hussein, G. A. (1996). Rare earth metal oxides: formation, characterization and catalytic activity thermoanalytical and applied pyrolysis review. Journal of analytical and applied pyrolysis, 37(2), 111-149.

Im, J. K., Sohn, E. J., Kim, S., Jang, M., Son, A., Zoh, K.-D., & Yoon, Y. (2021). Review of MXene-based nanocomposites for photocatalysis. Chemosphere, 270, 129478.

Kennedy, E. M., & Cant, N. W. (1991). Comparison of the oxidative dehydrogenation of ethane and oxidative coupling of methane over rare earth oxides. Applied catalysis, 75(1), 321-330.

Leger, J., Yacoubi, N., & Loriers, J. (1981). Synthesis of rare earth monoxides. Journal of Solid State Chemistry, 36(3), 261-270.

Liu, T., Zhang, Shao, & Li, X. (2003). Synthesis and characteristics of Sm2O3 and $Nd_2O_3$ nanoparticles. Langmuir, 19(18), 7569-7572.

Liu, Y., Guo, R., Shen, G., Li, Y., Li, Y., Gou, J., & Cheng, X. (2021). Construction of CuO@ CuS/PVDF composite membrane and its superiority for degradation of antibiotics by activation of persulfate. Chemical Engineering Journal, 405, 126990.

Lundeen, A. J., & VanHoozer, R. (1967). Selective catalytic dehydration. Thoria-catalyzed dehydration of alcohols. The Journal of Organic Chemistry, 32(11), 3386-3389.

Narasimharao, K., & Ali, T. T. (2020). Influence of synthesis conditions on physico-chemical and photocatalytic properties of rare earth (Ho, Nd and Sm) oxides. Journal of Materials Research and Technology, 9(2), 1819-1830.

Patil, A. S., Patil, A. V., Dighavkar, C. G., Adole, V. A., & Tupe, U. J. (2022). Synthesis techniques and applications of rare earth metal oxides semiconductors: A review. Chemical Physics Letters, 796, 139555.

Singh, K., Kumar, K., Srivastava, S., & Chowdhury, A. (2017). Effect of rare-earth doping in $CeO_2$ matrix: correlations with structure, catalytic and visible light photocatalytic properties. Ceramics International, 43(18), 17041-17047.

Sudha, D., & Sivakumar, P. (2015). Review on the photocatalytic activity of various composite catalysts. Chemical Engineering and Processing: Process Intensification, 97, 112-133.

Tanabe, K., Misono, M., Hattori, H., & Ono, Y. (1990). New solid acids and bases: their catalytic properties: Elsevier.

Truong, T. K., Nguyen, T. Q., La, H. P. P., Le, H. V., Van Man, T., Cao, T. M., & Van Pham, V. (2021). Insight into the degradation of p-nitrophenol by visible-light-induced activation of peroxymonosulfate over Ag/ZnO heterojunction. Chemosphere, 268, 129291.

Van Gerven, T., Mul, G., Moulijn, J., & Stankiewicz, A. (2007). A review of intensification of photocatalytic processes. Chemical Engineering and Processing: Process Intensification, 46(9), 781-789.

Wen, X.-J., Niu, C.-G., Ruan, M., Zhang, L., & Zeng, G.-M. (2017). AgI nanoparticles-decorated CeO2 microsheets photocatalyst for the degradation of organic dye and tetracycline under visible-light irradiation. Journal of colloid and interface science, 497, 368-377.

# Temperature and frequency dependence of the dielectric properties of novel chalcone based methacrylate polymer

Mahmut Yılmaz[1*], Fatih Biryan[1], Eray Çalışkan[2]
[1]*Firat University, Department of Chemistry, Elazig, 23200 Türkiye*
[2]*Bingol University, Department of Chemistry, Bingöl, 12000 Türkiye*

[*]**Corresponding E-mail:** yilmaz886@hotmail.com

Polymer-based dielectric materials have been extensively studied in recent years. Herein, we report the effect of temperature and frequency on the dielectric properties of novel chalcone based polymer. For this purpose, new methacrylate monomer was synthesized and its homopolymer was obtained according to free radical polymerization. The structures of monomer and homopolymer were characterized using FT-IR, $^{1}$H-NMR and $^{13}$C-NMR techniques. Dielectric properties play an important role in identifying electronic materials. Low dielectric constant and dielectric loss values in electronic materials shorten the signal transmission time and reduce heating.

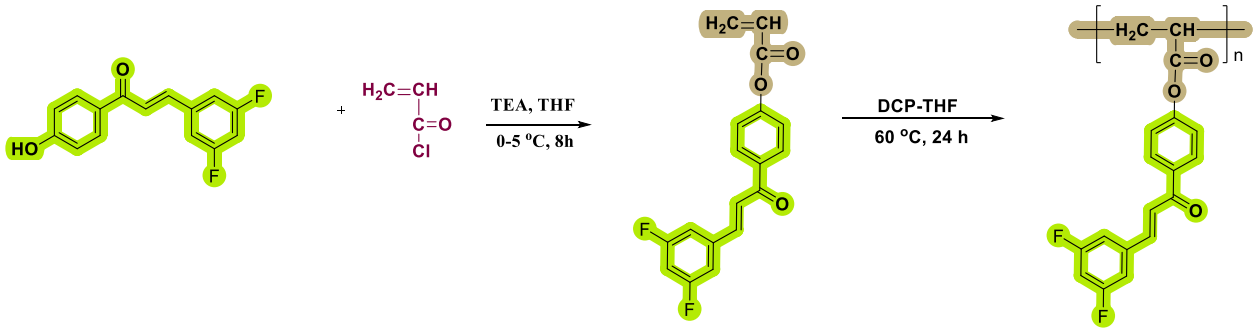


Fig.1 Synthesis of chalcone based monomer and polymer

The dielectric measurements of the composites were investigated using the impedance analyzer technique in the frequency range of 1-100 kHz. Dielectric constant (ε') Dielectric Loss (ε') and AC conductivity (σac) of polymer/MoS2 composites were measured. In addition, the dielectric properties of composites were examined as a function of temperature. It can be clearly that the dielectric constants of the polymer decrease slightly with increasing the frequency. In addition, the dielectric properties of polymer were increased by increasing the temperature. Conjugation and polar functional in the polymer structure groups have a significant effect on the dielectric constant.

**References**

1- Tamilvanan M, Pandurangan A, Subramanian K, Reddy BSR, 2008. Synthesis and characterization of mono- and di-methoxy substituted acrylate polymers containing photocrosslinkable pendant chalcone moiety. Polymers and Advanced Technologies, 19: 1218-1225.
2- Yakuphanoglu F, Okutan M, Zhuang Q, Han Z, 2005. The dielectric spectroscopy and surface morphology studies in a new conjugated polymer poly(benzobisoxazole-2,6-diylvinylene), Physica B: Condensed Matter, 365: 13-19.

# Investigation of Possible Current Transport Mechanisms (CTMs) of Quaternary Functional Semiconductor Device in a wide temperature and voltage range

S. Altındal Yerişkin[1], K. Yıldız[1], A. Dere[3], Y. Orman[4], F. Yakuphanoğlu[4], Ş. Altındal[5]

[1] *Gazi University, Vocational Highschool of Technical Sciences, Department of Chemistry and Chemical Processing Technologies, Turkey*
[2] *Department of Advanced Technologies, Faculty of Science, Gazi University, Ankara, Turkey*
[3] *Department of Electric and Energy, Vocational School of Technical Science, Firat University, Elazig, Turkey*
[4] *Department of Physics, Faculty of Science, Fırat University, Elazıg, Turkey*
[5] *Department of Physics,Faculty of Science, Gazi University, Ankara, Turkey*

[*]**Corresponding E-mail:** altundal@gazi.edu.tr

**ABSTRACT**

The Al/(Zn:Cd:Ni:$TiO_2$)/p-Si device with (4:2:2:2) ratios were prepared and then investigated possible CTMs of them in temperature range of 80-380 K and voltage range of ±4.5V using current-voltage (I-V) measurements. Reverse saturation-current (Io), ideality-factor (n), and barrier-height (BH)/($F_{bo}$) values were calculated from the semi-logarithmic $I_F$-$V_F$ curve for each-temperature. Experimental results show that while $F_{bo}$ value increases with increasing temperature, n decreases. The observed deviation from the linearity in the conventional Richardson plot (ln(Io/T2)-q/kT) at low-temperatures, very lower-value of Richardson-constant ($A^*$) calculated from this-plot when compared its theoretical-value (=32 A. $(cm.K)^{-2}$ for p-Si), and higher-values of n at lower-temperatures shows that deviation from the thermionic-emission (TE) theory. To explain this-situation; nkT/q-kT/q, $F_{bo}$-n and $F_{bo}$ -q/2kT graphs were drawn to obtain some-evidence to other possible-CTMs, and they show that both the tunnelling and Double-Gaussian-distribution (DGD) of BH are also effective CTMs rather than TE. Because experimental A* value obtained from the modified Richardson-plot by using standard-deviation from $F_{bo}$ -q/2kT plot was found very closer its theoretical-value. Energy-dependent density of surface-states/traps ($N_{ss}$/$D_{it}$) was also extracted from the $I_F$-$V_F$ data by taken into acount voltage-dependent variation of both effective-BH ($F_e$(V) and n(V) for each-temperature and they were found decrease with increase in temperature due to the restructuring of electrons at interface-states under the influence of temperature.

Keywords: Current-transport mechanisms (CTMs); Temperature dependent; Energy dependent of surface-states (Nss), Double Gaussian distribution of BH, Temperature sensitivity

# Over- Grinding of Biocoal-Chalcopyrite Concentrate Mixture

Selman YILMAZ[1], Canan AKSU CANBAY[2*], Mustafa SÜNER[1], Emrah ÇELİK[1], Elif ARANCI ÖZTÜRK[3], Oktay KARADUMAN[4], Güneş BAŞBAĞ[1], Mustafa BOYRAZLI[1]

[1]Fırat University, Faculty of Engineering, Department of Metallurgical and Materials Engineering, Elazig, TURKIYE

[2]* Department of Physics, Faculty of Science, Firat University, Elazig, TURKIYE

[3]Balıkesir University, Vocational School of Balıkesir, Department of Mechanical and Metal Technologies, Balıkesir, TURKIYE

[4]Rare Earth Elements Application and Research Center, Munzur University, Tunceli, TURKIYE

ABSTRACT

In this study, the biochar- chalcopyrite concentrate mixture prepared for the direct reduction of chalcopyrite were examined the changes in the physical structure in as a result of subjecting it to over-grinding. For this purpose, biochar, concentrated chalcopyrite and quicklime mixed in stoichiometric ratio were over-grinded in a spex type mill for different periods of time and the XRD images of the resulting products were examined. In the XRD images, it was seen that there was a large amount of amorphization in the crystal structure as a result of over- grinding of the material for 60 minutes.

*Keywords: Chalcopyrite, Biochar, Over-Grinding*

Corresponding author: caksu@firat.edu.tr

## 1. Introduction

The production from sulphurous ores Cu, Ni, Co and Pb metals by traditional pyrometallurgical methods involves different roasting, melting and conversion steps. The sulphur dioxide gas released during these steps causes major environmental problems. Therefore, these non-ferrous metals related industries in general and the copper industry in particular are under intense pressure towards reducing sulfur oxide emissions. In older methods, the $SO_2$ concentration in the exit gases is too low to allow economical sulfuric acid production. Although the concentration of $SO_2$ is higher in modern processes and sulfuric acid can be produced economically, the large amount of the gas creates new problems. Therefore, in recent years, many attempts have been made to develop new processes for the purification of copper sulfide concentrates that do not cause significant air pollution through $SO_2$ emissions [1-9].

The pyrometallurgical production technology of copper changed towards the end of the last century, from reverberatory, flash, vertical and electric furnaces towards converter. However, the reverberatory furnace proved to be an inefficient and polluting reactor, and as a result, many attempts were made to replace the system. Over the past 50 years, new successful melting processes that are more energy efficient and less polluting have been introduced on an industrial scale. Additionally, melting and conversion were carried out in a single reactor where the concentrate was fed and raw copper was produced [10].

Over-grinding, which is one of the pre-treat processes of mechanochemistry, increases the specific surface area of the mineral grains, making it easier for new surfaces to emerge and for these surfaces to come into contact with reagents. During grinding is happening mechanical activation most of the energy generated by transferring to the mineral [11-13].

Mills used for extreme grinding; They are classified as ball mill, planetary mills, spindle mills, centrifugal mills, eccentric vibrating mills, rolling mill, jet mills and vibrokinetic mills. Mills are shown schematically in Figure 1.

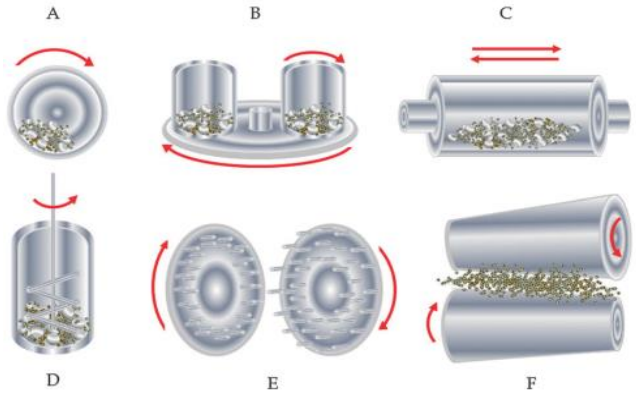


***Figure-1.*** *Mill Types Used for Advanced Grinding Process, A-Ball Mill, B-Planetary Mill, C-Vibrating Mill, D-Agitated Ball Mill (Atritor), E-Spindle Mill, F-Rolling Mill (10).*

In this full text, the first stage of the study aimed at obtaining directly reduced copper from chalcopyrite is presented. The changes in the physical structure of the biochar-chalcopyrite concentrate mixture as a result of subjecting it to over-grinding were examined.

**2. Experimental details**

2.1 Material

In the studies, chalcopyrite concentrate supplied from Yıldızlar Holding A.Ş. located in Elazığ Maden district, commercially purchased calcium oxide and almond shells carbonized as biochar were used. In the analysis of almond shells after carbonization, it was determined that they had 92.36% C and 0.018% S content. The analysis of the chalcopyrite concentrate used is given in Table 1.

***Table 1.*** *Analysis of chalcopyrite concentrate.*

| Component | Amount | Component | Amount |
|---|---|---|---|
| Cu | 19.03 (%) | Ag | 12.06(ppm) |
| Fe | 33.32 (%) | Al | 0.60 (%) |
| S | 26.56 (%) | Co | 1159.0 (ppm) |

Calcium oxide

CARLO ERBA brand calcium oxide with CAS No: 1305-78-8 was used in the preparation of the mixtures.

Balls

Steel balls with a diameter of 6 mm were used in spex mill experiments used for mechanical grinding.

- Speks Chamber

The spex chamber shown in Figure 2, where the mechanical grinding process is carried out, is a chamber specially manufactured from tungsten carbide with a depth of 56 mm, an inner diameter of 48 mm and a wall thickness of 7 mm.

***Figure-2.*** *Spex chamber.*

- Speks Mill

For mechanical grinding processes, MTI Corporation SFM-3 Desk-Top High Speed Vibrating Ball Miller branded shown in Figure 3, spex mill, a high energy ball mill, was used.

***Figure-3.*** *Spex mill.*

After the advanced grinding process, the spex chamber was opened in the nitrogen gas atmosphere in the glove-box shown in Figure 4, and the ground powders were removed and placed in ziplock bags.

- Glove-box

It is an airtight box specially designed from a plastic storage container with a length of 400 mm, a width of 270 mm, a depth of 280 mm and a volume of 30 liters. A gas valve was installed in the plastic box to ensure gas entry, and a gaz valve with an internal diameter of 15mm was installed to ensure gas exit. Plastic gaskets were attached to the inner and outer sides of the valves, and the operations made inside the box were carried out in a nitrogen gas atmosphere.

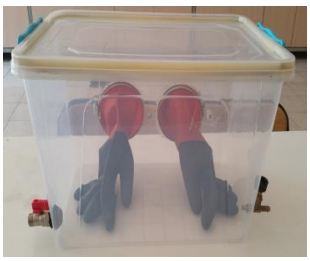

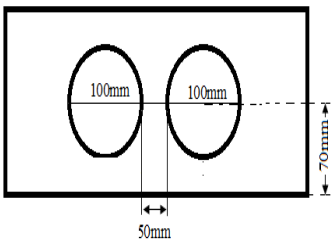

***Figure-4.*** *Glove box*

- XRD Analysis

XRD analysis of samples and original mixture after over-grinding were performed on the Rigaku Mini Flex 600 brand X-Ray Diffractometer.

- TG/DTA analyzes

After the over-grinding process, the samples thermal characterization analyzes were performed a Shimadzu brand DTG-60AH model differential thermal analysis (DTA) device. TG/DTA curves characterizing the behavior of the samples against thermal effects were obtained by measurements made by heating and cooling the samples between room temperature and 750 $^{o}$C, at a heating/cooling rate of 20 $^{o}$C/minute in an air environment with a constant flow of 100 ml/minute.

2.2. Method

Before starting the studies, the chalcopyrite concentrate was a grain size analysis and it was determined that it had a grain size of -200 µm. Then, biochar and CaO were pretreated to be in size of -200 µm and experiments were started.

In the study, biochar, chalcopyrite concentrate and quicklime (CaO) were prepared in stoichiometric ratio according to the equation (1) given below and over-grinding was done in the spex mill. In the over - grinding process, the powder mixture/ball ratio was determined as 1/20, so that one third of the spex chamber was filled with the mixture prepared stoichiometrically, and 7.5 g of powder mixture and 150 g of balls were weighed and placed in the spex chamber. The over-grinding process was determined as 15 min, 30 min and 60 min. After the $CuFeS_2$ concentrate was subjected to over-grinding in the spex mill with C and CaO for different periods of time, the resulting product was removed from the spex mill chamber in the argon gas atmosphere in the glove-box and the samples were name into S15, S30 and S60 depending on the grinding times.

$$CuFeS2(s) + 2CaO(s) + C(s) = Cu(s) + FeO(s) + 2CaS(s) + CO(g) \quad (1)$$

**3. Results and discussion**

- XRD and Grain Size Analyzes

XRD images of the samples applied over-grinding and the original mixture without grinding are given in Figure 5. Literature peak data of chalcopyrite are seen in Table 2.

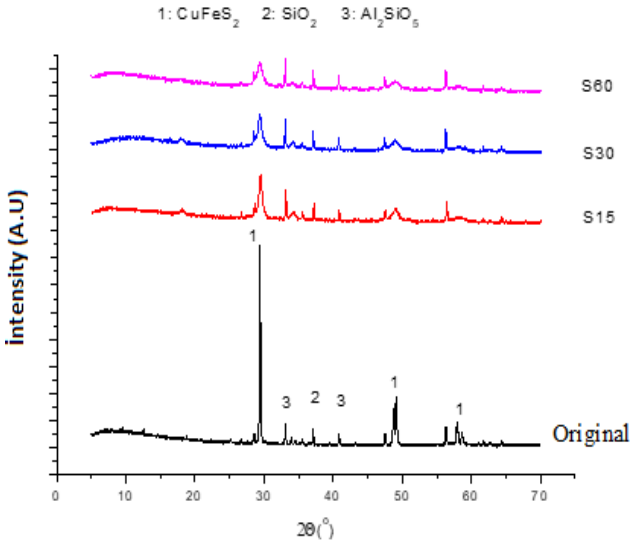


***Figure-5.*** *XRD images of the original mixture and the samples subjected to over-grinding.*

***Table 2.*** *XRD literature peak data of chalcopyrite [14].*

| 2 θ (°) | Intensity (A.U) | 2 θ (°) | Intensity (A.U) |
|---|---|---|---|
| 29.25 | 100.00 | 58.30 | 10.50 |
| 33.73 | 6.06 | 60.67 | 1.75 |
| 34.26 | 2.89 | 70.93 | 4.56 |
| 48.44 | 18.43 | 72.18 | 2.15 |
| 48.84 | 35.88 | 78.51 | 3.47 |
| 57.60 | 21.93 | 79.11 | 6.77 |

It is seen that the dominant peak of chalcopyrite in the original sample decreased due to excessive grinding time. It can be said that nanostructures are formed by grinding processes in the mill chamber. Grinding temperature is expected to have a significant effect on the formation of these structures. During grinding, two types of temperature effects are generally taken into account: local temperatures resulting from the collision of the balls with each other and with the powder material, and temperatures created by the balls hitting the walls inside the chamber. It can be said that with over-grinding, the powders in the concentrate are affected by these two temperatures and the crystal structure is disrupted. However, it appears that the silicate structure remains intact. Whereas according to the Mohs Hardness Scale, the hardness of quartz is 7, the hardness of steel balls is around 5.5-6. Considering the grinding environment and grinding materials selected for the over-grinding process, the peaks of these minerals should not change after grinding. However, the chalcopyrite peak should be expected to decrease with grinding time.

Grain size distribution analysis of the milled material was performed and these results are given in Table 3 and Figure 6.

***Table 3.*** *Grain size distribution analysis of the milled material*

| Grinding time | Size of more than 80% of material ($d_{80}$) (µm) |
|---|---|
| 15 | 9,46 |
| 30 | 5,240 |
| 60 | 6,042 |

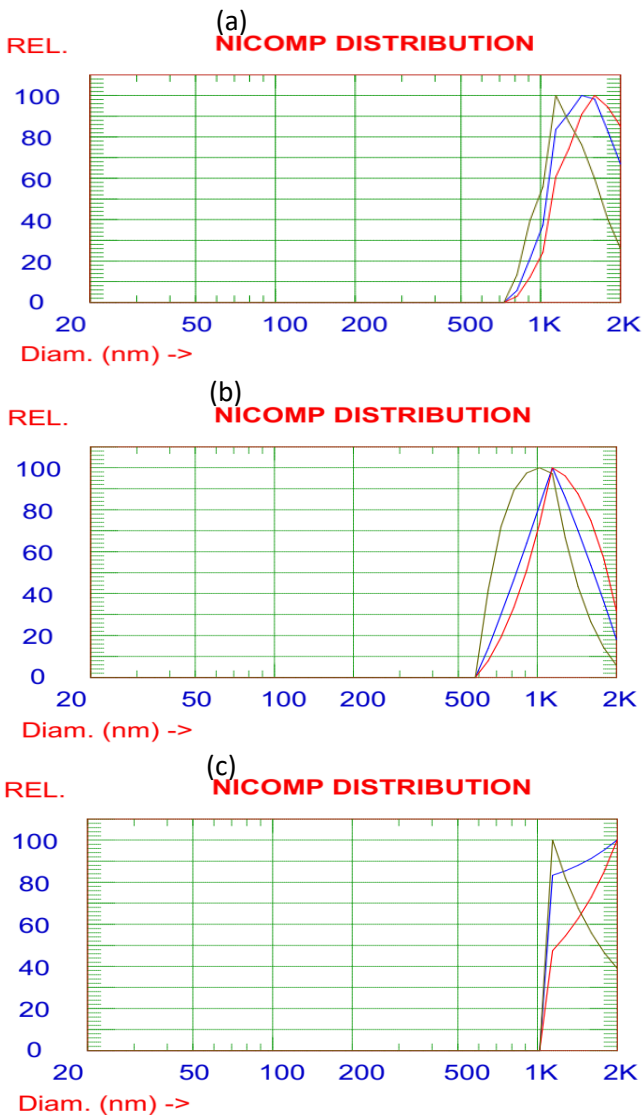


***Figure-6.*** *Grain size distribution analysis of the milled material (a) 15 minutes, (b) 30 minutes, (c) 60 minutes*

When the grain size distribution analyzes (Figure 6) made as a result of the grinding processes are examined, it is seen that 80% of the material falls below 5 µm, especially after 30 minutes of grinding.

- TG/DTA Analysis

Thermogravimetric analysis (TGA) is a technique that records the change in mass of the sample as a function of temperature. Whereas the differential thermal analysis (DTA) method, the same temperature program is applied to the sample and a thermally inert reference material, and the difference between the two is measured as a function of

temperature. These two substances are heated together by increasing the temperature smoothly. Dehydration, decomposition, melting, evaporation and sublimation events are endothermic, while amorphization, crystallization from amorphous state, solidification, formation of a new crystal structure from the crystal structure are exothermic [15].

TG/DTA curves characterizing the behavior of the original mixture against thermal effect after the over-grinding process are given in Figure 7.

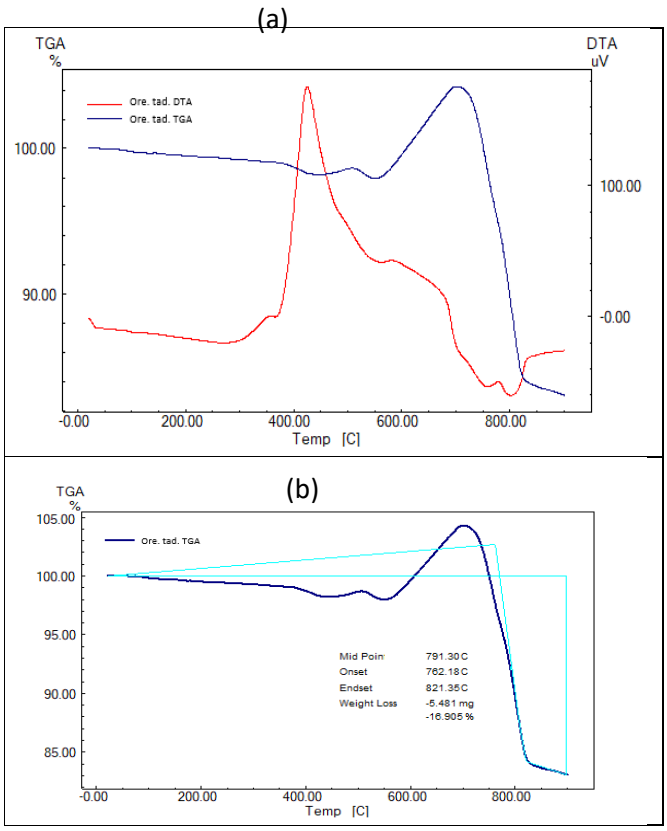


***Figure-7.*** *a)TG/DTA analysis, b) TGA analysis peak values of the original sample in air.*

From the TG/DTA images given in Figure 7 (a), it can be seen that endothermic reactions start at 380 °C and continue until 700 °C, and exothermic reactions start and continue after 700 °C. These analyzes performed in the atmospheric environment show that the oxygen in the environment reacts with the sulfur in the chalcopyrite, therefore, first, endothermic reactions occur until a weight increase and the ignition temperature of the sulfur, and then exothermic reactions begin as a result of the burning of the sulfur. At a temperature of approximately 400 °C, the burning of carbon is starting. When the TGA values given in Figure 7 (b) are examined, it is seen that the sample experienced approximately 16.905% weight loss.

For the temperatures at which TG/DTA analysis were taken, it is stated in the literature that the reactions and fundamental changes occurring can be explained by the following reactions.

Pirit: 200-300 °C :

$FeS_{2(S)} \rightarrow FeS_{(S)} + 1/2S_{2(g)}$ (2)

It breaks down according to the reaction (2).

Chalcopyrite: thermal decomposition:

$2CuFeS_{2(S)} \rightarrow Cu_2S_{(S)} + 2\ FeS_{(s)} + 1/2S_{2(S)}$ (3)

The result of give elemental sulfur.

Kovellin: from 358 °C:

$2CuS_{(s)} \rightarrow Cu_2S_{(s)} + 1/2\ S_{2(g)}$ (4)

In TG/DTA analyzes of the original sample performed in air, it is seen that these endothermic reactions occur between approximately 300-700 °C. In thermogravimetric analysis, the increase in weight after 400 °C can be said that iron sulphide and copper sulphide compounds reacting with the oxygen of the air are oxidized, causing weight increase first, and then with the start of exothermic reactions, these oxidized structures move away from the structure, causing weight decrease.

It is claimed that sulfation reactions occur directly between sulfur and oxygen, not through oxides, and that the formation of copper sulfate starts at 350 °C and is maximum at 550 °C. At around 500 °C, it is suggested that CuSO4 and CuO can combine to form basic sulfate ($CuO.CuSO_4$), likewise at 650 °C the sulfate will decompose to basic sulfate and at 700 °C with the increase in temperature it will turn into CuO and $SO_3$ [16].

$FeSO_4 + Fe_2O_3 \rightarrow FeO.\ Fe_2O_3 + SO_3$ (5)

$CuSO_4 + Fe_2O_3 \rightarrow CuO.Fe_2O_3 + SO_3$ (6)

These reactions cause the breakdown of sulfates and the formation of ferrites. Copper ferrite formation is starting at 600 °C.

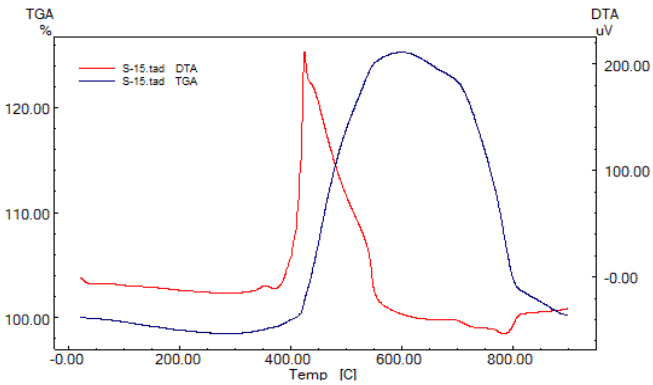


***Figure-8.*** *a) TG/DTA analysis of the sample subjected to 15-minute over-grinding.*

TG/DTA analysis of the sample subjected to 15 minutes of over-grinding is given in Figure 8. The reactions that may occur when chalcopyrite is grinding mixed with carbon and then subjected to heat treatment should be expected to be as follows.

$CuFeS_{2(s)} + 2CaO_{(s)} + C_{(s)} = Cu_{(s)} + FeO_{(s)} + 2CaS_{(s)} + CO_{(g)}$ (7)

$CuFeS_{2(s)} + 2CaO_{(s)} + CO_{(g)} = Cu_{(s)} + FeO_{(s)} + 2CaS_{(s)} + CO_{2(g)}$ (8)

In this case, we can say that the reactions that sulfur have give in the original sample (Figure 7 (a) and (b)) did not occur here. Here, sulfur is being held by CaO and $CO_2$ or CO gas is released into the environment. Therefore, weight loss too will remain low depending on the amount of carbon added in stoichiometric ratio.

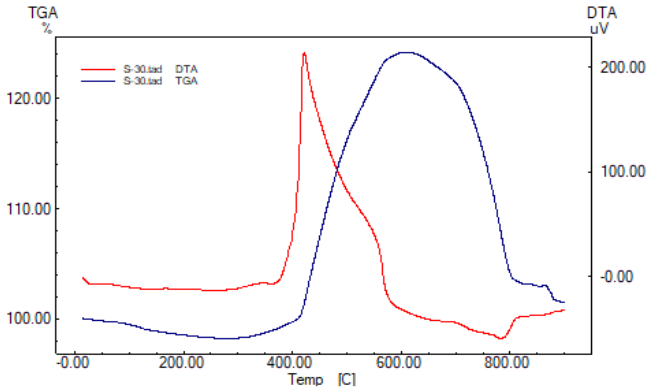


***Figure-9.*** *TG/DTA analysis of the sample subjected to 30-minute over-grinding in air.*

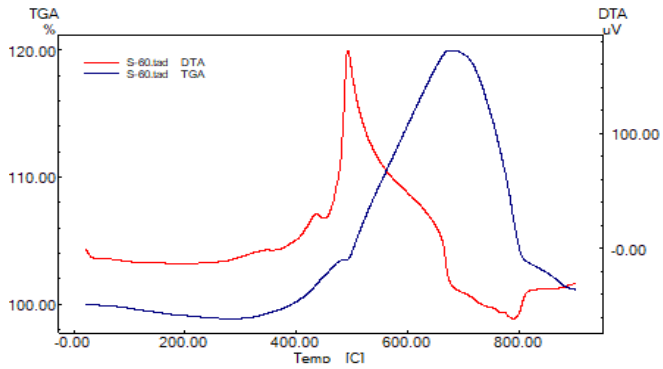


***Figure-10.*** *TG/DTA analysis of the sample subjected to 60-minute over-grinding in air.*

Figure 9 and Figure 10 show the TG/DTA analyzes of samples subjected to over-grinding for 30 minutes and 60 minutes, respectively. When the images are examined, it can be said that after an almost 20% weight increase that started with endothermic reactions, an exothermic reaction started (~620 °C) and a tendency to decrease in weight began from after this temperature. However, the total weight loss was not the same as in the original sample and remained lower. We can attribute the low weight loss to equation (1) above.

**4. Conclusion**

In this study, the changes in the physical structure of the biochar-chalcopyrite concentrate mixture prepared for the direct reduction of chalcopyrite were examined as a result of subjecting it to over-grinding. Biochar, chalcopyrite concentrate and quicklime (CaO) were blended in a stoichiometric ratio and subjected to over-grinding in a spex mill.

It was observed that with excessive grinding, the dominant peak of chalcopyrite in the original sample decreased depending on the excessive grinding time. The formation of nanostructures through grinding processes triggered this. Especially after 30 minutes of grinding, it is seen that 80% of the material falls below 5 µm. Grinding temperature is expected to have a significant effect on the formation of nanostructures. It can be said that the powders in the concentrate are affected by these temperature increases as a result of both the local temperatures resulting from the

collision of the balls with each other and the powder material during grinding, and the temperatures created by the balls hitting the walls in the chamber, and the crystal structure is deteriorated. However, it was observed that the silicate structure remained intact.

When TG/DTA analyzes were examined, it was seen that after an almost 20% weight increase that started with endothermic reactions, an exothermic reaction started (~620 °C) and a tendency to decrease in weight began from after this temperature. However, it was observed that the total weight loss was not as in the original sample and remained lower.

**References:**

[1] JHA A., GRIEVESON, P., JEFFES, J.H. (1989), An Investigation on The Carbothermic Reduction of Copper Sulfide Minerals: Kinetic and Thermodynamic Considerations, Scandinavian Journal of Metallurgy, 18, pp. 31-45.

[2] MOINPOUR, M., RAO, Y. K., (1985). Direct Reduction of Copper Sulfide with Carbon in The Presence of Lime, Canadian Metallurgical Quarterly, Vol. 24, No. 1, pp. 69-81.

[3] MACHINGAWUTA, N., JHA, A., GRIEVESON, P., (1989). Mechanism of Carbothermic Reduction of Nickel Sulfide Minerals in The Presence of Lime, Scandinavian Journal of Metallurgy, 18, pp. 81-88.

[4] EL-RAHAIBY, S. K., RAO, Y. K., (1984). Cell Measurements of The Reduction Potentials of Gas-Phase Emanating from Pbs/Cao/C at Elevated Temperatures, Metall. Trans. 15B, 19.

[5] BRONSON, M. C., SOHN, H. Y., (1983). The Carbothermic Reduction of Nickel Sulfide in The Presence of Lime, Metallurgical Transaction B, Vol. 14B, December, pp. 605-615.

[6] TERRY, B. S., RIVEROS, G., SANCHEZ, M., JEFFES, J. H. E., (1984). Lime-Concentrate Process for Roasting of Copper-Bearing Sulphides-Part 1 : Analysis of Optimum Roasting Conditions, Trans. Instn Min. Metall. (Sec. C: Mineral process, Extr. Metall.), 103, C193-200.

[7] TERRY, B. S., RIVEROS, G., SANCHEZ, M., JEFFES, J. H. E., (1984). Lime-Concentrate Process for Roasting of Copper-Bearing Sulphides-Part 2: Effect of Sulfide: Lime Ratio, Air Flow Rate, Pellet Size and Porosity on Reaction Kinetics, Trans. Instn Min. Metall. (Sec. C: Mineral process, Extr. Metall.), 103, C201-209.

[8] TERRY, B. S., RIVEROS, G., SANCHEZ, M., JEFFES, J. H. E.,(1984). Lime-Concentrate Process for Roasting of Copper-Bearing Sulphides-Part 3 : Mechanism of Roasting Reactions, Trans. Instn Min. Metall. (Sec. C: Mineral process, Extr. Metall.), 103, C210-216.

[9] KHAKI, J. V., SOLEIMANI, S. H., NEJAD, M. M. (2007). Direct Reduction of Sarcheshme Copper Sulfide Concentrate with Carbon in The Presence of Lime. Iranian Journal of Materials Science, 4(1).

[10] HABASHI, F. (2007). Copper Metallurgy at The Crossroads. Journal of Mining and Metallurgy B: Metallurgy, 43(1), 1-19.

[11] BALÁŽ, P., ACHIMOVIČOVÁ, M., BALÁŽ, M., BILLIK, P., CHERKEZOVA-ZHELEVA, Z., CRIADO, J. M., WIECZOREK-CIUROWA, K. (2013). Hallmarks of Mechanochemistry: From Nanoparticles to Technology. Chemical Society Reviews, 42(18), 7571-7637.

[12] BALÁŽ, P. (2003). Mechanical Activation in Hydrometallurgy. International journal of mineral processing, 72(1-4), 341-354.

[13] WANG, Y., and FORSSBERG, E. (2007). Enhancement of Energy Efficiency for Mechanical Production of Fine and Ultra-Fine Particles in Comminution. China Particuology, 5(3), 193-201.

[14] https://rruff.info/chalcopyrite/display=default/

[15] ARANCI, E.Ö., 2018, Manyetit Cevheri Konsantresinin Karbonize Çay Tesis Atıkları İle Mikrodalga Redüksiyonuna Mekanik Aktivasyon İşleminin Etkisinin Araştırılmas, Phd Thesis submitted to the Department of Metallurgical and Materials Engineering, Firat University

[16] BOR F. Y. (1989). Ekstraktif Metalurji Prensipleri-Part:2. ITU Printing House.

# POSTER PRESENTATIONS

# Investigation of Voltametric Behavior of Vanillin-Based Chalcone Compound

*Fatma Tuba Çoğalmış[a], Gulcemal Yildiz[a], Berkay Sütay[a], Burak Korkmaz[a], Zeynep Aydogmus[b], Bahire Filiz Şenkal [a*]*
[a] Department of Chemistry, Faculty of Science and Letters, Istanbul Technical University, 34469 Maslak, Istanbul, Turkey
[b] Department of Analytical Chemistry, Faculty of Pharmacy, Istanbul University, 34116 Beyazıt, Istanbul, Turkey
E-mail: *bsenkal@itu.edu.tr*, *gyildiz@itu.edu.tr*

**ABSTRACT**

In this study, a new chalcone derivative, vanillin chalcone (VC) was synthesized and electrochemical behavior of VC, was investigated using carbon paste electrode in Britton Robinson (BR) buffer solution by cyclic voltammetry (CV) method. The oxidation mechanism of VC was investigated by using density functional theory (DFT) computation. The effects of pH and scanning rate were investigated. The electrochemical process was adsorption controlled.

*Keywords*: *Chalcone, Aniline, Cyclic Voltammetry, DFT*

Corresponding author:

## 1. Introduction

Chalcone compounds have a widespread distribution in many natural compounds such as vegetables, fruits, teas and some herbs. These compounds have anti-cancer, anti-inflammatory, antimicrobial, antioxidant and antiparasitic properties. Electrochemical methods are very sensitive in identifying organic molecules. The applicability of carbon-based electrodes to the study of redox reactions in electrochemical measurements has increased in recent years. The redox properties of organic molecules that may be drug active ingredients can give an idea about the pharmaceutical activity of these molecules[1-6].

In this study, a chalcone substituted aniline monomer (VC) was synthesized starting from vanillin and 3-aminoacetohenone using Claisen–Schmidt condensation reaction in the presence of 40% KOH aqueous solution. Electrochemical properties of the VC monomer were investigated

## 2. Experimental details

VC was prepared according to the literature [29]. 1.4 g (10.0 mmol) of 3-amino acetophenone and 1.50 g (10.0 mmol) of Vanillin (4-hydroxy-3-methoxybenzaldehyde) were reacted in 40% KOH aqueous solution. VC was polymerized oxidatively using HBr (40%) as doping agent and ammonium persulfate (APS) as initiator at room temperature.

### Electrochemical Measurements

For electrochemical measurements, 5.0 mL of BR buffer was placed in the cell and nitrogen gas was passed through the solutions for 5 minutes to maintain an inert atmosphere. Then, the carbon paste electrode (CPE) was activated in the potential range of -0.1 and 1.1 V in the supporting solution selected by cyclic voltammetry.

## 3. Results and discussion

In this study, 3-amino acetophenone, which is an aniline derivative, was reacted with vanillin to obtain chalcone substituted aniline compound, named as vanillin chalcone, VC. This compound was polymerized oxidatively using APS to obtain PANI-VC (Scheme 1).

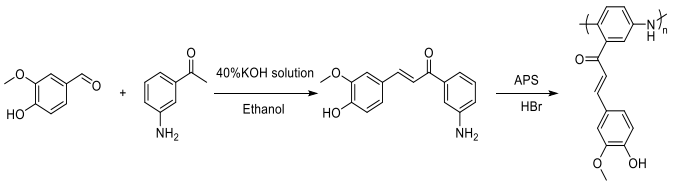


**Scheme 1.** Preparation of VC and PANI-VC

### Electrochemical behavior of Vanillin Chalcone(VC)

The voltammetric behavior and electro activity of 1 x 10-4 M VC was investigated on CPE in BR buffer solutions. Two well-defined oxidation peaks and one reduction peak were seen in the first cycle.

In Fig. 1, the first CV is given with a dashed line and the third CV with a solid line. The negative shift of the peak potentials (Fig. 1 solid line) at longer deposition times can be explained by the increase in the number of molecules adsorbed on the electrode surface at longer deposition times. Two oxidation peaks (peak I at 480 mV and peak III at 730 mV) and one reduction peak (peak II at 340 mV) have seen.

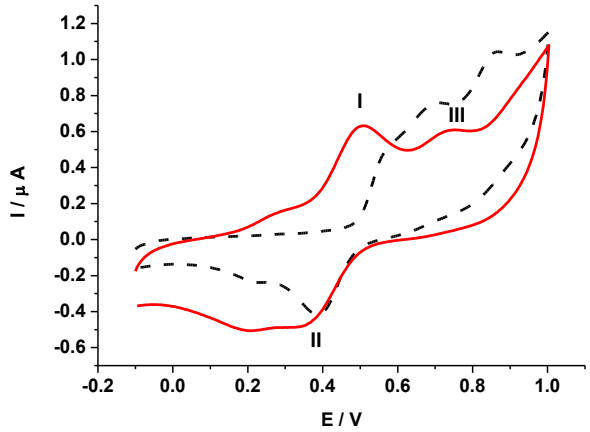


**Figure 1**. CVs of 1x10$^{-4}$ M VC solution at pH 3 (v = 50 mV/s) Dashed line: First CV and solid line: Third CV

The reduction peak (peak II at 340 mV) can be thought that this is due to the reduction of the C=O group in the molecule to C-OH. Also, a broadening has occurred at peak II and a posterior peak at 200 mV. It can be thought that this has occurred as a result of the reduction of adsorbed oxidation products.

Some theoretical considerations were considered to get more detail on the oxidation process. For this purpose, the molecular geometries of neutral, monocation and dication species were optimized by using density functional theory (DFT) at B3LYP level of theory in 6-31G(d,p) balanced basis, Figure 3.

**Table 1.** The partial atomic charges and the total partial atomic charges on each unit

| | $\delta_{O(OH)}$ | $\delta_{H(OH)}$ | $\delta_{N}$ | $\delta_{H(NH2)}$ | $\sum\delta_{A,i}$ | $\sum\delta_{B,i}$ | $\sum\delta_{C,i}$ |
|---|---|---|---|---|---|---|---|
| *neutral* | -0.696 | 0.521 | -0.856 | 0.417 | 0.075 | -0.082 | 0.007 |
| *monocation* | -0.595 | 0.547 | -0.851 | 0.420 | 0.821 | 0.115 | 0.064 |
| *dication* | -0.579 | 0.552 | -0.647 | 0.466 | 0.925 | 0.190 | 0.885 |

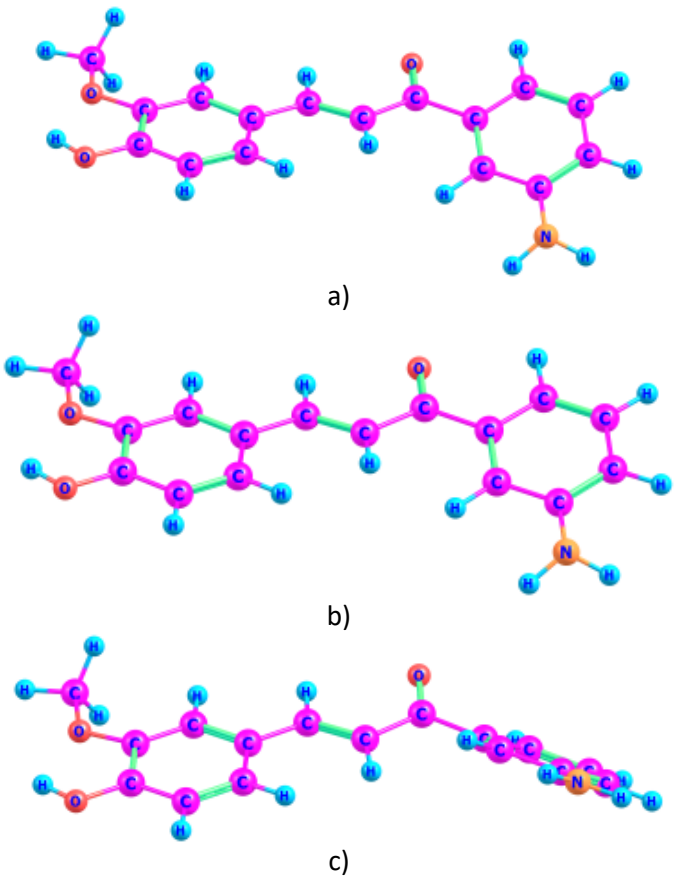


**Figure 2.** The optimized geometries of **a.** neutral chalcone, **b.** monocation and **c.** dication.

The conductor-like polarizable continuum solvent model (CPCM) [7] was used in all calculations in water media (ε = 78.4). All computations were performed in Gaussian '16 program package [8].

The partial atomic charges were calculated to investigate the changes upon oxidation of the molecule. Natural bound orbital (NBO) type charges were calculated and summarized in Table 1.

It was investigated whether VC (monomer) and PANI-VC (polymer) have the same electrochemical properties.

**4. Conclusion**

In this study, a new chalcone based aniline derivative (VC) was synthesized reaction with vanillin and 3-amino acetophenone using Claisen-Schmidt Condensation. Electrochemical properties of VC and PANI-VC were investigated by cyclic voltammetry method. Possible oxidation and reduction products are interpreted.

**5. Acknowledgement**

This work is supported by the Scientific Research Project Center of the Istanbul Technical University (Project number: TDK-2022-43604).

**6. References**

[1] DEMİRCİGİL B.T.; ÖZKAN S.A.; ÇORUH Ö.; YILMAZ S., 2002. Electrochemical behavior of formoterol fumarate and its determination in capsules for inhalation and human serum using differential-pulse and square-wave voltammetry, Electroanalysis: An International Journal Devoted to Fundamental and Practical Aspects of Electroanalysis, 14, pp. 122–127. https://doi.org/10.1002/1521-4109(200201)14:2 <122: AID-ELAN122>3.0.CO;2-1.

[2] KUMAR S.A.; TANG C.F.; CHEN S.M., 2008, Poly (4-amino-1-1'-azobenzene-3, 4'-disulfonic acid) coated electrode for selective detection of dopamine from its interferences, Talanta. 74, pp.860–866. https://doi.org/10.1016/j.talanta.2007.07.015.

[3] DICULESCU V.C.; KUMBHAT S.; OLIVEIRA-BRETT A.M. 2006. Electrochemical behaviour of isatin at a glassy carbon electrode, Anal Chim Acta.,575, pp. 190-197. https://doi.org/10.1016/j.aca.2006.05.091.

[4] LI G.; QI X.; WU J.; XU L.; WAN X.; LIU Y.; CHEN Y.; LI Q., 2022. Ultrasensitive, label-free voltammetric determination of norfloxacin based on molecularly imprinted polymers and Au nanoparticle-functionalized black phosphorus nanosheet nanocomposite, J Hazard Mater, 436, pp129107.https://doi.org/10.1016/j.jhazmat.2022.129107.

[5] XIA Y.; LI G.; ZHU Y.; HE Q.; HU C. 2023. Facile preparation of metal-free graphitic-like carbon nitride/graphene oxide composite for simultaneous determination of uric acid and dopamine, Microchemical Journal.190, pp108726. https://doi.org/10.1016/j.microc.2023.108726.
[6] LI G.; WU J.; QI X.; WANX.; LIU Y.; CHEN Y.; XU L.,
2022. Molecularly imprinted polypyrrole film-coated poly (3, 4-ethylenedioxythiophene): polystyrene sulfonate-functionalized black phosphorene for the selective and robust detection of norfloxacin, Mater Today Chem., 26, pp 101043.https://doi.org/10.1016/j.mtchem.2022.101043
[7] COSSI, M., REGA, N., SCALMANI, G., and BARONE, V, 2003. Energies, structures, and electronic properties of molecules in solution with the c-pcm solvation model. J. Comput. Chem. 24, pp. 669–681. doi:10.1002/jcc.10189
[8]FRISCH, A. J., IRELAND, M., RIZZARI, J. R., LONNSTEDT, O. M., MAGNENAT, K. A., MIRBACH, C. E., & HOBBS, J. P. A. 2016b. Reassessing the trophic role of reef sharks as apex predators on coral reefs. Coral Reefs, 35, pp. 459–472.

**Transition Metal Chalcogenide Supercapacitors**

Emre Gür[1*], Hasan Feyzi Budak and Ufuk Perişanoğlu

[1]*Eskişehir Omangazi University, Department of Physics, Eskişehir, 26040 TURKEY*

[*]**Corresponding E-mail:** emre.gur@ogu.edu.tr

Supercapacitors (SC) attract a lot of attention due to their higher power density compared to that of Li-ion batteries. Although variety of materials have been utilized so far as a high-performance SC device, a newly group of material, so called transition metal dichalcogenides (TDMC), has been noticed to be the next generation materials for energy applications because of their valuable properties such as rich chemical activity, high-conductivity, large absorption coefficient, high surface the volume ratio and relative high stability. In this study, graphenated carbon nanotubes was used to grow vertical 2D materials of layered sulfides both sputtering and chemical vapor deposition (CVD) methods. A vertical 2D structure are grown perpendicular to the carbon nanotubes. The electric double layer capacitors are realized for fabricated devices. The best supercapacitor performance achieved is about 224.0 mF/cm$^2$ for CVD grown MoS2 structures.

**Breaking Barriers: Lithium Manganese Oxide (LiMnO2) Cathode Paves the Way for Next-Generation Aqueous Ammonium Ion Batteries**

Melisa Uçan, Sevval Melek Şensoy, Dilara Özgenç, Yıldıray Topcu, Burak Tekin*

[1] *Ondokuz Mayıs University, Chemical Engineering Department, Samsun, 55139, TURKEY*

***Corresponding E-mail:** burak.tekin@omu.edu.tr

Aqueous ammonium ion batteries have garnered considerable attention due to the small hydrated ionic radius and light molar mass of ammonium ions, offering high security, environmental friendliness, and low cost. However, a significant challenge remains in the lack of suitable electrode materials with high specific capacity. To address this issue, we developed lithium manganese oxide ($LiMnO_2$) that is known for good electrochemical performance in Li-ion batteries. This cathode has attracted special attention due to the low cost of raw materials and the environmentally friendly nature of manganese compared to other transition metal oxide systems. In the quest for an ideal cathode material, lithium manganese oxide ($LiMnO_2$) emerges as a promising candidate, offering a high theoretical capacity of 285 mAh $g^{-1}$, attributed to the $Mn^{3+}/Mn^{4+}$ redox couple. $LiMnO_2$ was synthesized via the hydrothermal method, and XRD analysis revealed that this material has an orthorhombic crystal structure. the The electrochemical reaction mechanism was investigated using cyclic voltammetry, revealing a two-step oxidation process where lithium ions are extracted from the active $LiMnO_2$ during the first cycle. In the subsequent cycles, The cyclic voltammogram displays that the active cathode host facilitates ammonium ion reversibly insertion/de-insertion in an aqueous ammonium ion solution. The cut-off voltage of $LiMnO_2$ in the studied aqueous solution was determined to be 0-1.25 V vs. Ag/AgCl. Galvanostatic cycling of the $LiMnO_2$ cathode at 1 mA/$cm^2$ between 0 and 1.15 V demonstrated a specific capacity of approximately 45 mAh/g with 99% Coulombic efficiency over approximately 50 cycles. Additionally, changes in internal resistance were investigated using Potentiostatic Electrochemical Impedance Spectroscopy, revealing alterations in the half-cell configuration's internal resistance under alternative current before and after the phase change.

**Keywords**: $LiMnO_2$ Cathode, Aqueous electrolyte, Ammonioum ion battery, Electrochemical Characterization

**Spinel-Derived LiMn2O4: A Promising Cathode for Environmentally Friendly Ammonium Ion Batteries**

Dilara Özgenç[1], Şevval Melek Şensoy[1], Melisa Uçan[1], Burak Tekin[1], Yıldıray Topcu[1]*

[1] *Ondokuz Mayıs University, Chemical Engineering Department, Samsun, 55139, TURKEY*

***Corresponding E-mail:** ytopcu@omu.edu.tr

The pursuit of high-performance, cost-effective, and environmentally friendly energy storage systems has sparked significant interest in aqueous ammonium ion batteries. These batteries offer several advantages, including heightened security, environmental friendliness, and low cost, owing to the small hydrated ionic radius and light molar mass of ammonium ions. However, a primary challenge in ammonium-based batteries is finding an appropriate host electrode capable of electrochemical operation in aqueous electrolytes while enabling reversible insertion/extraction of ammonium ions into/from the active structure under a constant electric field. Addressing this challenge, this study proposes lithium manganese oxide ($LiMn_2O_4$) as a promising cathode material for ammonium ion batteries. Spinel-derived $LiMn_2O_4$ has garnered attention due to its cubic-crystal system, offering large 3D-diffusion channels, low raw material costs, and environmental friendliness compared to other transition metal oxide systems. With a theoretical capacity of approximately 148 mAh $g^{-1}$, $LiMn_2O_4$ offers high specific capacity, crucial for maximizing battery energy density. Furthermore, its structural stability in aqueous electrolytes during cycling ensures prolonged cycle life and consistent performance. $LiMn_2O_4$ spinel was synthesized using a high-temperature solid-state reaction method, and XRD analysis confirmed its orthorhombic crystal form. Electrochemical characterization via cyclic voltammetry revealed a two-step Li extraction process in aqueous ammonium-based electrolytes. Subsequent cycling induced the appearance of oxidation and reduction peaks at various voltages, reflecting the ammonium insertion and extraction process within the host cathode structure. As cycle number increased, redox peaks became more pronounced, indicating the reversible facilitation of efficient ammonium ion insertion/de-insertion in aqueous electrolytes. The compatibility of $LiMn_2O_4$ with ammonium ion electrolytes further bolstered battery performance, ensuring robust ion transport and reversible electrochemical reactions. Galvanostatic charge-discharge experiments demonstrated that the $MnO_2$ electrode exhibited a specific capacity of around 47 mAh/g upon $NH_4^+$ intercalation/de-intercalation. In conclusion, the utilization of $LiMn_2O_4$ cathode materials holds significant promise for advancing the development of high-performance and environmentally sustainable ammonium ion batteries. This study offers valuable insights into the key attributes, challenges, and future directions in leveraging $LiMn_2O_4$ for ammonium ion battery technologies.

**Keywords**: Aqueous ammonium ion batteries, Spinel cathode materials, Electrochemical energy storage

# Evaluation of the Potential of Two-Dimensional (2D) Borophene Material for Hydrogen Storage Applications

C. Can[1*], B. Buyuk[2*], M. Kamislioglu[3,4*], H. Disbudak[5*]

[1]*Bandırma Onyedi Eylül University, Department of Alternative Energy Sources, Bandırma, 10200 TURKEY*

[2]*Bandırma Onyedi Eylül University, Faculty of Engineering and Natural Sciences, Bandırma, 10200 TURKEY*

[3]*Turkish Energy, Nuclear and Mineral Research Agency – Boron Research Institute, Çankaya, Ankara, 06510, TURKEY*

[4]*Bandırma Onyedi Eylül University, Department of Medical Imaging, Vocational School of Health Services, Bandırma, 10200 TURKEY*

[5]*Turkish Energy, Nuclear and Mineral Research Agency – Nuclear Research Institute, Çankaya, Ankara, 06510, TURKEY*

**ABSTRACT**

Today, the rise of green hydrogen as an alternative to fossil fuels is being discussed due to increasing energy demand and the imperative to reduce carbon emissions. Solid-state hydrogen storage, with its safety and energy density advantages, is gaining traction, especially with the potential of two-dimensional (2D) materials like borophene. As a 2D allotrope, Borophene has garnered attention for its diverse properties such as high electron transport, anisotropic behavior, and superconductivity. Its unique structure facilitates stronger binding of molecular hydrogen compared to carbon layers, making it is a promising material for hydrogen storage. Because of the distinctive structure of boron layers, characterized by a notable distance between adjacent atoms that form a stable lattice, molecular hydrogen binds more firmly to boron layers (0.05 eV) than to carbon layers. Despite theoretical studies, experimental research on borophene remains limited. In this study, it is emphasized that the chemical and physical properties of the promising borophene regarding hydrogen storage and binding energy should be investigated for experimental studies.

*Keywords: Borophene, hydrogen storage, 2D materials*

Corresponding author: canan.can92@hotmail.com

## 1. Introduction

In the current environment where fossil fuel reserves are decreasing and environmental concerns are increasing, hydrogen is ready to serve as an energy carrier. The limited nature and environmental consequences of fossil fuels highlight the need to transition to alternative energy sources. As resources become scarce and environmental awareness increases, there is a growing trend to embrace alternative energy options [1]. The drive to reduce carbon emissions has highlighted green hydrogen as an attractive alternative to traditional fossil fuels. Green hydrogen, obtained sustainably from renewable energy sources, stands out with its environmentally friendly production process. Using a solid matrix, solid-state hydrogen storage offers greater safety and improved energy density compared to traditional methods such as compressed gas or liquid hydrogen [2].

Over the past two decades, two-dimensional (2D) nanomaterials have emerged as a highly innovative area of research in chemistry, physics, materials science, energy storage, production, and nanotechnology.

Borophene, a monolayer boron sheet, has garnered significant scientific interest due to its recent transition from theoretical concept to practical realization. Borophene is a two-dimensional, atomically thin crystalline structure characterized by its corrugated form and covalent bonds between boron atoms. It was first experimentally observed on a silver substrate under ultra-high pressure in 2015. To date, theoretical calculations and modeling have identified four phases of borophene, all of which have been synthesized on silver (Ag) or aluminum (Al III) substrates under ultra-

high vacuum conditions. These four synthesized borophene phases—2-Pmmn, $\beta_{12}$, χ3, and graphene-like are reported to be metallic. Various methods have been employed to synthesize these borophene allotropes.

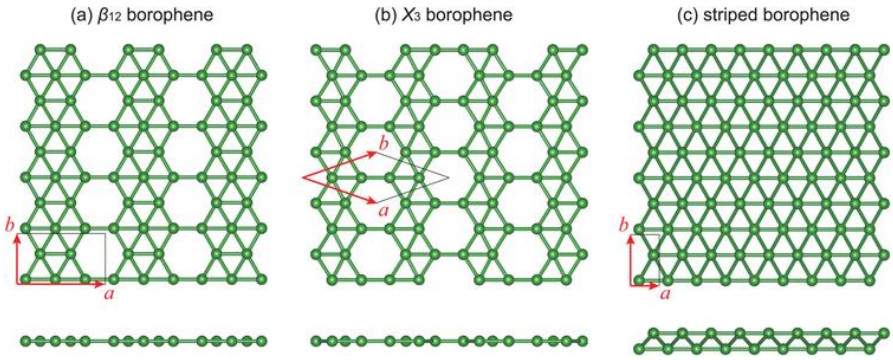


**Figure 1.** Three main crystal structures of experimentally obtained borophene (a) $\beta_{12}$ borophene, (b) $\chi_3$ borophene (c) striped borophene [3].

The families of 2D materials hold immense promise in revolutionizing energy conversion and hydrogen storage technologies. Borophene, a two-dimensional material, has potential as an intermediate hydrogen storage medium because of its moderate binding energy and reversible properties. This boron monolayer is a highly promising material with exceptional characteristics, including anisotropic metallic behavior, superconductivity and high carrier mobility [4-7].

Two main indices such as adsorption energy and $H_2$ adsorption capacity are required to evaluate the hydrogen storage ability. Adsorption energy is important to provide a certain energy range so that $H_2$ molecules can be stably and easily adsorbed onto the surface of the material. This range should generally be between 0.2 and 0.6 eV. $H_2$ adsorption capacity refers to how many $H_2$ molecules the material can hold at a certain weight. The target value set by the US Department of Energy is 7.5% by weight. Recent research shows that borophene has potential in $H_2$ storage with its light weight and large specific surface area properties, especially when used with graphene or transition metals. Thus, borophene is considered to be a significant candidate in the field of hydrogen storage [8].

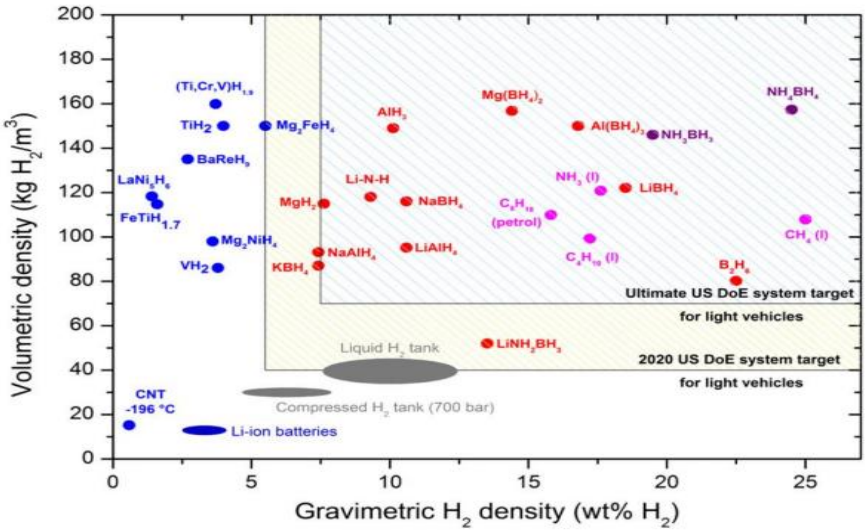


**Figure 2.** The gravimetric and volumetric hydrogen densities of selected materials are shown and compared with the U.S. Department of Energy's targets for hydrogen storage systems [9].

Recent research has examined the hydrogen storage capabilities of both pristine and metal-decorated monolayer borophene. For instance, Li et al. (2017) found that borophene decorated with lithium achieved a gravimetric density of 13.7 wt%, while Chen et al. (2017) reported a density of 1.3 wt% for borophene decorated with calcium [10-11]. However, these studies have primarily concentrated on single-metal decorations. Therefore, broader investigations involving multiple alkali atoms are required to enhance comparisons and advance our understanding of this phenomenon [12].

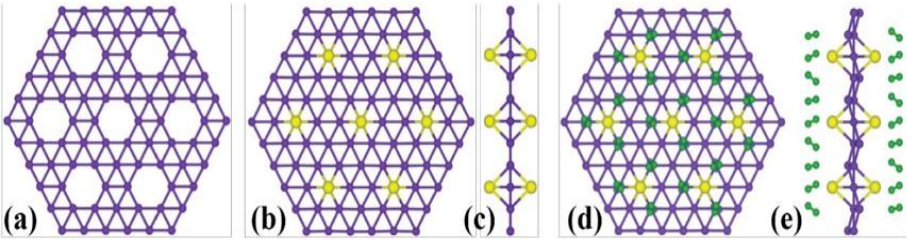


**Figure 3.** Crystal structures of α-sheet borophene are shown without (a) and with (b), Additionally, (c) Li adsorption. (d) and (e) Illustrate the crystal structures of Li-decorated α-sheet borophene with adsorbed hydrogen molecules [13].

Borophene's discovery has sparked considerable excitement due to its exceptional properties, holding promise across multiple sectors. Borophene's prowess extends to energy applications, where it could enhance supercapacitors, batteries, and hydrogen storage, bolstering renewable energy solutions. Its high conductivity and surface area make it an ideal candidate for energy storage and conversion devices, potentially improving the efficiency and performance of renewable energy systems. Besides energy applications, its application potential in biomedicine ranges from diagnostics to therapeutics, leveraging its unique properties for bioimaging, drug delivery and photonic therapy. Overall, the discovery of borophene represents an exciting development with far-reaching implications, from healthcare to renewable energy, signaling a new era of innovation driven by advanced materials science. As scientists continue to uncover its capabilities and refine production methods, borophene's transformative potential across various industries becomes increasingly apparent.

This study emphasizes borophene's considerable potential in energy applications, especially for hydrogen storage. Borophene is synthesized and modified with different metals transition metals, alkali metals, and alkaline earth metals to boost its hydrogen storage capacity.

**2. Experimental Synthesis and Theoretical Studies**

There are two main methods for producing 2D nanomaterials: top-down and bottom-up. Top-down methods include mechanical cleavage, ultrasonication, ion intercalation exfoliation, and etching. On the other hand, the bottom-up approach involves techniques such as physical vapor deposition (PVD), chemical vapor deposition (CVD), and various methods of wet chemical synthesis [14].

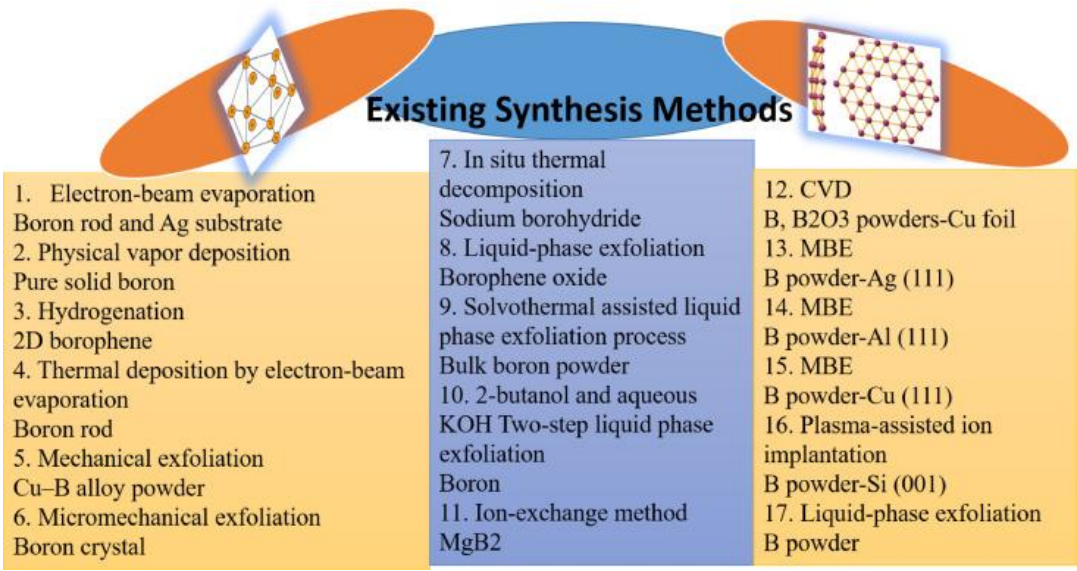


**Figure 4.** Overview of available methods for borophene synthesis [15].

### 2.1. Physical vapor deposition (PVD) methods

PVD techniques, involving vaporization and condensation in a vacuum, are crucial for borophene synthesis. Epitaxial growth methods like Molecular Beam Epitaxy (MBE), segregation-enhanced epitaxy, and van der Waals epitaxy have shown promise in producing high-quality borophene films at scale.

#### 2.1.1. Molecular beam epitaxy (MBE) methods

Epitaxy techniques, notably Molecular Beam Epitaxy (MBE), have become crucial for precise borophene synthesis. They provide exceptional control over film morphology, structure, and electronic properties [16].

Kong et al. (2018) utilized molecular beam epitaxy to fabricate two-dimensional boron layers on an Al (111) substrate. The aluminum surface's three free electrons effectively compensated for borophene's electron deficiency. Experiments were conducted at low temperatures using an ambient scanning tunneling microscope-molecular beam epitaxy system under a base pressure of 10 mbar. Prior to deposition, the substrate underwent cleaning, and borophene layers were synthesized by evaporating 99.99% pure boron onto Al (111) using an electron beam evaporator. The boron flux was maintained at 500 K, with a deposition rate of 0.1 monolayer per minute throughout the procedure [17].

### 2.2. Chemical vapor deposition (CVD) methods

Chemical Vapor Deposition (CVD) is a flexible and scalable technique where a precursor gas breaks down on a heated substrate to create a borophene layer. Ongoing research in this area actively refining CVD to improve the quality of borophene and enhance control over its growth. However, despite its effectiveness in producing borophene, CVD typically involves higher expenses and longer processing durations [18].

Tai et al. (2015) produced ultrathin two-dimensional (2D) γ-boron films on copper (Cu) foils via chemical vapor deposition (CVD). They utilized a blend of boron and boron oxide powder as the source material, and hydrogen gas as the carrier gas. This research opens avenues for utilizing boron films in diverse applications such as nanoelectronics and nanophotonics [19].

### 2.3. Exfoliation techniques as a synthesis strategy for Borophene

Exfoliation methods, involving the separation of individual or few layers from the bulk precursor materials, have emerged as promising approaches for the synthesis of 2D borophene. Exfoliation methods offer cost-effectiveness and the potential for tailored properties. Various strategies, like liquid phase, micromechanical, ball milling-induced, and electrochemical exfoliation, have been explored [16].

#### 2.3.1. Liquid phase exfoliation (LPE)

Liquid-phase exfoliation (LPE) is a common method for synthesizing 2D materials like borophene. It involves dispersing bulk materials in a suitable solvent and then using techniques such as ultrasonication to break them down into individual layers or few-layer nanosheets. LPE has advantages for borophene synthesis, like scalability, simplicity, and the ability to produce large quantities of borophene nanosheets with controlled thickness. However, challenges such as achieving high yield and maintaining the structural integrity of borophene during exfoliation remain areas of active research.

Many 2D material synthesis methods rely on sonochemical processes, involving immersion of bulk material in an organic solvent and exposure to ultrasound for extended periods. Ranjan et al. (2020) used this technique to exfoliate bulk boron into borophene. They conducted experiments using a variety of organic solvents (methanol, ethanol, isopropanol, acetone, DMSO, DMF) and confirmed ultrasound-assisted exfoliation as an efficient method for producing large, thin borophene flakes. Additionally, they demonstrated the applicability of the modified Hummers method for boron exfoliation [20].

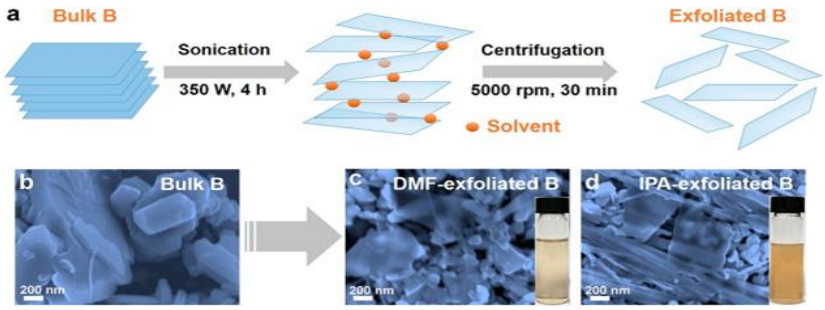


**Figure 5.** (a) Schematic representation of the sonication-assisted liquid phase exfoliation process [21].

### 2.4. Theoretical studies into borophene's potential for hydrogen storage

Computational studies on the varying crystal structures of borophene with different alkali or transition metals, using first principles methods such as DFT and Molecular Dynamics, highlight the use of DFT as an effective theory for predicting solid crystal properties. These investigations offer valuable insights into electronic structures, lattice constants, binding energies, and magnetic properties. Studies on borophene has specifically explored factors such as adsorption energy, potential hydrogen storage capacity, and the amount of hydrogen molecules bonded to borophene modified with alkali or transition metals [22].

Alkali and transition metals were selected due to their capability to alter the electronic properties of borophene, enhancing its conductivity and interaction with hydrogen molecules. These metals can act as catalysts to accelerate the breakdown of hydrogen molecules, enhancing both adsorption and release kinetics. Metal doping also improves borophene's resistance to oxidation and its ability to maintain thermal stability, essential for effective long-term hydrogen storage [23].

Zhang et al. (2022) decorated the surface of $\beta_{12}$ borophene with superalkaline $NLi_4$ with a large binding energy, and the gravimetric $H_2$ storage capacity reached up to 7.66 wt% [24].

Kerimzadeh et al. (2022) utilized first principles density functional calculations to investigate the effect of Yttrium (Y) doping on $\beta_{12}$-borophene for hydrogen storage. The negative adsorption energy results indicate that hydrogen molecule adsorption on Y-doped $\beta_{12}$-borophene (Y doped borophene) was both energetically favorable and thermodynamically stable. Moreover, the calculated adsorption energies demonstrate strong bonding between doped Y atoms and the $\beta_{12}$-borophene surface, preventing the formation of metal clusters. The study achieved a hydrogen storage capacity of 5.74 wt% with 4Y-doped $\beta_{12}$-borophene [25].

## 3. Results and Discussion

Boron sheet surface functionalization with alkali, alkaline earth, and transition metal atoms has been extensively studied. Initially, Li, Ca, Ti, Na, and Mg were commonly used metals. Li emerged as the preferred choice due to its low cohesive energy in bulk structures and favorable hydrogen molecule binding energy on decorated complexes. Density functional theory (DFT) calculations indicate hydrogen storage capacities of 7.94 wt % and 15.26 wt % for Li-decorated zigzag (2, 2) boron nanotubes and borophene, respectively. Wen et al. (2020) investigated χ3 borophene doped with titanium transition metal via DFT. Ti-doped borophene significantly increased $H_2$ storage capacity, reaching 15.065%, surpassing alkali metals. This capacity was much higher than Li-decorated borophene, nearly 15.07 wt%, exceeding the DOE's target by over threefold [26]. **Table 1** gives the hydrogen capacities of select 2D materials, emphasizing borophene's superior storage capacity.

**Table 1.** Hydrogen storage capacity of various 2D materials

| 2D based material | Hydrogen storage capacity(wt%) | Reference |
|---|---|---|
| Li decorated η = 1/7-borophene | 9.22 | [27] |
| Li decorated η = 1/8-borophene | 15.26 | [28] |
| Ti decorated $X^3$-borophene | 15.065 | [26] |
| Na decorated 2pmmn borophene | 8.36 | [29] |
| Ca decorated $\beta_{12}$-borophene | 9.5 | [30] |
| N decorated α sheet-borophene | 6.22 | [31] |
| Y decorated $\beta_{12}$-borophene | 5.74 | [25] |
| $NLi_4$ decorated $\beta_{12}$-borophene | 7.66 | [24] |

## 4. Conclusion

The emergence of borophene, two-dimensional nanomaterial consisting of hexagonally arranged boron atoms, presents significant potential for reshaping the energy landscape and reducing reliance on fossil fuels. Borophene, originally proposed as a theoretical concept, has been synthesized successfully, leading to thorough investigation of its properties, particularly its potential for hydrogen storage. However, practical applications encounter challenges that require attention despite its high storage capacity. To enhance stability and storage capability, strategies such as doping with alkali metals or other 2D materials are proposed. To achieve the best hydrogen adsorption, a profound understanding of how hydrogen interacts with the borophene surface is crucial.

Borophene's distinct geometry and electronic properties enable it to achieve a higher hydrogen adsorption capacity compared to metal-based complex hydrides. Ongoing research on borophene nanomaterials is crucial to overcome current limitations and unlock its full potential for efficient and sustainable hydrogen storage solutions. Despite the advantages of borophene nanomaterial, it is not yet ready for commercial use, indicating the need for further research and development to optimize its properties. This study underlines the importance of borophene in the development of hydrogen storage technologies and highlights the challenges that need to be addressed for its practical application.

This study suggests future research directions including exploring the effects of metal dopants on the stability and charge transfer of borophene, scaling up synthesis methods, investigating dual doping with alkali and transition metals, and examining borophene's applications in hydrogen storage and fuel cell catalysis.

**References**

[1] Rosen, M. A., & Koohi-Fayegh, S. (2016). The prospects for hydrogen as an energy carrier: an overview of hydrogen energy and hydrogen energy systems. *Energy, Ecology and Environment*, *1*, 10-29.

[2] Ledwaba, K., Karimzadeh, S., & Jen, T. C. (2023). Emerging borophene two-dimensional nanomaterials for hydrogen storage. *Materials Today Sustainability*, *22*, 100412.

[3] Peng, B., Zhang, H., Shao, H., Ning, Z., Xu, Y., Ni, G., ... & Zhu, H. (2017). Stability and strength of atomically thin borophene from first principles calculations. *Materials Research Letters*, *5*(6), 399-407.

[4] Kaneti, Y. V., Benu, D. P., Xu, X., Yuliarto, B., Yamauchi, Y., & Golberg, D. (2021). Borophene: two-dimensional boron monolayer: synthesis, properties, and potential applications. *Chemical Reviews*, *122*(1), 1000-1051.

[5] Ranjan, P., Lee, J. M., Kumar, P., & Vinu, A. (2020). Borophene: New sensation in flatland. *Advanced Materials*, *32*(34), 2000531.

[6] Zhang, X., Hu, J., Cheng, Y., Yang, H. Y., Yao, Y., & Yang, S. A. (2016). Borophene as an extremely high capacity electrode material for Li-ion and Na-ion batteries. *Nanoscale*, *8*(33), 15340-15347.

[7] Leng, S., Sun, X., Yang, Y., & Zhang, R. (2019). Borophene as an anode material for Zn-ion batteries: A first-principles investigation. *Materials Research Express*, *6*(8), 085504.

[8] Ou, M., Wang, X., Yu, L., Liu, C., Tao, W., Ji, X., & Mei, L. (2021). The emergence and evolution of borophene. *Advanced Science*, *8*(12), 2001801.

[9] Møller, K. T., Jensen, T. R., Akiba, E., & Li, H. W. (2017). Hydrogen-A sustainable energy carrier. *Progress in natural science: Materials International*, *27*(1), 34-40.

[10] Li, L., Zhang, H., & Cheng, X. (2017). The high hydrogen storage capacities of Li-decorated borophene. *Computational Materials Science*, *137*, 119-124.

[11] Chen, X., Wang, L., Zhang, W., Zhang, J., & Yuan, Y. (2017). Ca-decorated borophene as potential candidates for hydrogen storage: a first-principle study. *International Journal of Hydrogen Energy*, *42*(31), 20036-20045.

[12] Haldar, S., Mukherjee, S., & Singh, C. V. (2018). Hydrogen storage in Li, Na and Ca decorated and defective borophene: a first principles study. *RSC advances*, *8*(37), 20748-20757.

[13] Er, S., de Wijs, G. A., & Brocks, G. (2009). DFT study of planar boron sheets: a new template for hydrogen storage. *The Journal of Physical Chemistry C*, *113*(43), 18962-18967.

[14] Rahman, A., Rahman, M. T., Chowdhury, M. A., Ekram, S. B., Uddin, M. K., Islam, M. R., & Dong, L. (2023). Emerging 2D borophene: Synthesis, characterization, and sensing applications. *Sensors and Actuators A: Physical*, 114468.

[15] Chowdhury, M. A., Uddin, M. K., Shuvho, M. B. A., Rana, M., & Hossain, N. (2022). A novel temperature dependent method for borophene synthesis. *Applied Surface Science Advances*, *11*, 100308.

[16] Adekoya, G. J., Adekoya, O. C., Muloiwa, M., Sadiku, E. R., Kupolati, W. K., & Hamam, Y. (2024). Advances In Borophene: Synthesis, Tunable Properties, and Energy Storage Applications. *Small*, 2403656.

[17] Li, W., Kong, L., Chen, C., Gou, J., Sheng, S., Zhang, W., ... & Wu, K. (2018). Experimental realization of honeycomb borophene. *Science Bulletin*, *63*(5), 282-286.

[18] Mishra, R. K., Sarkar, J., Verma, K., Chianella, I., Goel, S., & Nezhad, H. Y. (2024). Borophene: A 2D wonder shaping the future of nanotechnology and materials science. *Nano Materials Science*.

[19] Tai, G., Hu, T., Zhou, Y., Wang, X., Kong, J., Zeng, T., ... & Wang, Q. (2015). Synthesis of atomically thin boron films on copper foils. Angewandte Chemie International Edition, 54(51), 15473-15477.

[20] Sielicki, K., Maślana, K., Chen, X., & Mijowska, E. (2022). Bottom up approach of metal assisted electrochemical exfoliation of boron towards borophene. *Scientific Reports*, *12*(1), 15683

[21] Li, H., Jing, L., Liu, W., Lin, J., Tay, R. Y., Tsang, S. H., & Teo, E. H. T. (2018). Scalable production of few-layer boron sheets by liquid-phase exfoliation and their superior supercapacitive performance. *Acs Nano*, *12*(2), 1262-1272.

[22] Saal, J. E., Kirklin, S., Aykol, M., Meredig, B., & Wolverton, C. (2013). Materials design and discovery with high-throughput density functional theory: the open quantum materials database (OQMD). *Jom*, *65*, 1501-1509.

[23] Yadav, G. M., Bajre, W. K., Mayilswamy, N., & Kandasubramanian, B. (2024). Alkali/transition metal decorated borophene in hydrogen storage through adsorption: A review. *Hybrid Advances*, 100149.

[24] Zhang, Y., & Liu, P. (2022). Hydrogen storage on superalkali NLi4 decorated β12-borophene: A first principles insights. *International Journal of Hydrogen Energy*, *47*(32), 14637-14645.

[25] Ledwaba, K., Karimzadeh, S., & Jen, T. C. (2022). Enhancement in the hydrogen storage capability of borophene through yttrium doping: A theoretical study. *Journal of Energy Storage*, *55*, 105500.

[26] Wen, T. Z., Xie, A. Z., Li, J. L., & Yang, Y. H. (2020). Novel Ti-decorated borophene χ3 as potential high-performance for hydrogen storage medium. *International Journal of Hydrogen Energy*, *45*(53), 29059-29069.

[27] Wang, Y. S., Wang, F., Li, M., Xu, B., Sun, Q., & Jia, Y. (2012). Theoretical prediction of hydrogen storage on Li decorated planar boron sheets. *Applied surface science*, *258*(22), 8874-8879.

[28] Li, J., Zhang, H., & Yang, G. (2015). Ultrahigh-capacity molecular hydrogen storage of a lithium-decorated boron monolayer. The Journal of Physical Chemistry C, 119(34), 19681-19688.

[29] Zhang, Y., & Cheng, X. (2019). Hydrogen adsorption property of Na-decorated boron monolayer: A first principles investigation. *Physica E: Low-dimensional Systems and Nanostructures*, *107*, 170-176.

[30] Tang, X., Gu, Y., & Kou, L. (2018). Theoretical investigation of calcium-decorated β12 boron sheet for hydrogen storage. *Chemical Physics Letters*, *695*, 211-215.

[31] Baraiya, B. A., Som, N. N., Mankad, V., Wu, G., Wang, J., & Jha, P. K. (2020). Nitrogen-decorated borophene: An empowering contestant for hydrogen storage. Applied Surface Science, 527, 146852.

**Glycoconjugates based on Mesoporous silica nanoparticles**

D.S. Salmanoglu[1*], I.Yazgan[2], E.Tut[3], O.Kozgus Guldu[3], D.Odaci[4]
[1] *Ege University, Department of Biomedical Technologies, Izmir, 35040 TURKEY*
[2]Kastamonu University of Department of Biology, Kastamonu, 37200 *TURKEY*
[3]*Institute of Nuclear Sciences, Ege University, Izmir, 35100, TURKEY*
[4]*Ege University, Department of Biochemistry, Izmir, 35100 TURKEY*

[*]**Corresponding E-mail:** dilekodaci.od@gmail.com
selcenderya@gmail.com

Most existing approaches to cancer treatment rely heavily on traditional chemotherapy, which lacks specificity in drug delivery to cancer cells, thereby impacting both malignant and healthy cells. Inorganic nanostructures have attracted great interest in the biomedical field due to their flexible design and ease of surface chemistry modelling as well as their improved performance as drug carriers. Mesoporous silica nanoparticles (MSNs), categorized among inorganic nanostructures, have become very attractive for drug development in the fight against cancer. Mesoporous silica nanoparticles are extensively employed as targeted drug delivery owing to their structural characteristics such as uniform and tunable pore size, uniform and modifiable nanoparticle size and shape, possibility of surface functionalization, high surface area, large pore volume, low toxicity. Cancer cells typically exhibit distinct glycan profiles in comparison to normal cells. This characteristic of cancer cells makes carbohydrates attractive appealing as ligand for targeted drug delivery to tumors. Many glycoconjugates have emerged as promising anticancer treatments, offering enhanced cancer specificity, reduced systemic toxicity, and improved anticancer efficacy. In this study, MSNs was synthesized and the surface of MSNs was functionalised with amine groups. Carbohydrate derivatives were synthesised in the laboratory (e.g. mannose, galactose and lactose derivatives) to target cancer cells. Mannose (M) and galactose (G) based glycoconjugates which contain 5-aminosalicylic acid (5-AS) and lactose (L) based glycoconjugate which contains thiol group were synthesized. The synthesis of sugar derivatives, the coating of MSNs with sugars and the characterization of targeted carriers were performed.

**Keywords***: Nanobiotechnology, glycoconjugate, nanoparticle, carbohydrate, cancer*

**REFERENCE**

Sancak, S., Yazgan, İ., Bayarslan, A. U., Ayna, A., Evecen, S., Taşdelen, Z., Gümüş, A., Sönmez, H. A., Demir, M. A., Demir, S., Bakar, F., Dilek-Tepe, H., Kasemets, K., Otsus, M., & Çeter, T. (2023). Surface chemistry dependent toxicity of inorganic nanostructure glycoconjugates on bacterial cells and cancer cell lines. *Journal of Drug Delivery Science and Technology*, *79*. https://doi.org/10.1016/j.jddst.2022.104054

**Development of Hydrogen Peroxide Biosensors Based on Poly-L-Histidine, Multi-walled Carbon Nanotubes and Ionic Liquid**

E.ULUKAN[1*] F.OZTURK[2*]

[1,2] *Namık Kemal University, Department of Chemistry, Faculty of Science and Arts, Tekirdag, 59030 TURKEY*

[*]**Corresponding E-mail:** elifulukan1997@gmail.com

[*]**Corresponding E-mail:** fozturk@nku.edu.tr

In recent years, studies have shown that the excessive use of $H_2O_2$ in food industry is harmful to human health. Various techniques, such as chemiluminescence, spectrophotometry, titrimetry, chromatography, and electrochemistry have been reported in literature with regard to the determinaion of $H_2O_2$. Among these techniques, enzymatic biosensors are more attractive than others since they are inexpensive, simple, sensitive, and selective. In this study, an amperometric biosensor has been fabricated by immobilizing horseradish peroxidase on poly-L-histidine, multi-walled carbon nanotube, and ionic liquid modified glassy carbon electrode (HRP/PLH/MWCNT-IL/GCE) for the sensitive quantification of $H_2O_2$. HRP was electrostatically immobilized on the PLH/MWCNT-IL/GCE. The surface morphology was analyzed by scanning electron microscopy, cyclic voltammetry, and impedance spectroscopy. The electrode composition, buffer, pH, and operating potential were all optimized in order to achieve the best analytical performance. The designed biosensor shows wide operating range, high sensitivity, low detection limit, good stability, and good storage stability. These results indicate that the limited biosensor application involving electrostatic immobilization of HRP should be more widely used in future[1].

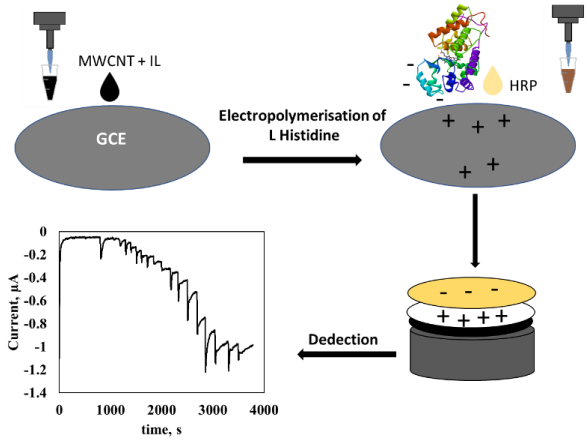


Fig.1. Fabrication of HRP/PLH/MWCNT-IL/GCE

ACKNOWLEDGEMENT

This study was supported by Tekirdag Namık Kemal University Scientific Research Projects Coordination Unit (Project No: NKUBAP.01.GA.23.481)

REFERENCES

1. Ulukan, E., & Öztürk, F. (2023). The electrostatic immobilization of the horseradish peroxidase on poly-L-histidine modified multiwall carbon nanotube – ionic liquid composite glassy carbon electrode for the amperometric determination of hydrogen peroxide. *Monatshefte für Chemie-Chemical Monthly*, *154*(6), 585-594. https://doi.org/10.1007/s00706-023-03071-6

**Ternary rGO/MnO2/PANI hybrid nanocomposite materials in 1M KOH for Supercapacitor evaluations**

Fatih NACAK* Prof. Dr. Murat ATEŞ**

*Tekirdag Namık Kemal University, Department of Chemistry, Tekirdağ, 59030 TURKEY*

***Corresponding E-mail:** fnacak@nku.edu.tr

****Corresponding E-mail:** mates@nku.edu.tr

Nowadays, supercapacitors have gained importance in energy storage. It has higher power and energy density and longer life cycle than conventional capacitors. Supercapacitor electrode materials are chosen from carbonaceous materials with high surface area, transition metal oxides, and conductive polymers. In this study, it is aimed to synthesize new nanocomposites and to develop supercapacitor devices with superior electrochemical performances. $MnO_2$, GO, rGO, PANI, rGO/$MnO_2$, rGO/$MnO_2$/PANI, materials were synthesized to show the applicability on equivalent circuit. The synthesized materials were characterized by various methods, such as SEM-EDX, FTIR-ATR, thermal gravimetric analysis (TGA-DTA), 4-point probe solid state conductivity measurements, surface analysis (BET) and Atomic force microscopy (AFM). Electrochemical performances of supercapacitor devices were measured by various methods, such as cyclic voltammetry (CV), galvanostatic charge/discharge (GCD), electrochemical impedance spectroscopy (EIS). 1M potassium hydroxide (KOH) solution is used as electrolyte in supercapacitor devices. The surface area, pore sizes and conductivities of the electrode materials of binary and ternary nanocomposites and their effects on the electrochemical performance of supercapacitors were examined in detail. The highest specific capacitance value of all materials was obtained for the rGO/$MnO_2$/PANI nanocomposite as $C_{sp}$=1541.7 (2 mV/s) by the CV method. $MnO_2$ based materials were tested by ladder equivalent circuit model [$R_1(C_1(R_2(C_2(R_2(C_3R_3))))$] using ZSimpWin 3.22 simulation programme.

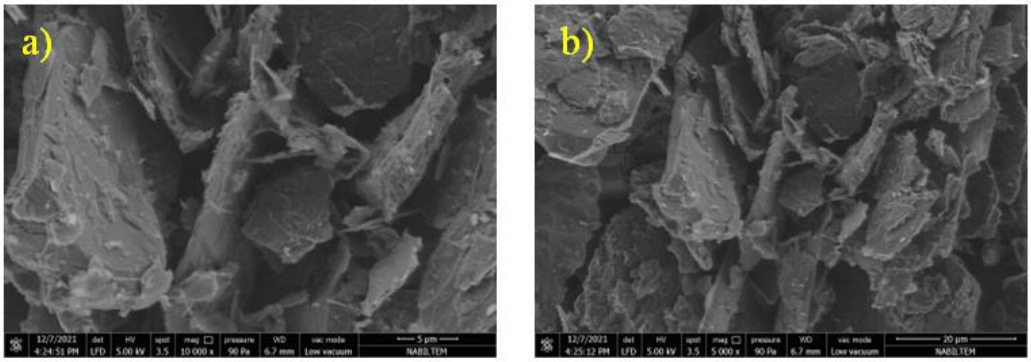


Fig.1. SEM images of rGO/$MnO_2$/PANI at different sizes; a) 5 µm magnification; b) 20 µm magnification

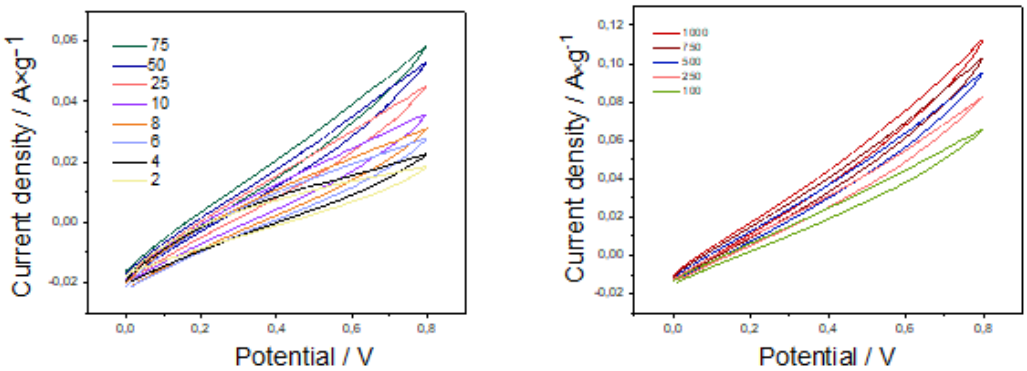


Fig.2. CV graphs of rGO/$MnO_2$/PANI at a scan rate of a) 2-75 mV/s, b) 100-1000 mV/s.

**Synthesis and Characterization of Shape and Size-Controlled Mesoporous Silica Nanoparticle Spheres**

Fatmanur Uyan[1], Merve Kucukoflaz Korkmaz[1], Hümeyra Karakaya[1], Serkan Dayan [*1,2]

[1] *Drug Application and Research Center, Molecular Synthesis & Industrial Application Research Laboratory, Erciyes University, 38039 Kayseri, Turkey.*

[2] Faculty of Pharmacy, Department of Pharmaceutical Sciences, Kayseri, Turkey.

[*]**Corresponding E-mai:** serkandayan@erciyes.edu.tr

Silica nanospheres have many applications due to their easy synthesis and unique properties such as high surface/volume ratio, tunable pore size, high stability, adsorption capacity, and biocompatibility. In materials science, it is used as a surface coating template with its water-repellent properties, in energy to increase the efficiency of solar cells, and in cosmetics to provide mattness to the skin in skin products. In pharmacy, it is used as a controlled drug delivery system [1]. Nanoparticle-based materials offer several advantages over free and unformulated drugs. In particular, mesoporous silica nanoparticles (MSNs) as nanosized porous silica carriers provide more sustained and controlled drug release or enhanced oral bioavailability. Therefore, in this study, we will investigate the advantages of nanostructured silica nanospheres such as particle size, particle shape, surface roughness or surface functionalization as drug delivery systems. In particular, we will elucidate the synthesis and characterization of mesoporous silica nanocarriers for oral drug delivery [2].

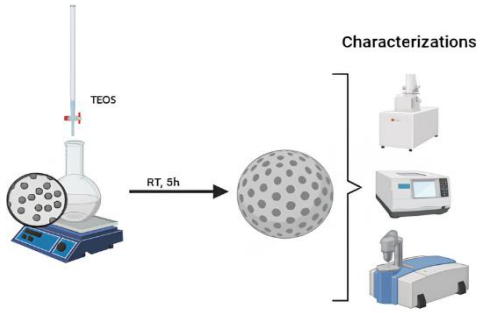


Figure 1. Synthesis and characterization of silica nanoparticle.

In this study, silica nanospheres were synthesised using a wet chemical method (Figure 1). The synthesised nanospheres were characterised by field emission scanning electron microscopy, transmission electron microscopy, elemental mapping, energy dispersive X-ray analysis, dynamic light scattering and Fourier transform infrared spectroscopy. The aim of this comprehensive analysis was to determine the structural and chemical properties of the synthesised nanomaterials and their use as drug delivery systems.

[1] Nayl, A. A., Abd-Elhamid, A. I., Aly, A. A., & Bräse, S. (2022). Recent progress in the applications of silica-based nanoparticles. RSC advances, 12(22), 13706-13726.

[2] J. Florek, R. Caillard and F. Kleitz, (2017). Evaluation of mesoporous silica nanoparticles for oral drug delivery – current status and perspective of MSNs drug carriers. RSC advances, 9(40), 15252-15277.

**Synthesis of rGO@L-Arginine/Co Nanoparticles and Application Enzyme-Free Glucose Sensing**

Rümeysa Kisi[1], Mehtap Ceyran[1], Merve Kucukoflaz Korkmaz[1], Serkan Dayan [*1,2]

[1] *Drug Application and Research Center, Molecular Synthesis & Industrial Application Research Laboratory (MSIA-Lab), Erciyes University, 38039 Kayseri, Turkey.*

[2] *Faculty of Pharmacy, Department of Pharmaceutical Basic Sciences, Kayseri, Turkey.*

[*]**Corresponding E-mail:** serkandayan@erciyes.edu.tr

Biosensors are devices that exhibit selectivity towards biological substances and convert a sensitive, specific analyte concentration into an electrical signal [1]. Biosensors can be investigated both with and without enzymes for the detection of biomolecules in samples. Current studies focus on enzyme-free biosensors, as enzymatic biosensors have a limited lifetime and enzyme activity decreases over time [2]. L-arginine is a molecule that is found at different active sites of different proteins and is of great importance in medicine. Due to its highly effective therapeutic properties, it is currently used as one of the most effective dietary supplements [3]. Graphene oxide (GO) and reduced graphene oxide (rGO) have excellent mechanical strength as well as chemical and physical stability. The most important reason for choosing graphene oxide (GO) is its large surface area on the ribbon, as it forms a regular structure between carbon atoms [4].

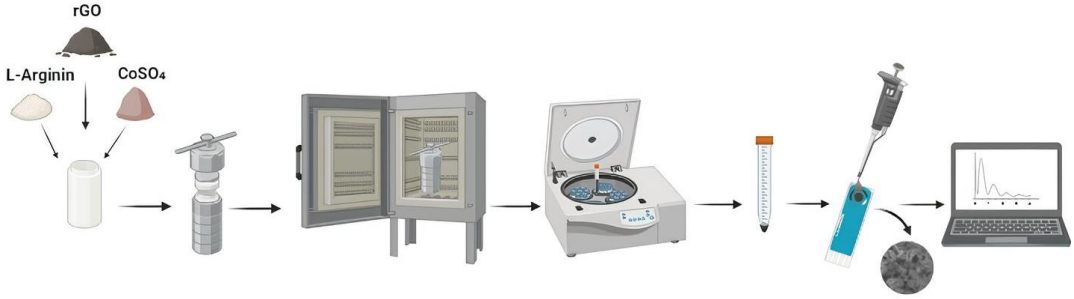


Figure 1. Synthesis of rGO@L-arginine/Co nanomaterial

The study deals with the synthesis of rGO@L-arginine/co-nanomaterials by a hydrothermal process. It was observed that rGO@L-arginine/co-nanocomposites cause strong changes in the optical properties of L-arginine. Characteristic X-ray elemental analysis, Fourier transform infrared spectroscopy and scanning electron microscopy (SEM) were used for the structural, optical and morphological properties of the samples.With regard to the methods used for recent advances in the field of nanoparticle (NP)-based electroanalysis, the functionalization of the electrode surface and its ability to cover a larger area were considered.

[1] Kissinger, P. T. (2005). Biosensors—A perspective. Biosensors and Bioelectronics, 20(12), 2512-2516.

[2] Franceschini, F., & Taurino, I. (2022). Nickel-based catalysts for non-enzymatic electrochemical sensing of glucose: A review. Physics in Medicine, 100054.

[3] Dayan, S., Özdemir, N., Erdener, D., Dayan, O., & Çetinkaya, B. (2023). Synthesis of a cationic ruthenium (ii) complex and its non-enzymatic glucose-sensing properties. New Journal of Chemistry, 47(21), 10187-10194.

[4] Rahsepar, M., Foroughi, F., & Kim, H. (2019). A new enzyme-free biosensor based on nitrogen-doped graphene with high sensing performance for electrochemical detection of glucose at biological pH value. Sensors and Actuators B: Chemical, 282, 322-330.

**Synthesis, characterization, optical and electrochemical properties of poly(azomethine)s containing aliphatic chain and biphenylsulfonic acid unit**

Ruhiye Nilay Tezel[1,2*], İsmet Kaya[1]

[1]*Çanakkale Onsekiz Mart University , Department of Chemistry, Çanakkale, 17020 TURKEY*

[2]*Çanakkale Onsekiz Mart University, Lapseki Vocational School, Department of Chemistry and Chemical Processing Technologies, Çanakkale, 17800 TURKEY*

[*]**Corresponding E-mail:** nilaytezel@comu.edu.tr

Conjugated oligomers and polymers are used as viable alternatives to conventional inorganic-based compounds in various optoelectronic or electronic devices due to their excellent optoelectronic behavior, light-weight, large area processing, flexibility and low fabrication cost. P0ly(azomethine)s (also called poly(imine)s or polymeric Schiff bases) are among the large variety of conjugated compounds of increasing interest with great potential for optoelectronic and photonic applications. They exhibit high thermal stability, optical and semiconducting properties, liquid crystalline potential, complexation capability or biological activity, which enabled their use in light emitting diodes, solar cells, catalysts or detectors. In the current work, we describe the synthesis of three poly(azomethine) compounds. Structural characterizations of the synthesized poly(azomethine)s were performed by NMR and FT-IR techniques and they were also characterized with UV-Vis, CV, TG-DTA, fluorescence measurements. According to obtained results, the structure–property relationships of these compounds were investigated.

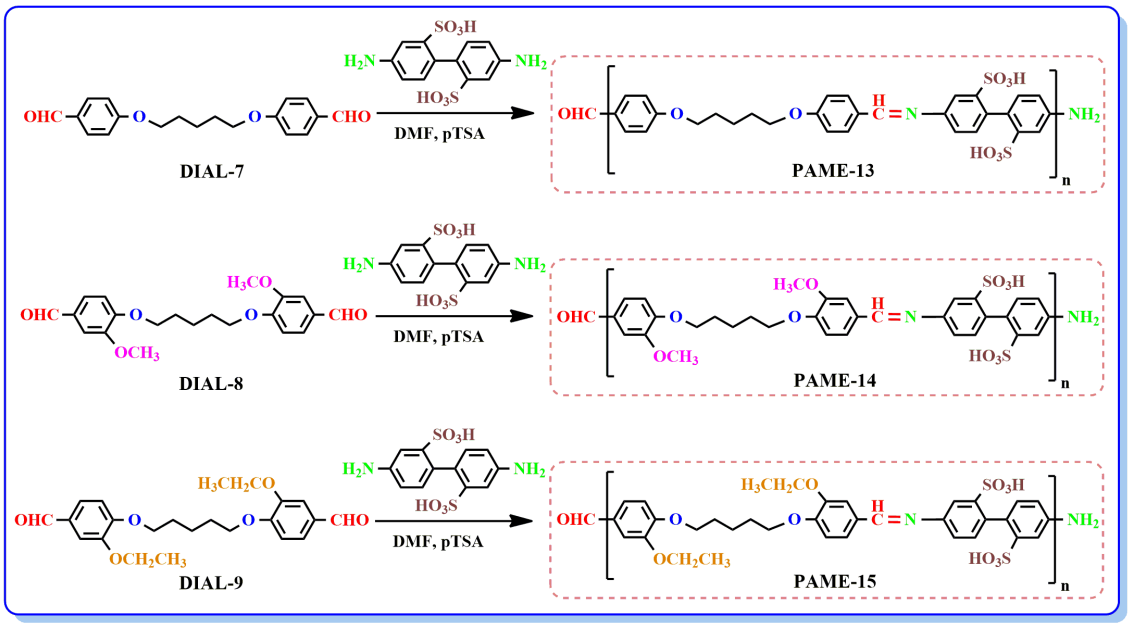


Fig.1. Synthesis and structures of poly(azomethine)s.

**Characterization of Electrical Properties in MIS Schottky Barrier Diodes with N-Doped DLC Thin Films**

N.Urgun[1*] , A.Feizollahi Vahid[2],Ş.Altındal[3]

[1]*Department of Mechatronics Engineering, Faculty of Engineering, Karabük University, Karabük, 78050, Turkey*
[2]*Department of Nanotechnology Engineering, Zonguldak Bülent Ecevit University, Zonguldak, 67100, Turkey*
[3]*Department of Physics, Faculty of Sciences, Gazi University, Ankara, 06500, Turkey*

[*]**Corresponding E-mail:** nuray1erkutlu@gmail.com

In this study, nitrogen-doped DLC thin film is grown on p-type silicon by utilizing the electrochemical method. Then, the surface properties of the fabricated thin film are characterized in detail using XPS (X-ray photoelectron spectroscopy) and SEM (scanning electron microscopy) to investigate its chemical and surface features. After deconvolution, C1s and N1s peaks are separated into several sub-peaks. According to the XPS analysis results, C1s spectrum analysis corresponds to the peaks at 284.78 eV for the $sp^2$ C-C bond, 286.13 eV for the $sp^3$ C-C bond, and 288.35 eV for C-O bonds. The additional peak at 289.3 eV indicated the C-N bond. In the N1s XPS scan analysis, the observed peaks in our N-DLC thin film were 399.76 eV for the N-$sp^2$ bond and 400.84 eV for the N-O bonds. The image obtained by scanning electron microscopy (SEM) shows that the surface of the nitrogen-doped diamond-like carbon (N-DLC) film comprises spherical grains of various sizes and shapes distributed randomly. This result indicates that the incorporation of nitrogen atoms into the carbon cage during the doping process affects grain growth and creates this granular structure. In order to characterize the obtained nitrogen-doped thin film as a Schottky diode interface, an Au/(N-DLC)/p-Si structure was prepared. Then, both C-V (capacitance-voltage) and G/ω analyses are performed at low frequency (3 kHz) and high frequency (1 MHz) in the range of -3 and 3 Volts. These analyses showed that this interface is entirely frequency and voltage-dependent and changes in a compatible manner. In order to investigate the electrical parameters of the structure, the basic electrical parameters of the structure are extracted using the slope and intercept of the linear part of the C-2 graph. These parameters include diffusion potential ($V_D$), acceptor atom doping concentration ($N_A$), Fermi energy ($E_F$), maximum electric field ($E_m$), depletion layer width ($W_D$) and barrier height ($\Phi_B$). The interface states ($N_{ss}$) of the structure are obtained using the high-low frequency capacitance method, depending on voltage and frequency.

According to the results of this study, N-DLC thin film has exhibited superior properties as an interlayer in electronic devices. It can be a superior alternative to oxide or other insulating layers to reduce Nss and other defects. In addition, this study shows that the integration of nitrogen-doped DLC layer significantly contributes to the reduction of unwanted electrical effects in semiconductor devices.

Keywords: XPS, SEM, C-V characterization, electrical parameters.

**Preparation of Alumina-Supported Pd@Ru Nano-Catalysts and Their applications**

Ezginur Güleriş, Osman Dayan*

* Department of Chemistry, Faculty of Science, Çanakkale Onsekiz Mart University, 17020- Çanakkale, Turkey.

***Corresponding E-mail:** osmandayan@comu.edu.tr

Toxic dyes, such as azo dyes and nitrophenols, pose a significant environmental and health risk, particularly in the textile industry. These synthetic organic compounds are widely used in many industries, including plastics, paper, food, pharmaceuticals, cosmetics, and textiles. These pollutants in water systems can harm ecosystems, prevent photosynthesis, and cause health issues. To address this issue, industries should use sustainable practices such as natural dyes and appropriate wastewater treatment technologies. Chemical catalytic conversion methods utilizing transition metal catalysts could be a strategic solution due to their speed, efficiency, and cost-effectiveness. Transition metal nanoparticles are efficient, fast, and cost-effective dye degradation catalysts. Alumina, also known as aluminum oxide ($Al_2O_3$), is a popular support material for the production of metal nanoparticles due to its low toxicity, chemical stability, and abundance. Ruthenium and palladium nanoparticles are widely used due to their high surface area, ease of production, and catalytic properties. In this study, the reduction of a real sample-like dye mixture was investigated using a bimetallic catalytic system (Ru-Pd) attached to Al2O3.

**Determination of potential use of halloysite nanotube filled alginate film for food packaging**

Bilge Unat[1], Özde Ipsalalı[1], Filiz Ugur Nigiz[1]

[1] *Çanakkale Onsekiz Mart University, Department of Chemical Engineer, Çanakkale, 17100, Türkiye*

[*]**Corresponding E-mail:** filiz.ugur@comu.edu.tr

The packaging sector occupies a large place within the plastic industry. Most of the materials used in packaging today are petroleum derived. However, natural degradation of these materials is not possible. They also cause irreversible damage to the environment and life when exposed to sunlight. It has been reported that, especially in Europe, food packaging will be completely biodegradable by 2030. For this reason, the production of biodegradable, environmentally friendly food packaging materials has gained importance. In addition to being natural, food packaging has important features that it must have. These; To protect food from external factors, to ensure food safety, to extend the shelf life of food, to be mechanically durable, to facilitate food transport and to degrade in nature. In this study, food packages were produced from alginate, an important biodegradable material obtained from brown seaweeds and used in the medical, food and chemical industries. Halloysite nanotube material was added (wt.1-5%) to increase the mechanical strength and water-steam resistance of alginate. Additionally, thyme oil was added to the package to benefit from the antimicrobial and antioxidant properties of thyme oil. The material's mechanical strength, opacity, water and moisture retention rates, and antimicrobial activity were tested and its potential use was determined. As a result, the swelling capacity of the films increased up to a certain value as HNT was added and it decreased in films containing thyme oil. The highest swelling value %121,57 values were obtained from Alg-%1 HNTs and %76,74 values Alg-%3 HNT-10 microL Thyme oil. The addition of HNT to the alginate-based matrix resulted in the formation of porous structures in the films, affecting their WVP. The porous structure makes the films more flexible and allows water vapour to pass through. The opacity value of the films obtained from alginate ranged from 8.5 to 10.5 A/mm and these films were transparent enough. The values for tensile strength were maximum 47.3 MPa Alg-3% HNTs films and maximum 44 MPa Alg-3% HNT-20 microL Thyme oil. The results show that the HNT addition improved all packaging property of the films. It is suggested that the developed films should be tested for biodegradability, shelf life in food and controlled release systems of essential oils such as thyme in the films should be improved.

**Acknowledgements**

This research was supported by the Çanakkale Onsekiz Mart University Scientific Research Projects Coordination Unit (BAP) and Grant Number FLÖAP-2023-4595, Turkey.

**Key words:** Biopolymer, Packaging, Antimicrobial, Film

**Effect of Sulphurization Duration on Cu rich $CuSbS_2$ Films Produced by a Two-step Process**

Uğur Yorulmaz and İdris Akyüz

*Department of Physics, Eskişehir Osmangazi University, Eskişehir*

***Corresponding E-mail:** uyorulmaz@ogu.edu.tr; iakyuz@ogu.edu.tr

Alternative materials that can be used in sustainable, renewable and cost-effective energy technologies are one of the most important topics that attract the attention of researchers working in the field of materials science. At this point, solar energy and photovoltaic solar cells stand out among renewable technologies. Currently, in addition to polycrystalline and monocrystalline Si solar cells, which are leading the photovoltaic market, CIGS and CdTe-based thin-film solar cell technologies are also attracting attention as an alternative. However, CIGS and CdTe materials have some limitations, such as the shortage of In, the use of heavy metals, when it comes to mass-scale production. In recent years, new materials containing earth-abundant, non-toxic components have emerged as promising photovoltaic absorbers, and one of these materials is $CuSbS_2$ films. Although research on these films is ongoing, the number of systematic studies on the structural, optical and electrical properties of $CuSbS_2$ is insufficient to clearly reveal the phase formations in the films and the effects of these phases on the physical properties. In this study, using a two-step process, layered Cu and $Sb_2S_3$ coatings were formed by thermal evaporation method in the first stage, and in the second stage, the films were subjected to sulphurization in a home-made borosilicate cell as shown in Fig. 1. Effect of sulphurization process performed for 30, 60, 90 and 120 minutes on the structural, optical and electrical properties of the films and phase formation/surface texture have been revealed.

**Keywords:** Thermal Evaporation, Absorber Layer, Solar Cell, Sulphurization.

**Acknowledgement:** Authors would like to acknowledge the Eskisehir Osmangazi University Scientific Research Projects Commission through its research support (Project code: FDK-2022-2547).

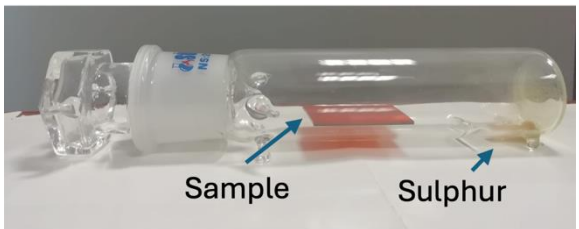


Fig.1. Set-up used for sulphurization process.

**Cu-Based MPOF Immobilization to Strip Electrodes: Fabrication of a Glucose Biosensor**

Yaren CANATAN[1], Neşe DEMİR[1], Funda ÖZDEMİR GÜNEY[1], Serkan DAYAN[1,2*]

[1]*Drug Application and Research Center, Molecular Synthesis and Industrial Application Laboratory (MSIA-Lab), Erciyes University, 38280 Kayseri, Turkey*

[2]*Erciyes University, Faculty of Pharmacy, Department of Pharmaceutical Basic Sciences 38039, Kayseri, Turkey*

[*]**Corresponding E-mail:** yarencanatann@gmail.com or serkandayan@erciyes.edu.tr

Metal-organic frameworks (MOFs) are polymeric coordination structures formed by the combination of metal ions or clusters and various organic connecting elements. Metal-organic frameworks exhibit a variety of unique properties: a special surface area, a high pore volume, a large and ordered structure as well as favorable thermal and mechanical stability [1]. Due to these excellent properties, MOF nanomaterials are widely used in areas such as biosensing, bacterial control, therapeutics bioimaging, etc. [2]. In the present study, a Cu-based organic metal phosphate framework (MPOF) was synthesized at different pH values. Subsequently, characterization was carried out by techniques such as Fourier transform infrared spectroscopy (FT-IR), X-ray diffraction (XRD), field emission scanning electron microscopy (FESEM), energy dispersive X-ray analysis (EDX), and elemental mapping. The synthesized MPOFs were immobilized on the strip electrode, and then electrochemical measurements were performed for glucose determination. As a result, the fabricated strip electrodes can be used as new candidates for biosensors, catalysts, and drug release studies.

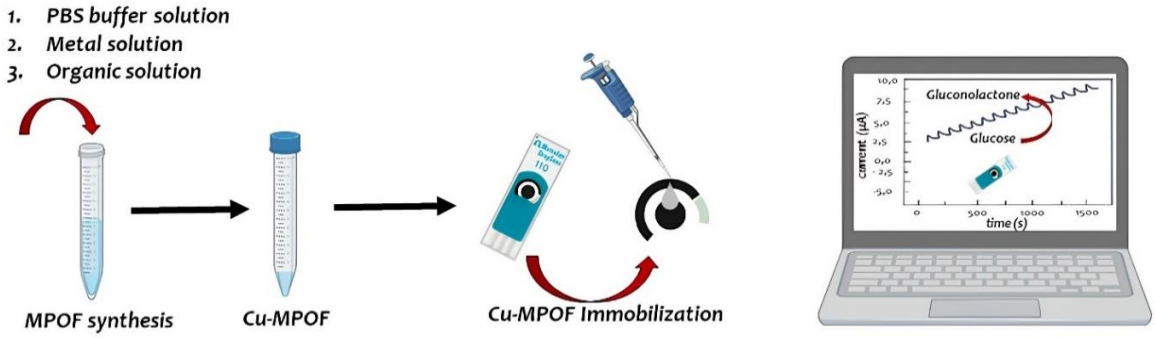


**Fig.1.** Schematic illustration of MPOF synthesis and strip electrode process.

**References:**

[1] Al Sharabati, M., Sabouni, R., & Husseini, G. A. (2022). Biomedical applications of metal− organic frameworks for disease diagnosis and drug delivery: a review. *Nanomaterials*, *12*(2), 277.

[2] Wang, D., Jana, D., & Zhao, Y. (2020). Metal–organic framework derived nanozymes in biomedicine. *Accounts of chemical research*, *53*(7), 1389-1400.

# Production and Electrical/Optical Characterization of Al/$NiCo_2O_4$ /n-Si/Al Schottky Photodiode Structure

Y.Atmaca [1*],Ş.Çavdar[2]

[1] *Gazi University, Department of Advanced Technologies, Graduate School of Natural and Applied Sciences, Ankara, Turkey, 06500 TURKEY*

[2]*Gazi University, Department of Physics, Faculty of Science, Ankara, Turkey, 06500 TURKEY*

[*]**Corresponding E-mail:** yusuf.atmaca1@gazi.edu.tr

In this study, Schottky structured photodiodes were produced using $NiCo_2O_4$ (nickel cobaltite) thin films and their electrical and optical characterizations were performed. $NiCo_2O_4$ thin film structure on $Co_3O_4$ (cobalt oxide) seed layer was created using spin coating technique on n-type Si, quartz and FTO (fluorine doped tin oxide) surfaces. Surface analysis of the produced samples was performed using scanning electron microscopy (SEM). In SEM analysis, the surface morphology of the samples is examined. Optical transmittance and absorption analyze were performed using UV/VIS spectroscopy of the $NiCo_2O_4$ thin film structure on quartz and FTO glass structures. Al/ $NiCo_2O_4$/n-Si/Al Schottky diode structure was created, and its electro-optical and electrical properties were examined at different illumination intensities in visible light wavelengths. Using I-V graphs, the ideality factor (n), barrier height ($\Phi_b$) and saturation current ($I_0$) values of the materials were calculated. It was determined that as the illumination intensity increased, the photocurrent in the reverse bias increased, the samples were sensitive to light and showed photodiode properties. When examined in the light of all these data, it was seen that $NiCo_2O_4$ is a suitable material that can be used as a photodiode in optoelectronic applications in different fields with these properties.

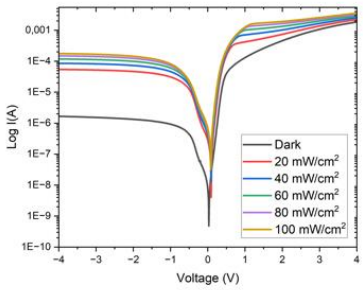


Fig.1. The I-V Curve of Al/ NiCo2O4/n-Si/Al Schottky Diode

# Synthesis And Optimization Of Polyvinylimidazole By Photopolymerization Type II

M. Danisman[1*], A. Oral[2]

[1] *Canakkale Onsekiz Mart University, Bayramic Vocational School, Department of Chemistry and Chemical Processing Technologies, Canakkale, 17700 TURKEY*

[2] *Canakkale Onsekiz Mart University, Faculity of Science, Department of Chemistry, Canakkale, 17020 TURKEY*

[*]**Corresponding E-mail:** mervedanisman@comu.edu.tr

Imidazole ring-containing polymers, or their derivatives, are recognized as valuable biomaterials due to their enhanced biodegradability and antimicrobial properties. Poly (N-vinyl imidazole), a well-known water-soluble polymer, was used to modify various synthetic or natural polymers via grafting, which displayed several biological properties, such as antibacterial activity, biocompatibility, and biodegradable. PVI has a dual nature, consisting of a hydrophobic main structure and hydrophilic side chains. PVI readily forms molecular complexes with a wide range of organic and inorganic compounds, which explains its utilization in many industrial processes, printing, ion removal, preparation of adsorbents, catalyst supports, gene delivery carriers. Furthermore, imidazole is recognized for its susceptibility to analytes that have the ability to establish hydrogen bonds and coordinate with imidazole rings, particularly in the presence of metal ions. This attribute makes PVI very suitable for the production of biosensors and membranes used in the complexation and removal of metal ions. In this study, the synthesis of polyvinylimidazole using photopolymerization type II with 1-imidazole monomer was carried out and the photopolymerization conditions were optimized. In addition, free radical polymerization of polyvinylimidazole was also carried out and compared with the reaction efficiency of photopolymerization.

***Keywords:*** *Polyvinylimidazole, Photopolymerization, Free Radical polymerization*

# Detailed analysis of possible current transport mechanisms (CTMs) in Au/(P3DMTFT)/n-GaAs Schottky diodes (SDs) over a wide temperature range

Ahmet Faruk Özdemir[1*], Yılmaz Kansız[1], Durmuş Ali Aldemir[1] & Şemsettin Altındal[2]

[1]*Department of Physics, Faculty of Sciences and Arts, Süleyman Demirel University, Isparta, Turkey*
[2] *Department of Physics, Faculty of Science, Gazi University, 06500 Ankara, Turkey*

[*]**Corresponding E-mail:** afozdemir@hotmail.com

The aim of this study is to fabricate Au/(P3DMTFT)/n-GaAs SDs and then their current transport mechanisms (CTMs) have been investigated in wide-temperature range of 80-300K by using current-voltage (I-V) measurements. For this aim, the basic electrical parameters of them such as reverse saturation-current ($I_o$), zero-bias barrier-height ($\Phi_{bo}$), and ideality-factor (n) were extracted the linear-part of forward bias $\ln(I_F)$-$V_F$ plots for each-temperature by using standard Thermionic-Emission (TE) theory. The observed an increase in $\Phi_{bo}$ and decrease in n with increasing temperature was attributed to barrier-inhomogeneities by assuming double Gaussian-distribution (DGD) of barrier-heights (BHs) at metal/semiconductor interface. Conventional Richardson-plot ($\ln(I_o/T^2)$ vs q/kT) was also deviated from linearity and obtained experimental Richardson-constant (A*) from its linear-part was found considerably lower theoretical value. Therefore, $\Phi_{bo}$ versus n and q/2kT were drawn to obtain some evidence of GD of BH. By using the standard-deviation ($\sigma_s$) values obtained from the slope two linear-part of $\Phi_{bo}$-q/2kT, the modified Richardson plot ($(\ln(I_o/T^2)-0.5(q\sigma_s/kT)^2$ vs q/kT) was drawn and also the experimental value of A* was found closer to its theoretical value. Additionally, the energy dependent profile of surface state density ($N_{SS}$) obtained from the $I_F$-$V_F$ data for various temperatures by considering voltage dependent BH and n values.

**Keywords:** Thermionic-Emission (TE) theory, Temperature dependent, Current transport mechanisms (CTMs), Surface states ($N_{ss}$), Basic electrical parameters, Double Gaussian-distribution (DGD) of barrier height, Richardson plots